The background is an abstract, artistic representation of water or a molecular structure. It features several large, semi-transparent blue spheres of varying sizes, some of which have a small, glowing globe of the Earth inside them. The background is a mix of teal, light blue, and green, with a soft, out-of-focus effect. The overall aesthetic is clean and scientific.

Integrated modeling of ozonation for optimization of drinking water treatment

A.W.C. van der Helm

Stellingen

behorende bij het proefschrift

Integrated modeling of ozonation for optimization of drinking water treatment

Alexander Wilhelmus Cornelis van der Helm

Delft, 3 december 2007

- 1 Overheden en waterleidingbedrijven moeten zich richten op een onberispelijke kwaliteit van kraanwater. (dit proefschrift)
- 2 Bij ozonisatie door middel van het doseren van opgelost ozon met een statische menging gevolgd door contacttijd in een propstroom reactor, is de verhouding desinfectie tot desinfectie-bij-producten groter dan bij ozonisatie door middel van conventionele bellenkolommen en contact kamers. (dit proefschrift)
- 3 De reactiesnelheid van snelle ozon consumptie volgt de kinetiek van diffusie limitatie. (dit proefschrift)
- 4 Assimileerbaar organisch koolstof (AOC) vorming tijdens ozonisatie kan worden bepaald aan de hand van on-line differentie UV absorptie spectra. (van den Broeke et al., Proceedings of the IWA AutMoNet 2007 conference, Gent, Belgium, 2007)
- 5 Of bromaat nou mogelijk (IARC) of waarschijnlijk (USEPA) kankerverwekkend is, het zorgt zeker voor buikpijn, hoofdpijn en slapeloosheid bij onderzoekers en water managers. (IARC Monographs on the evaluation of carcinogenic risks to humans, 1999; USEPA 2006 edition of the drinking water standards and health advisories)
- 6 De mens kan niet aan de thermostaat van de aarde draaien. (S. Kroonenberg, ACADEMY® Magazine, 2007)
- 7 Proberen brengt alles tot stand. (Herodotus, Historiae 7,9: Mardonius to Xerxes)
- 8 Later is al lang begonnen. (Klein orkest, 1984)
- 9 De belemmering die iemand ervaart van een handicap is omgekeerd evenredig met zijn acceptatie ervan.
- 10 Het is wonderlijk dat een thesis begint met 10 thesen.

Deze stellingen worden opponeerbaar en verdedigbaar geacht en zijn als zodanig goedgekeurd door de promotor, prof. ir. J.C. van Dijk.

Propositions

belonging to the thesis

Integrated modeling of ozonation for optimization of drinking water treatment

Alexander Wilhelmus Cornelis van der Helm

Delft, 3 December 2007

- 1 Governments and drinking water supply companies should aim for impeccable tap water quality. (this thesis)
- 2 For ozonation by means of dosing dissolved ozone with a static mixer and subsequent contact time in a plug flow reactor, the disinfection to disinfection-by-products ratio is greater compared to ozonation by means of conventional bubble columns and contact chambers. (this thesis)
- 3 The rate of rapid ozone consumption follows diffusion-limited kinetics. (this thesis)
- 4 Assimilable organic carbon (AOC) formation during ozonation can be determined on-line from differential UV absorbance spectra. (van den Broeke et al., Proceedings of the IWA AutMoNet 2007 conference, Gent, Belgium, 2007)
- 5 Whether bromate is possibly (IARC) or probably (USEPA) carcinogenic to humans, it definitely gives stomachaches, headaches and insomnia to researchers and water board managers. (IARC Monographs on the evaluation of carcinogenic risks to humans, 1999; USEPA 2006 edition of the drinking water standards and health advisories)
- 6 Mankind cannot turn the earth's thermostat. (S. Kroonenberg, ACADEMY® Magazine, 2007)
- 7 Trying will accomplish everything. (Herodotus, Historiae 7,9: Mardonius to Xerxes)
- 8 Later started long ago. (Klein orkest, 1984)
- 9 The hindrance that a person experiences from a handicap is inversely proportional to his acceptance of it.
- 10 It is curious that a thesis starts with 10 theses.

These propositions are considered opposable and defensible and as such have been approved by the supervisor, Prof. ir. J.C. van Dijk.

Integrated modeling of ozonation for optimization of drinking water treatment

Water Management Academic Press

Published by
Water Management Academic Press
PO Box 5048
2600 GA Delft
the Netherlands
Tel.: +31 15 278 3347

Author A.W.C. van der Helm
Printed Gildeprint Drukkerijen BV
ISBN 978-90-8957-001-7
NUR 956

Integrated modeling of ozonation for optimization of drinking water treatment

Copyright © 2007 by Water Management Academic Press

All rights reserved. This book, or parts thereof, may not be reproduced in any form or by any means, electronic or mechanical, including photocopying, recording or any information storage and retrieval system now known or to be invented, without written permission from the Publisher.

Integrated modeling of ozonation for optimization of drinking water treatment

Proefschrift

ter verkrijging van de graad van doctor
aan de Technische Universiteit Delft,
op gezag van de Rector Magnificus prof. dr. ir. J.T. Fokkema,
voorzitter van het College voor Promoties,
in het openbaar te verdedigen

op maandag 3 december 2007 om 15:00 uur

door
Alexander Wilhelmus Cornelis VAN DER HELM

civiel ingenieur
geboren te Nootdorp

Dit proefschrift is goedgekeurd door de promotor:

Prof. ir. J.C. van Dijk

Toegevoegd promotor:

Dr. ir. L.C. Rietveld

Samenstelling promotiecommissie:

Rector Magnificus, voorzitter

Prof. ir. J.C. van Dijk, Technische Universiteit Delft, promotor

Dr. ir. L.C. Rietveld, Technische Universiteit Delft, toegevoegd promotor

Prof. dr. ir. R. Babuška, Technische Universiteit Delft

Prof. dr. G.L. Amy, UNESCO-IHE

Prof. dr. ir. W.G.J. van der Meer, Universiteit Twente

Prof. dr. U. von Gunten, Eidgenössische Technische Hochschule Zürich

Ir. Th.G.J. Bosklopper, Waternet

Summary

In the Netherlands, drinking water treatment plants are robust and designs are based on the performance of individual processes with pre-set boundary conditions. In the operation of drinking water treatment plants, the processes are usually optimized individually on the basis of “rules of thumb” and operator knowledge and experience. However, changes in operational conditions of individual processes can affect subsequent processes and an optimal operation is different for every operator. At the beginning of this research it was assumed that an integrated approach to the entire treatment plant could lead to a more efficient operation, and it was recognized that decisions of an integrated nature could be complex and difficult to make. It was expected that an integrated model of the entire water treatment plant could be used as an instrument for operational support and process control to further improve the operation of a drinking water treatment plant, making maximal use of the installed infrastructure and postponing new investments.

In order to perform an integrated optimization of operation of a drinking water treatment plant, explicit objectives for the operation of drinking water production have to be identified and defined. Three possible objectives were assessed: environmental impact, costs and water quality. The assessments were carried out for the case of the drinking water treatment plant Weesperkarspel and its pre-treatment plant Loenderveen of Waternet (the water cycle company for Amsterdam and surrounding areas). The possible decrease in environmental impact and costs of operation at Weesperkarspel was found to be small compared to the possible increase in environmental impact and costs for the society as a whole when more bottled water is used for drinking as a result of insufficient (confidence in) tap water quality. Based on social, environmental and economical considerations, it can be concluded that governments and drinking water supply companies should aim for an impeccable tap water quality and a reliable, healthy and environmentally sound image of tap water in order to at least stop the increase in bottled water use. Thus, the objective for integrated optimization of the operation of drinking water treatment plants should be the improvement of water quality and not an *a priori* reduction of environmental impact or costs.

From the water quality assessment it follows that ozonation plays a key role in the Weesperkarspel treatment scheme and therefore the focus of integrated modeling in this research was on ozonation. Assimilable organic carbon (AOC), bromate formation and the CT value for ozone exposure were recognized as important parameters. For the development and calibration of a model describing these parameters, experiments in different bench-scale and pilot-scale ozone installations with different natural waters were performed in combination with fundamental modeling studies.

By using different experimental setups such as dosing of dissolved ozone, dosing of ozone in bubble columns, contact time between ozone in water in a pipe with plug flow reactor characteristics and in a vessel with completely stirred tank reactor characteristics, the model was calibrated and validated for a wide range of applications. This has resulted in an integrated model for ozonation that is able to predict ozone decay, CT value, *E. coli* disinfection, the decrease in UV absorbance at 254 nm (UVA_{254}), the increase in AOC concentration and bromate formation on the basis of influent water quality parameters, and the applied ozone dosage under different hydraulic conditions. This model was used for evaluating the current control strategy of the full-scale ozone installation at Weesperkarspel and for assessing other control strategies for operational support and process control of ozonation. It is a tool that directly shows the consequences of changes in operation of the ozone installation. It enables water supply companies to make more objective choices for operational settings and, thus, is a valuable tool for controlling the balance between disinfection, bromate formation and AOC formation.

From the experimental work and modeling studies, the importance of the hydraulic conditions was demonstrated. It was found that the disinfection capacity for the ozone-sensitive organism *E. coli* is 3 to 5 times higher when ozone contactor hydraulics approaches a plug flow reactor compared to a completely stirred tank reactor. For an efficient disinfection, it is important that the dosed ozone be completely mixed with the water flow as quickly as possible to avoid having water parts with ozone concentrations lower than the average concentration. This specifically holds true at relatively low ozone dosages, as is the case for the drinking water treatment plants of Waternet. The dissolved ozone plug flow reactor (DOPFR) concept developed in this research addresses both issues. In the DOPFR, ozone is dissolved in a pre-treated side stream and dosed to the main stream just before a static mixer. By dosing dissolved ozone, the gas transfer of

ozone into water is eliminated from the mixing process. Two liquid flows mix much better and more quickly than a gas and a liquid flow. In this way, with a static mixer, the dosed ozone can be almost instantly mixed with the total water flow. Subsequently, contact time in the DOPFR is created in a pipe with plug flow characteristics. From research with pilot-plant ozone bubble columns with relatively good hydraulic characteristics compared to full-scale installations, it was found that large short-circuit flows can occur in the bubble columns. Realizing the importance of hydraulics, the application and design of conventional ozone installations needs to be reconsidered.

Natural organic matter (NOM) has a large influence on processes taking place during ozonation and, thus, is an important parameter for ozonation efficiency and for integrated modeling of ozonation. In the tested bench-scale DOPFR and pilot-scale DOPFR it was possible to measure ozone concentrations starting from a contact time of 1 to 2 seconds, in contrast to other research where the first samples are usually taken after 30 seconds or one minute. This allowed for the possibility of measuring rapid ozone consumption that occurs due to the reaction between ozone and NOM upon the first contact of ozone with natural water. From modeling the measured rapid ozone consumption it was found that the rate of rapid ozone consumption in the first 20 seconds of contact time follows diffusion-limited kinetics.

The effects of the character and the removal of NOM on the formation of AOC and the formation of bromate and CT during ozonation were evaluated in order to determine what amount and which part of the NOM should be removed for improvement of ozonation efficiency. Natural waters from two locations with different dissolved organic carbon (DOC) concentrations were tested. In addition, the DOC concentration of one of the natural waters was reduced either by ion exchange (IEX) or by granular activated carbon (GAC) filtration. The resulting four water types were tested in conventional pilot-scale ozone bubble column reactors and in a bench-scale plug flow reactor with dissolved ozone dosing. It was concluded that for the same ozone dosages the CT is higher when NOM is removed by IEX or GAC compared to the situation without NOM removal. In addition it was concluded that ozonation efficiency improved more with the removal of humic substances (molecular weight ~ 1000 g/mol) as compared to the removal of the building blocks fraction (molecular weight 300-500 g/mol) of NOM, as determined by size exclusion chromatography with DOC detection, because it led

to less bromate formation and less AOC formation. It was concluded that for NOM removal before ozonation, IEX is preferred, because the IEX resin that was tested removed more humic substances than the GAC tested.

During this research, integrated modeling has proven to be the driving force for optimization of operation based on explicit objectives (control strategies), for new developments in design (DOPFR) and for exploring changes in the concept of a drinking water treatment plant (NOM removal). In general it can be stated that in order to be able to model a process, the process has to be understood. Thus, modeling efforts lead to the increase in knowledge, application of knowledge and recordation of knowledge.

Samenvatting

In Nederland zijn drinkwaterzuiveringen robuust en ontwerpen zijn gebaseerd op de prestaties van deelprocessen met voorafgestelde grenzen aan de procescondities. Verbeteringen in de bedrijfsvoering zijn gewoonlijk gericht op optimalisatie van deelprocessen, gebaseerd op vuistregels, kennis van bedrijfsvoerders en ervaring. Echter, veranderingen in stuurparameters van deelprocessen kunnen navolgende deelprocessen beïnvloeden en bedrijfsvoerders kunnen verschillend denken over de beste instellingen voor een drinkwaterzuivering. Bij aanvang van dit onderzoek was verondersteld dat een integrale aanpak van de gehele zuivering kan leiden tot een meer efficiënte bedrijfsvoering en was onderkend dat het nemen van beslissingen met een integraal karakter complex en moeilijk kan zijn. De verwachting was dat een integraal model van de gehele drinkwaterzuivering gebruikt kan worden voor ondersteuning van de bedrijfsvoering en voor procesbesturing, om de bedrijfsvoering van een drinkwaterzuivering verder te verbeteren en maximaal gebruik te maken van de bestaande installaties waardoor nieuwe investeringen kunnen worden uitgesteld.

Om een integrale optimalisatie van de bedrijfsvoering van een drinkwaterzuivering uit te voeren, dienen expliciete doelen voor de bedrijfsvoering geïdentificeerd en gedefinieerd te worden. Drie mogelijke doelen zijn beoordeeld: waterkwaliteit, milieubelasting en kosten. Drinkwaterzuivering Weesperkarspel van Waternet, het watercyclusbedrijf voor Amsterdam en 25 omliggende gemeenten, is gebruikt als voorbeeld. De mogelijke verlaging van de milieubelasting en kosten van de bedrijfsvoering van Weesperkarspel bleek klein te zijn in vergelijking met de mogelijke stijging van de milieubelasting en kosten voor de maatschappij wanneer meer flessenwater gedronken zou gaan worden als gevolg van onvoldoende (vertrouwen in de) kwaliteit van het kraanwater. Op basis van sociale, economische en milieutechnische overwegingen is geconcludeerd dat overheden en waterleidingbedrijven zich moeten richten op een onberispelijke kwaliteit van kraanwater en een betrouwbaar, gezond en milieuvriendelijk imago van kraanwater om op zijn minst de stijging van het gebruik van flessenwater te stoppen. Daarom dient de verbetering van de waterkwaliteit het doel te zijn voor integrale

optimalisatie van de bedrijfsvoering en niet a-priori de verlaging van de milieubelasting of de kosten.

Uit het onderzoek naar de doelen voor optimalisatie van de bedrijfsvoering van Weesperkarspel, volgde dat ozonisatie een sleutelrol vervult in de zuivering. Om deze reden is de integrale modellering in dit onderzoek gericht op ozonisatie, waarbij assimileerbaar organisch koolstof (AOC), bromaat en de CT waarde (maat voor blootstelling aan ozon) de belangrijkste parameters zijn. Voor de ontwikkeling en kalibratie van een model dat deze parameters beschrijft zijn experimenten uitgevoerd in verschillende proefinstallaties op testbank schaal en proefinstallatie schaal, met water van verschillende locaties, in combinatie met fundamentele modelstudies.

Door gebruik te maken van verschillende opstellingen waarbij ozon in opgeloste vorm is gedoseerd en in gasvorm in conventionele bellenkolommen, en waarbij contact tijd tussen ozon in water is gecreëerd in een leiding met een propstroom karakteristiek en in een vat met een volledig gemend vat karakteristiek, is het model gekalibreerd en gevalideerd voor een breed toepassingsgebied. Dit heeft geresulteerd in een integraal model voor ozon dat in staat is om voor verschillende hydraulische condities de ozonafbraak, de CT waarde, *E. coli* inactivatie, de afname van UV absorptie bij 254 nm (UVA_{254}), de toename van de AOC concentratie en bromaatvorming te voorspellen op basis van influent waterkwaliteitsparameters en de toegepaste ozondosering. Het model is gebruikt voor het evalueren van de huidige bedrijfsvoeringstrategie van de ozon praktijkinstallatie van Weesperkarspel en voor het testen en beoordelen van alternatieve bedrijfsvoeringstrategieën voor ondersteuning van de bedrijfsvoering en procesbesturing van de ozon installatie. Het is een hulpmiddel dat direct de consequenties zichtbaar maakt van veranderingen in de bedrijfsvoering. Het geeft waterleidingbedrijven de mogelijkheid om meer objectieve keuzes te maken voor de stuurparameters en is daarom een waardevol gereedschap voor het beheersen van de balans tussen desinfectie, AOC vorming en bromaatvorming.

Met het experimenteel onderzoek en de modelstudies is het belang van goede hydraulische condities aangetoond. Het is gebleken dat de desinfectiecapaciteit voor het ozongevoelige organisme *E. coli* 3 tot 5 keer groter is in een propstroomreactor dan in een volledig gemengd vat reactor. Voor een efficiënte desinfectie is het van belang dat het gedoseerde ozon zo snel mogelijk volledig

gemengd wordt over de te behandelen waterstroom, om te voorkomen dat delen van de waterstroom een ozonconcentratie hebben die lager is dan de gemiddelde concentratie. Dit geldt voornamelijk wanneer relatief lage ozonconcentraties worden toegepast zoals bij Waternet. Het concept van de opgelost ozon propstroomreactor (DOPFR, dissolved ozone plug flow reactor) dat is ontwikkeld tijdens dit onderzoek richt zich op deze twee punten. In de DOPFR wordt ozon opgelost in een voorbehandelde deelstroom die vlak voor een statische menger aan de hoofdstroom wordt toegevoegd. Door het doseren van opgelost ozon wordt de gasoverdracht van ozon naar water buiten het proces gehouden. Twee waterstromen mengen veel beter en sneller dan een gasstroom en een waterstroom. Op deze wijze kan het gedoseerde ozon door middel van de statische menger vrijwel instantaan gemengd worden met de totale waterstroom. Vervolgens wordt contacttijd gerealiseerd in een leiding met een propstroom karakteristiek. Uit proefonderzoek in ozon bellenkolommen op proefinstallatie schaal met relatief goede hydraulische eigenschappen ten opzichte van praktijkschaal installaties, bleek dat grote kortsluitstromen op kunnen treden in de bellenkolommen. Gezien het belang van de hydraulische condities dient de toepassing en het ontwerp van conventionele ozon bellenkolom installaties in heroverweging genomen te worden.

Natuurlijk organisch materiaal (NOM) heeft een grote invloed op de processen die optreden tijdens ozonisatie en is daarom een belangrijke parameter voor de efficiëntie van ozonisatie en voor de integrale modellering van ozonisatie. In de DOPFR was het mogelijk om ozon te meten vanaf 1 à 2 seconden verblijftijd, in tegenstelling tot andere onderzoeken waarbij de eerste ozon metingen over het algemeen na 30 seconden tot een minuut (kunnen) worden genomen. Dit gaf de mogelijkheid om snelle ozon consumptie te bepalen die optreedt door de reactie tussen ozon en NOM vanaf het moment dat ozon in het water aanwezig is. Uit de modellering bleek dat de snelheid van snelle ozon consumptie in de eerste 20 seconden contacttijd de kinetiek van diffusie limitatie volgt.

NOM bestaat uit een grote verscheidenheid aan organisch materiaal en kan worden gekarakteriseerd door onder andere de molecuul grootte. De effecten van het karakter van NOM en de verwijdering van NOM op de vorming van AOC, de vorming van bromaat en de CT waarde zijn onderzocht om de hoeveelheid NOM en het specifieke deel van NOM te bepalen dat kan worden verwijderd om de efficiëntie van ozonisatie te verbeteren. Hiervoor is water van twee locaties met

verschillende gehalten aan opgelost organisch koolstof (DOC) onderzocht. De DOC concentratie van de locatie met de hoogste waarde is verlaagd met behulp van ionenwisseling of met actieve koolfiltratie. De resulterende vier watertypen zijn onderzocht in een ozon bellenkolom proefinstallatie en in een testbank schaal DOPFR. Uit de experimenten is geconcludeerd dat voor dezelfde ozondoseringen de CT hoger is bij NOM verwijdering door ionenwisseling of actieve koolfiltratie dan voor de situatie waarbij geen NOM wordt verwijderd. Daarnaast is geconcludeerd dat de efficiëntie van ozonisatie sterker verbeterde door de verwijdering van humusachtige stoffen (moleculair gewicht ~ 1000 g/mol) uit NOM, dan door verwijdering van de bouwstenen fractie (moleculair gewicht 300-500 g/mol) uit NOM, omdat dit leidde tot minder AOC vorming en minder bromaatvorming. Hieruit is geconcludeerd dat ionenwisseling wordt verkozen boven actieve koolfiltratie voor NOM verwijdering voorafgaand aan ozonisatie, omdat de geteste ionenwisselaar meer humusachtige stoffen verwijderde.

Tijdens dit onderzoek is integrale modellering de drijvende kracht gebleken voor optimalisatie van de bedrijfsvoering gebaseerd op expliciete doelen (bedrijfsvoeringstrategieën), voor nieuwe ontwikkelingen in ontwerp (DOPFR) en voor het onderzoeken van veranderingen in het concept van een drinkwaterzuiveringsinstallatie (NOM verwijdering). In het algemeen kan gesteld worden dat voor het modelleren van een proces, het proces begrepen moet worden. Dit betekent dat modelleringwerkzaamheden leiden tot het vergroten van kennis, het toepassen van kennis en het vastleggen van kennis.

Acknowledgement

Four years after finishing my Master's thesis Luuk Rietveld asked me if I would like to do PhD research on integrated modeling for the operation of drinking water treatment plants. My first thought was that the project he was asking me to participate in was extremely interesting, and my second thought was that it would be great to take part in this project and at the same time get a PhD degree.

Looking back, it was great to be part of the Promicit project, as it was named, but the PhD degree didn't come as easily as I thought it would be. Earning that degree involved a lot of hard work, difficulties to overcome, plenty of (re)searching and then finding. I really enjoyed the process of researching and learning. It was a great opportunity for me to deepen my knowledge and broaden my views on water treatment. I have many people to thank for my growth and for helping me do the work described in this thesis.

Although my name is the only one on the cover, I could have never accomplished the work required for this thesis all by myself. I had a lot of help from many people and the cooperation of many organizations. The organizations I want to thank are DHV B.V., Waternet, Delft University of Technology and ABB B.V., the four partnering companies of the Promicit project. Without their vision and support, this thesis would not have been possible. Also thanks to SenterNovem agency of the Dutch Ministry of Economic Affairs that subsidized the Promicit project, Evers & Manders Consult that assisted in the project administration of Promicit, and Kiwa Water Research that made their laboratory facilities available for part of the experimental work.

The first persons I want to thank are my supervisor, Hans van Dijk, and my adjunct supervisor, Luuk Rietveld. Hans greatly helped me with focusing on the important issues, as well as placing the work in a larger context. As none other, he can inspire and create enthusiasm in people in our profession. Luuk Rietveld and I worked closely together on a 'daily' basis. Luuk always provided me with good comments on the contents and structure of all my writing and I have really enjoyed working and laughing with him.

I want to thank a few people from DHV, my primary employer. In particular, I want to thank Jan Timmer who did an excellent job defending our project proposal before the scientific committee of SenterNovem; my good friend Kim van Schagen, who always made time for my questions on modeling issues and for reflections on my work; Hans van der Kolk, who took over managing DHV's participation in Promicit from Jan Timmer, and Wim Kreijne, who made sure that Promicit's financial administration was very well organized.

Waternet is a great company and my 'colleagues' in the research department Drinking Water Technology made me really feel like one of them. The opportunity to work with them and share their facilities was great. I want to thank Karin Bosklopper, Alex Veersma, Eric Baars, René van der Aa, Fred van Schooten, Joost Kappelhof, Onno Kramer, Dolf Wind, Peter Huis, Mike Gillebaard, Peter Wind, Dirk Jan Sohl, Simon van Waveren, Harold Homburg and all the other employees of Waternet and Het Waterlaboratorium that I cannot mention by name.

From Delft University of Technology I owe thanks to Robert Babuška, for occasional feedback. Many thanks to Petra Ross, Patrick Smeets, Maarten Keuten, Anke Grefte, Luisa Nunes, Margarida Fernandes, Menno van Leenen and Jink Gude, they are great company and I enjoyed working with them.

Further, I would like to thank Ben Smaal from ABB B.V. for providing me with and sharing knowledge of the newest solutions on automation and control. I would like to thank Gary Amy, from IHE, from whom I learned a lot about scientific writing; and Maarten Siebel, Ramiro Barrios, and Mauricio Tapia with whom I worked on joint research with IHE. I also want to thank Joep van den Broeke from scan Messtechnik for the good cooperation and knowledge exchange and Adele Sanders for correcting my writing and improving my English.

Finally, I want to thank my family and friends and in particular my parents and my parents-in-law. Their support, interest in my work and wellbeing is overwhelming. I realize I am very fortunate to have such a loving family and good friends. I want to conclude this acknowledgement by thanking the two most important people in my life, my wife Liesbeth and my daughter Eva. They provided me with the stable and joyful environment at home. Liesbeth unconditionally supported me in my work and reminded me what is truly important in life when I needed reminding. I couldn't have done this without her.

Table of contents

1. Introduction	1
2. Objectives for integrated optimization of drinking water treatment plants	7
3. Modeling of ozonation for dissolved ozone dosing	29
4. Disinfection and by-product formation during ozonation in a pilot-scale plug flow reactor and CSTR	49
5. Effects of natural organic matter (NOM) character and removal on efficiency of ozonation	79
6. Integrated model for operational support and process control of ozonation	103
7. Conclusions	133
List of publications	147
Curriculum vitae	151

1. Introduction

Background of the thesis

In the Netherlands, drinking water treatment plants are robust and designs are based on the performance of individual processes with pre-set boundary conditions. In operation of drinking water treatment plants, the processes are usually optimized individually on the basis of “rules of thumb” and operator knowledge and experience. However, changes in operational conditions of individual processes can affect subsequent processes (see Figure 1) and an optimal operation, which can include a number of water quality parameters, costs and environmental impact, is different for every operator. The quality of drinking water is thus influenced by day-to-day decisions of individual operators (Bosklopper et al., 2004). Bosklopper et al. assumed that an integrated approach to the entire treatment plant can lead to a more efficient operation and concluded that decisions of an integrated nature can be complex and difficult to make. It was expected that an integrated model of the entire water treatment plant could be used as an instrument for operational support and for process control to further improve the operation of a drinking water treatment plant, making maximal use of the installed infrastructure and postponing new investments.

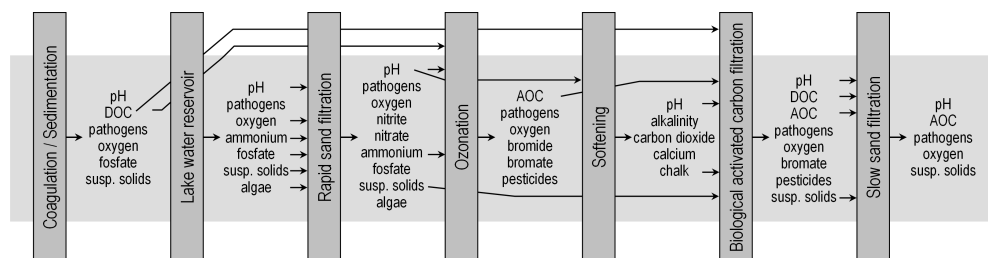


Figure 1 Influence of individual processes on subsequent processes (process scheme of drinking water pre-treatment Loenderveen and treatment plant Weesperkarspel of Waternet)

In 2003 Waternet, the water cycle company for Amsterdam and surrounding areas, DHV B.V., a consultancy and engineering company, ABB B.V., an engineering company for power and automation technology, and Delft University of Technology, department of Water Management and Delft Center for Systems and Control,

joined forces to perform research on drinking water quality control by developing an integrated model of the total water treatment and using this model as a basis for operation. This thesis is part of the defined joined research project 'Promicit' that was subsidized by SenterNovem, Ministry of Economic Affairs, the Netherlands. Evers & Manders Consult assisted in the project administration of Promicit.

The project is a first step towards realizing the visions for water utilities in 2050, according to Rosen (2000) and Trussel (2000). They envision that models predicting water quality and necessary treatment will be constantly run and assist operators, whose daily duties will be automated. Water quality data will be fed into control systems that will adjust the level of treatment needed to ensure safe water, while minimizing the use of chemicals. Treatment plants will become so rich in automation and intelligence that they will assume the role of a person, carrying on conversations with the operator – and the public – that closely approach human behavior. This means that computer models would therefore be needed to predict the quality of the source, the impact on the process, the quality of the product and the required, most effective control. Cooperation between process-engineers and automation and ICT-engineers would have to be intensified. As a consequence, the method for research would be changed from practical research to a combination of practical research with fundamental model studies (Rietveld, 2005).

From past and current research projects, Waternet, DHV B.V., ABB B.V. and the Delft University of Technology already have experience in modeling drinking water treatment processes and model-based control. In cooperation with several Dutch drinking water companies, DHV B.V. has developed a model-based water quantity control program called OPIR[®] that predicts the demand for drinking water, and controls the integrated production of several drinking water treatment plants efficiently (Bakker et al., 2003). In 2007 already over 3 million consumers in the Netherlands received drinking water produced using OPIR[®] water quantity prediction and control. Rietveld (2005) conducted a PhD study at Delft University of Technology on the modeling of individual drinking water treatment processes. These models are integrated in the Stimela environment, which is programmed in Matlab[®]/Simulink[®] (van der Helm and Rietveld, 2002). ABB B.V. has broad experience in plant optimization in many industries, amongst which is the water supply industry. Waternet is one of the drinking water companies in the Netherlands with a strong interest in drinking water treatment modeling. Waternet has two drinking water treatment plants where pre-treated surface water is

subsequently treated with ozonation, pellet softening, biological activated carbon (BAC) filtration and slow sand filtration. Emphasis on the modeling of BAC filtration and pellet softening is given in separate research (van der Aa et al., 2004; van Schagen et al., 2005 and 2006).

The focus for this PhD study is on optimization of drinking water treatment plants and on integrated modeling of ozonation. Ozonation plays a key role in integrated modeling of the treatment plants of Waternet. Ozonation is influenced by the pre-treatment and it influences softening and the BAC filtration. In addition, ozonation is the only process in which disinfection can be actively influenced.

Objectives of the thesis

This thesis has two objectives: to determine the objectives for optimization of operation of drinking water treatment plants and to develop an integrated model for ozonation that can be used for operational support and process control. The model has to be able to function as a part of an integrated model for the entire Weesperkarspel drinking water treatment plant of Waternet.

It is the purpose of the Promicit project that the models are able to function based on on-line calibration and validation, and that the modeling efforts lead to an increase in knowledge and understanding of the treatment processes. The consequence is that the models should be phenomenological models with an empirical model parameter estimation based on the on-line measurements available at that time. This results in the use of semi-empirical modeling techniques.

Content of the thesis

Each chapter is based on a published or submitted article. Since each chapter covers different subjects, the relationship between the chapters is explained.

In Chapter 2 what the objectives for optimization of operation of drinking water treatment plants should be is discussed. Three possible objectives are assessed: environmental impact, costs and water quality. The Weesperkarspel drinking water treatment plant is used as a case study. From the assessments it follows that

ozonation plays a key role in the Weesperkarspel treatment scheme and therefore the focus of integrated modeling is on ozonation. This chapter sets the framework for optimization and for this research in general.

In Chapter 3 an adapted version of the ozone model as proposed by Rietveld (2005) is provided and the model parameter estimation for predicting assimilable organic carbon (AOC) formation, bromate formation and CT value for ozone exposure is described. In Chapter 2 these parameters are recognized as important integrated parameters. The experimental data were obtained with a bench-scale installation where dissolved ozone was dosed and contact time was realized in a plug flow reactor.

In Chapter 4 the *E. coli* inactivation, bromate and AOC formation under optimal hydraulic conditions in a pilot-scale ozone plug flow reactor at the Leiduin drinking water treatment plant of Waternet are described. In addition, a comparison is made between *E. coli* inactivation in a plug flow reactor and in a completely stirred tank reactor. In both cases dissolved ozone was dosed. With this comparison the importance of the hydraulic design of ozonation reactors is shown. Rapid ozone consumption in the first 20 seconds of contact time between ozone and water is also assessed in Chapter 4 using different models. Since the results of the pilot-scale plug flow reactor experiments are obtained in a similar installation as the bench-scale plug flow reactor experiments described in Chapter 3, the determined ozonation modeling parameters are compared to each other in order to evaluate the effects of upscaling.

In Chapter 5 insight is provided into the additional improvement of ozonation efficiency compared to instant mixing of ozone and using a plug flow reactor for contact time as described in Chapter 4. Natural organic matter (NOM) has a large influence on processes taking place during ozonation and, thus, is an important parameter for ozonation efficiency and for integrated modeling of ozonation. The effects of the character and the removal of NOM on the formation of AOC, and the formation of bromate and CT during ozonation are evaluated. The main part of the experiments was performed at Weesperkarspel.

In Chapter 6 experimental research and modeling of ozone dosing in bubble columns with subsequent contact columns is described for two different natural waters. Model parameters determined in Chapters 3 and 4 are used and for a

number of model parameters relationships are determined for the two different water types, based on water quality parameters. The model is used for evaluating the current control strategy of the full-scale ozone installation at Weesperkarspel and for assessing other control strategies for operational support and for process control of ozonation.

In Chapter 7 overall conclusions are drawn from Chapters 3 to 6 in relation to Chapter 2. The consequences of the conclusions are discussed for operational optimization, process design and treatment concept of the drinking water treatment plant at Weesperkarspel. In Chapter 7, also an overview of related ongoing research is given.

References

- Bakker, M., Schagen, K.M. van and Timmer, J. (2003). Flow control by prediction of water demand. *J. Water Supply Res. Technol. AQUA*, 52(6), 417-424.
- Bosklopper, Th.G.J., Rietveld, L.C., Babuška, R., Smaal, B. and Timmer, J. (2004). Integrated operation of drinking water treatment plant at Amsterdam Water Supply. *Water Sci. Technol.: Water Supply*, 4(5-6), 263-270.
- Rietveld, L.C. (2005). *Improving operation of drinking water treatment through modelling*. PhD Thesis, Faculty of Civil Engineering and Geosciences, Delft University of Technology.
- Rosen, J.S. (2000). Computer-based technologies: predictions for water utilities. *Am. Water Works Assoc. J.*, 92(2), 62-63.
- Trussell, R.R. (2000). Treatment plant of 2050: a designer's view. *Am. Water Works Assoc. J.*, 92(2), 52-53.
- van der Aa, L.T.J., Achari, V.S., Rietveld, L.C., Siegers, W.G. and van Dijk, J.C. (2004). Modelling biological activated carbon filtration: determination adsorption isotherms of organic compounds. *Proceedings of the 2004 Water Institute of Southern Africa Biennial Conference*, Cape Town, South Africa, 2004.
- van der Helm, A.W.C. and Rietveld, L.C. (2002). Modelling of drinking water treatment processes within the Stimela environment. *Water Sci. Technol.: Water Supply*, 2(1), 87-93.
- van Schagen, K.M., Babuška, R., Rietveld, L.C., Wuister, J. and Veersma, A.M.J. (2005). Modeling and predictive control of pellet reactors for water softening. *Proceedings of 16th IFAC World Congress*, Prague, Czech Republic, 2005.

van Schagen, K.M., Babuška, R., Rietveld, L.C. and Baars, E.T. (2006). Optimal flow distribution over multiple parallel pellet reactors: a model-based approach. *Water Sci. Technol.*, 53(4-5), 493-501.

2. Objectives for integrated optimization of drinking water treatment plants

In order to perform an integrated optimization of operation of a drinking water treatment plant, explicit objectives for the operation of drinking water production have to be identified and defined. In this chapter, what these objectives should be is discussed. Three possible objectives were assessed: environmental impact, costs and water quality. Data from drinking water treatment plant Weesperkarspel of Waternet (the water cycle company for Amsterdam and surrounding areas) were used for a case study. It is concluded that the objective for integrated optimization for operation of drinking water treatment plants should be the improvement of water quality. The environmental impact and the financial impact of the operation of drinking water production should be regarded as constraints, not as objectives for operational optimization.

Introduction

In the past twenty years, drinking water research at Waternet (the water cycle company for Amsterdam and surrounding areas) was carried out for improvement of the water quality, sustainability and the robustness of their two drinking water treatment plants using surface water. One of the improvements realized was the abolition of the use of chlorine for main disinfection through a multi-barrier approach and through prevention of regrowth by distribution of biologically stable drinking water (Rook et al., 1982; van der Kooij et al., 1999). The introduction of biological activated carbon (BAC) filtration in combination with a pre-oxidation by ozone (Graveland, 1996) had a positive effect on the removal of natural organic matter (NOM). In addition ozone forms a barrier for a number of pathogenic microorganisms and BAC filtration forms an efficient barrier for pesticides such as bentazon (van der Hoek et al., 2000). In the pre-treatment of surface water, coagulation was introduced for the removal of phosphate preventing the growth of algae in reservoirs, resulting in an improvement in the disinfection by solar light,

and in nitrification in reservoirs (van der Veen et al., 1987). In addition, the NOM measured as dissolved organic carbon (DOC) was decreased during coagulation. In 1987 a softening process was introduced for producing drinking water with a total hardness of 1.5 mM (Graveland et al., 1983). Research, thus, generally focused on selecting new processes and on the optimization of individual process steps.

The quality of surface water varies over the seasons (temperature, algae concentration, DOC character and concentration, number concentration of micro-organisms), due to long-term trends (increase in the concentration of pesticides, hormones, chloride, bromide) and also as a result of natural events such as heavy rainfall or ice formation and process-related events such as the removal of sludge. In the current situation the operation of treatment plants is optimized on the basis of “rules of thumb” and operator knowledge and experience. The quality of drinking water is thus influenced by day-to-day decisions of individual operators (Bosklopper et al., 2004). In addition, choices for operation of an individual process may have a negative effect on one or more subsequent steps. It can be concluded that decisions of an integrated nature can be complex and difficult to make.

Because of the complexity of the relationships between and the effects of the different processes on the water quality parameters, an integrated model of the drinking water treatment plant can best determine the optimal settings for operation. It is assumed that an integrated approach to the treatment plant with model-based control, that takes into account the quality variations in surface water, leads to a more stable and efficient treatment with a better quality of the drinking water produced. In order to perform an integrated optimization of operation of a drinking water treatment plant, explicit objectives for optimization have to be identified and defined. In this study, what these objectives should be with respect to water quality, environmental impact and costs are discussed. Drinking water treatment plant Weesperkarspel (WPK) and its pre-treatment Loenderveen (LNV) of Waternet were used for a case study.

Materials and methods

Drinking water treatment plant Weesperkarspel

The drinking water treatment plant WPK receives pre-treated water from LNV for the production of drinking water (Figure 1). The raw water mainly consists of

seepage water from the Bethune polder, sometimes mixed with Amsterdam-Rhine Canal water. At LNV the raw water is coagulated with ferric chloride (FeCl_3) and flocs are removed in horizontal settling tanks, resulting in the removal of phosphate, DOC, suspended solids and heavy metals. The quality of the water further improves due to sedimentation, nitrification of ammonium, biodegradation, and other self-purification processes in a lake-water reservoir of 130 hectares during a retention time of about 100 days. The remaining ammonium, suspended solids and algae are removed during rapid sand filtration before the water is transported over 10 kilometers to the WPK treatment plant without chlorination.

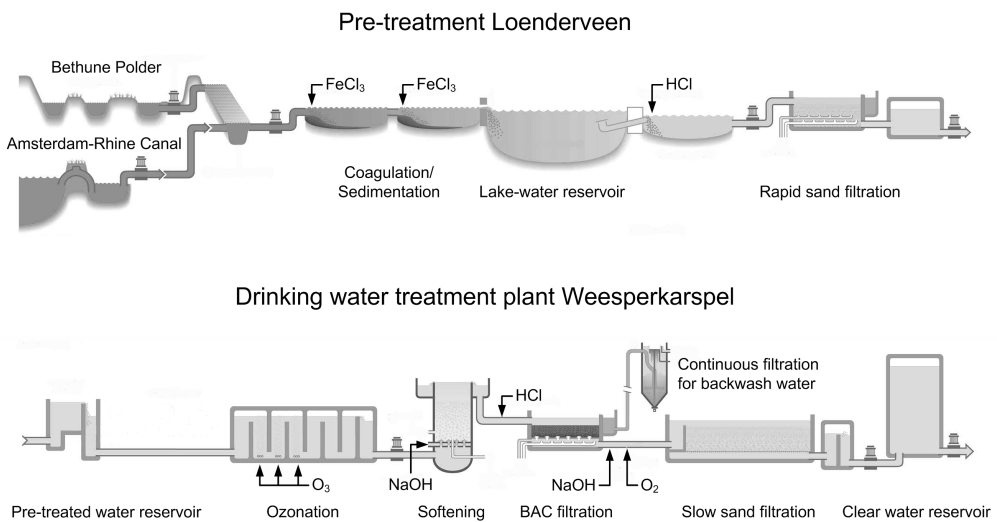


Figure 1 Process scheme of pre-treatment at LNV and drinking water treatment plant WPK

The first process at the treatment plant WPK is ozonation for disinfection and oxidation of NOM, which results in an increase in the biodegradability of the organic matter. Thereafter, pellet reactors are used to reduce hardness (softening) and BAC filtration is applied to remove NOM and pesticides. The last step in the treatment is slow sand filtration for further nutrient removal and reduction of suspended solids. This process is also the second important barrier in the treatment against pathogens and is especially important for removing persistent pathogens with low susceptibility to ozone (e.g., *Cryptosporidium*). Drinking water is transported and distributed without residual chlorine.

Water quality assessment

The main objectives of drinking water treatment plants are to produce safe drinking water for consumption (without pathogenic micro-organisms and toxic compounds), to produce attractive drinking water (free from taste, odor, and color), and to avoid the accumulation of solids, corrosion, and regrowth of bacteria in the distribution and transport pipelines (van Dijk and van der Kooij, 2004). This means that the water quality assessment has to incorporate microbiological safety, toxicity, chemical stability, and biological stability of the water.

To determine the microbiological safety of the water, the disinfection at WPK can be assessed. In separate studies it was concluded that the disinfection for viruses, *Giardia*, *Cryptosporidium*, and *Campylobacter* is sufficient (Dullemont 2006a,b,c).

For toxicity, the number and amount of organic micro-pollutants and disinfection by-products can be assessed. In the case of WPK the influent organic micro-pollutant concentrations were under the detection limit. A potential disinfection by-product at WPK is bromate, formed during ozonation of bromide-containing waters (von Gunten, 2003). The bromate concentration at WPK is less than 1 µg/l due to the relatively low ozone dosages (1.7 mg-O₃/l is dosed when water temperature is above 12°C and 2.2 mg-O₃/l is dosed when water temperature is below 12°C) in comparison with the concentrations of NOM (DOC concentration before ozonation is 5-7 mg-C/l).

Drinking water is chemically stable when the limestone carbonic acid equilibrium is approached. The commonly used parameter for chemical stability is the saturation index (SI). The SI is a function of pH, temperature, alkalinity, calcium concentration and ionic strength. At WPK it is influenced by sodium hydroxide (NaOH) and hydrogen chloride (HCl) dosages, by softening, and by biological removal of NOM, which results in the formation of carbon dioxide (CO₂).

The NOM in natural waters is a mixture of organic components with different molecular weights (MW). The biological stability of drinking water is determined by the amount of biodegradable organic matter in the water, which consists of low MW acids. It can be measured by the concentration of assimilable organic carbon (AOC). UV absorbance at 254 nm (UVA₂₅₄), expressed as the absorbance per meter of path length (1/m), is sensitive to unsaturated bonds. In natural water most unsaturated bonds are present in NOM as aromatic carbon, and it was found that

the increase in AOC during ozonation is a function of the decrease in UVA_{254} (van der Kooij et al., 1989). AOC, DOC, and UVA_{254} were assessed for determining biological stability. In order to assess the character of NOM, the specific UV absorbance (SUVA) defined as UVA_{254} divided by DOC concentration ($(1/m)/(mg-C/l)$) was also calculated (see Table 1).

Table 1 Guidelines on character of NOM (Edzwald and Tobiason, 1999)

SUVA ($(1/m)/(mg-C/l)$)	Composition
~ 4 or greater	Mostly aquatic humics, high hydrophobicity, high MW
2-4	Mixture of aquatic humics and other NOM, mixture of hydrophobic and hydrophilic NOM, mixture of MWs
<2	Mostly non-humics, low hydrophobicity, low MWs

The water quality assessments were performed by plotting the changes in water quality parameters throughout the drinking water treatment plant. The data used were from laboratory measurements from 2000 to 2005. Since UVA_{254} and DOC are not always measured on the same day, and UVA_{254} is measured less frequently than DOC, the UVA_{254} is determined by interpolation on the days DOC is measured. With the interpolated UVA_{254} data the SUVA is calculated.

Environmental assessment

Life cycle assessment (LCA) is a well-established methodology defined by the International Organisation for Standardisation in the ISO14040 Standard (ISO, 2000). LCA is developed to calculate the environmental impact of products or processes along its entire life cycle. In the present study, the LCA methodology is used to assess the operation of drinking water treatment, one of the stages of the life cycle. The functional unit is one cubic meter of drinking water produced ($1 m^3$).

This study considered the four stages of LCA methodology (Barrios et al., 2006):

1. Goal and scope definition; determine the environmental impact resulting from the current operation at LNV and WPK.
2. Inventory analysis; site specific data are used from 2002 and data from databases included in SimaPro 5.1.
3. Impact assessment; SimaPro 5.1 is used with the Eco-Indicator 99 method where a single score is obtained in EcoPoints/ m^3 for each single unit process and material, reflecting the various impacts (Goedkoop and Spriensma, 2000).
4. Interpretation of the results.

Financial assessment

For the financial assessment the methodology for life cycle costing (LCC) as proposed by the Department of Public-Works and Services of New South Wales, Australia (DPWS-NSW, 2001), was taken as a basis. The four stages of the life cost-planning phase of the LCC study were carried out:

1. Planning the LCC analysis.
2. Selection/development of an LCC model and inventory analysis to collect the necessary data.
3. LCC model application.
4. Documenting and reviewing the LCC results.

The principles underlying these stages are similar to those of the LCA method. The LCC methodology is used to only assess the operation of drinking water treatment. It is based on materials, energy flows, and other direct costs of production, such as maintenance and direct labor. As a consequence, investment and demolition costs are not taken into account.

Results

Water quality assessment

The water quality parameters for the assessment of the chemical stability are shown in Figure 2. The pH of the raw water is 7.5 on average. During coagulation, FeCl_3 is dosed and ferric hydroxide flocs are formed, resulting in a pH drop. In the lake-water reservoir, the CO_2 concentration decreases until equilibrium with the CO_2 concentration in air is reached. As a consequence the pH value rises to between 8.1 and 8.3 depending on the temperature, which ranges from 2°C to 23°C during the year. The influent calcium concentration is around 80 mg-Ca/l, with a maximum variation of ± 5 mg-Ca/l. In combination with the high pH, the water leaving the reservoir is supersaturated with calcium carbonate, this can be concluded from the saturation index (SI) which varies from 0.5 to 0.9 (see Figure 2, right). Due to the production of CO_2 by biological activity in the rapid sand filters, the pH decreases. To prevent calcium carbonate precipitation during transport to WPK, HCl is dosed after the reservoir, which results in a drop in pH. Subsequently, the pH influences the bromate formation during ozonation and ozone decay. In the softening process, calcium is removed by dosing NaOH, to make the water supersaturated with calcium carbonate that crystallizes on pellets in a fluidized bed reactor. After softening, HCl is dosed to prevent precipitation of calcium carbonate

in the BAC filters. Due to CO_2 production in the BAC filters, the pH decreases. The NaOH dosage applied after the BAC filters increases the pH in order to make the water supersaturated with calcium carbonate to prevent corrosion of the distribution network. In Figure 2, it is observed that the variation in the pH and in the SI is greater after each NaOH and HCl dosage and the variation becomes smaller in the water reservoir and in the filtration steps.

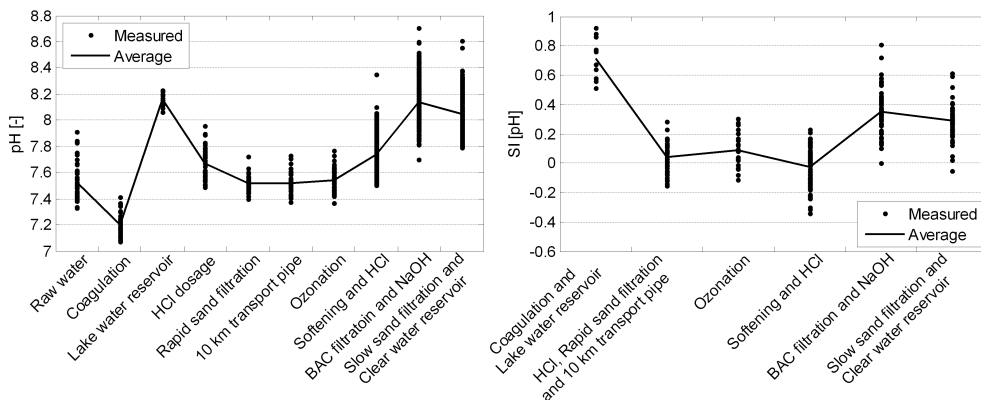


Figure 2 Water quality assessment for chemical stability: (i) pH (left); (ii) SI (right); data from 2004

The water quality parameters for the assessment of the biological stability are shown in Figures 3 and 4. During coagulation DOC is removed. The decrease in UVA_{254} during coagulation is higher than the decrease in DOC, which results in a decrease in SUVA. This can be explained by the fact that the part of NOM that is removed during coagulation contains the highest amount of aromatic carbon, which indicates that mainly large organic components ($\text{MW} > 1000 \text{ g/mol}$) are removed. In the reservoir and rapid sand filters, the concentration of DOC also decreases. This time the decrease is proportional to the UVA_{254} , so the SUVA stays constant and there is no observed change in the character of NOM.

During ozonation no DOC is removed, but the character of NOM is changed, as can be concluded from the decrease in the SUVA. Due to the attack of double bonds in NOM, the UVA_{254} decreases and large organic components are broken down into smaller organic components. Consequently, the AOC concentration increases.

During softening, the DOC concentration decreases due to biological activity in the pellet reactors. The decrease is approximately 0.40 mg-C/l. The decrease in AOC concentration is approximately 0.05 mg-C/l. Consequently, the part of the NOM that is biodegraded during softening is at least 8 times greater than the part of biodegradable organic matter measured as AOC.

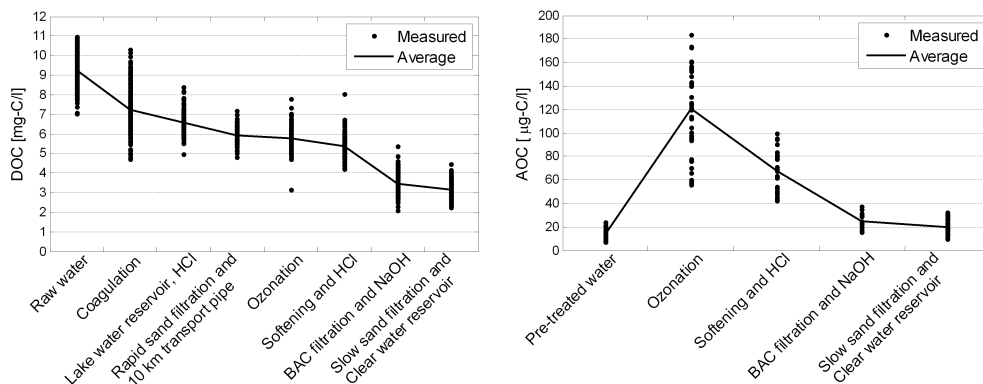


Figure 3 Water quality assessment for biological stability: (i) DOC (left); (ii) AOC (right); data from 2000 to 2005

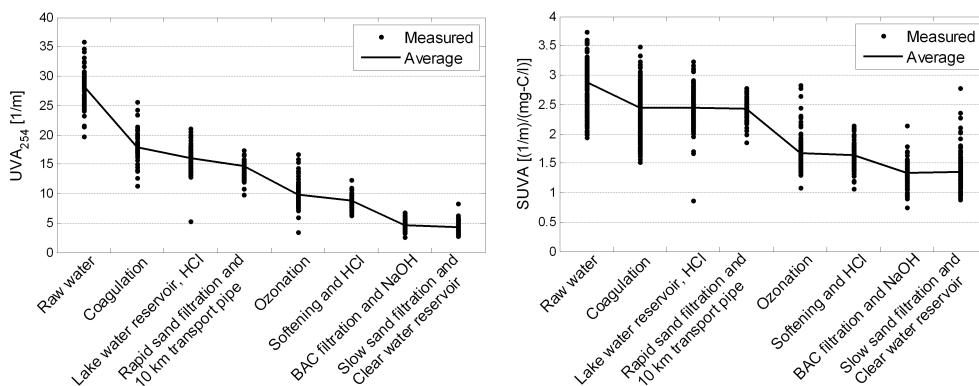


Figure 4 Water quality assessment for biological stability: (i) UVA₂₅₄ (left); (ii) SUVA (right); data from 2000 - 2005

During BAC filtration there is a decrease in the concentrations of DOC and AOC due to biological activity with additional NOM adsorbed onto the activated carbon. From the decrease in SUVA, it could be concluded that more high MW organic

components are removed than low MW organic components. This seems in contradiction with the fact that during BAC filtration mainly low MW organic carbon is removed biologically. A hypothetical explanation for this apparent contradiction can be given based on the structural concept of a humic acid molecule as proposed by Schulten and Schnitzer (1993), Figure 5 (left), and the structural concept of a fulvic acid molecule as proposed by Stevenson (1982), Figure 5 (right).

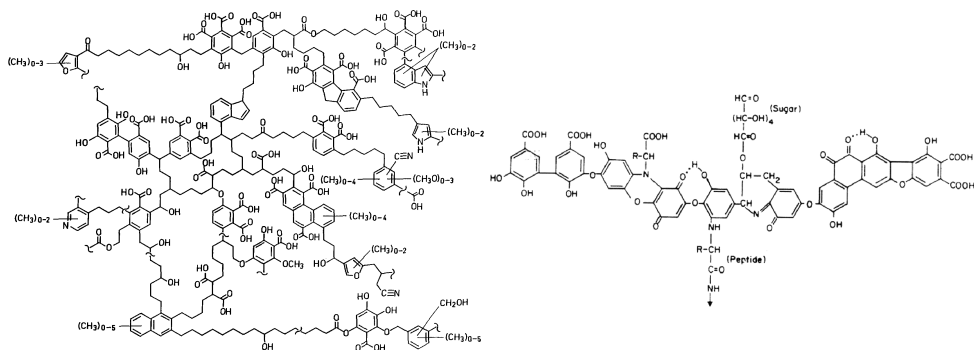


Figure 5 Structural concept for: (i) humic acid (Schulten and Schnitzer, 1993) (left); (ii) fulvic acid (Stevenson, 1982) (right)

From the literature it is known that biodegradable organic matter formed during ozonation consists of aldehydes, ketones, ketoacids, and carboxylic acids. Examples of this are acetaldehyde, glyoxal, methylglyoxal, glyoxalic acid, acetone, pyruvic acid, formic acid, acetic acid and oxalic acid (Glaze et al., 1989; van der Kooij et al., 1989; Carlson and Amy, 1997; Melin and Ødegaard, 2000; Richardson et al., 2002). Based on the MWs of these compounds that range from 44 g/mol to 90 g/mol, it is assumed that the average MW is 60 g/mol. Hammes et al. (2006) have proposed a mechanism for phenol oxidation leading to the formation of glyoxalic acid, formic acid and oxalic acid. Based on this mechanism it is assumed that biodegradable organic molecules are formed from aromatic carbon rings with a functional group (e.g., carboxyl and/or hydroxyl group). The attacked aromatic carbon rings can be either part of the humic or fulvic acid molecule, or can be simple aromatic rings with functional groups (e.g., phenol, benzoic acid and salicylic acid) that are detached from the humic or fulvic acid molecule and have an assumed average weight of 140 g/mol. Further, it is assumed that two aromatic carbon-carbon double bonds have to be broken in the humic or fulvic acid molecule to form either a biodegradable organic molecule or a simple aromatic compound.

From the structural concepts in Figure 5, it can be derived that the humic acid molecule has 73 aromatic carbon-carbon double bonds per molecule and an MW of 5540 g/mol and the fulvic acid molecule has 25 aromatic carbon-carbon double bonds per molecule and an MW of 1510 g/mol. From Figure 4 (left) it is observed that the UVA_{254} decreases by one third during ozonation. It is assumed that the entire UVA_{254} decrease is due to aromatic carbon-carbon double bonds broken down in the humic and fulvic acid molecules, leading to equal formation of biodegradable organic molecules and simple aromatic compounds. Consequently, 24 aromatic double bonds are broken down in the humic acid molecule, which gives 6 biodegradable organic molecules (0 carbon-carbon double bonds) and 6 simple aromatic compounds (6 times 3 carbon-carbon double bonds). The MW of the humic acid decreases 6 times 60 g/mol and 6 times 140 g/mol to 4340 g/mol and the carbon-carbon double bonds decrease from 73 to minus 24, and minus 18, leaving 31. The simple aromatic compounds have 3 carbon-carbon double bonds with a molecular weight of 140 g/mol. Thus, the remaining humic acid molecules have substantially less aromatic carbon-carbon double bonds per gram compared to the formed simple aromatic compounds. The same applies to the fulvic acid molecule. During BAC filtration mainly low MW organic carbon is removed. A higher removal of the simple aromatic compounds with a higher carbon-carbon double bond content per gram than the humic and fulvic acid molecules will lead to the observed decrease in SUVA during BAC filtration. So, the apparent contradiction can be explained by the formation of small organic compounds during ozonation, containing more aromatic carbon-carbon double bonds per unit of weight compared to humic and fulvic compounds.

During slow sand filtration a small amount of AOC and DOC is removed without changing the character of NOM. The removal of NOM can result in a decrease in the copper and lead uptake from the distribution network (Broo et al., 1998). The character of NOM is, in this respect, of importance and ozonation has a positive influence on that character because it decreases the surface activity of NOM, which has a clear association with dissolving lead in water according to Korshin et al. (2005). In the case of WPK, these effects are not yet quantified and the targeted value for the effluent DOC concentration is 3 mg-C/l (\pm 1 mg-C/l).

Environmental assessment

The most relevant data from the inventory used for the LCA of the operation at WPK is given in Table 2. The total environmental impact calculated per process

(Figure 6) is found to be 8.61 milli-Eco-points/m³ of drinking water. It can be observed that softening is the main contributor to operational environmental impact. Further analysis discloses that the NaOH dosage accounts for 79.5% of the softening impact and the HCl dosage for 7.2%. The second largest contributor is coagulation; 71.3% of its impact comes from the use of FeCl₃. The third largest contributor is BAC filtration; the use of steam, as the oxidant to activate and regenerate carbon, is responsible for 38.3% of its environmental impact and the NaOH dosage after BAC filtration for 30.9%. Eighty percent of the impact of the lake-water reservoir is due to HCl dosing. The total impact of the chemical dosages of NaOH, HCl and FeCl₃ is 5.81 milli-Eco-points/m³, which is 67.5% of the total environmental impact.

Table 2 Selection of the inventory data for the LCA

Parameter	Value	Unit
Raw water intake		
Energy used	0.01155	kWh/m ³
Coagulation and settling		
FeCl ₃ used (as 100% concentration)	0.03956	kg/m ³
Amount of dry sludge produced	0.03588	kg/m ³
Lake-water reservoir		
HCl used (as 100% concentration)	0.00942	kg/m ³
Pumping from lake		
Energy used	0.02296	kWh/m ³
Rapid sand filtration		
Amount of sludge produced	0.01408	kg/m ³
Pumping to WPK		
Energy used	0.02870	kWh/m ³
Ozonation		
Energy used	0.05052	kWh/m ³
Softening		
Energy used in pumping	0.15970	kWh/m ³
Sand transport weight times distance (Australia)	0.19410	10 ³ kg*km/m ³
NaOH used (as 100% concentration)	0.04229	kg/m ³
Number of pellets produced	0.08585	kg/m ³
HCl used (as 100% concentration)	0.00551	kg/m ³
BAC filtration		
New activated carbon	0.00443	kg/m ³
Steam used in AC regeneration	0.03661	kg/m ³
NaOH used (as 100% concentration)	0.00746	kg/m ³
Slow sand filtration		
Energy used	0.02413	kWh/m ³
Amount of sand replaced	0.01614	kg/m ³
Drinking water storage and distribution	Not considered	
Total volume of drinking water produced	27,873,000	m ³ /year

The pumping phases and ozonation, which are both high power-consuming processes, have only a modest environmental impact because Waternet uses 100% green energy produced from hydropower and biogas. Mohapatra et al. (2002) found that for the Leiduin drinking water treatment plant of Waternet a reduction of environmental impact up to 73% could be achieved by changing from conventional energy sources to green energy. With as a result that, Waternet changed from conventional to green energy. If conventional energy sources were still used at WPK, the environmental impact of the total treatment would be 57% higher (Barrios et al., 2006).

When construction and demolition would be included, the distribution of the environmental impact over the treatment processes would have been different. This is caused by the differences in building volumes, among others. For instance, softening is operated at average flow rates of around 70 m/h, and BAC filtration is operated at average flow rates of around 3.3 m/h. This represents a 21-fold difference in the needed surface area between softening and BAC filtration and thus large differences between building volumes and the materials used. However, this impact is spread over a lifetime of usually 30 years or more. Since this research focuses on optimization of operation of existing treatment plants, environmental impact of construction and demolition are not considered. However, for the design of new processes construction and demolition should be taken into account.

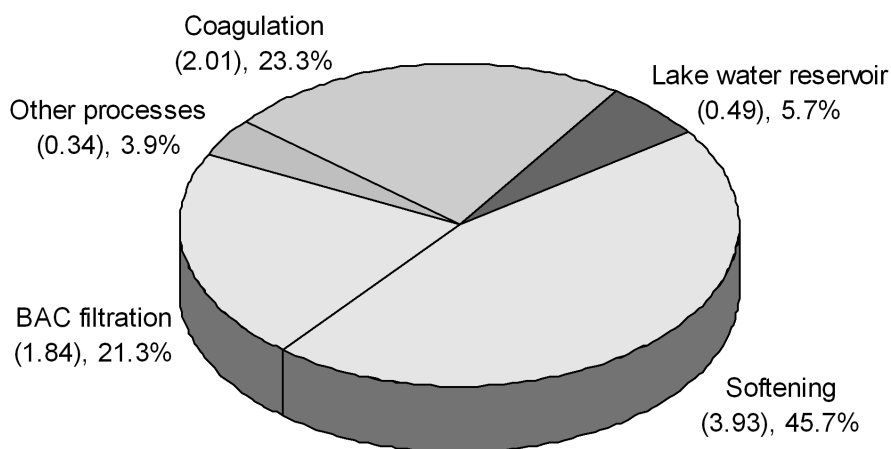


Figure 6 Contributions to environmental impact from processes of WPK: (as 10^{-3} EcoPoints/m³), as percentage of the total environmental impact

Financial assessment

The most relevant data from the inventory used for the LCC study of the operation at WPK are given in Table 3. The financial impact is 0.1259 €/m³ or 3.5 million €/y. Figure 7 presents the financial impact per process at LNV and WPK. BAC filtration is the main contributor, with the cost of purchasing new activated carbon and the regeneration of activated carbon being 62.0% of the financial impact and the dosage of liquid oxygen, 18.1%. The liquid oxygen is dosed when the oxygen concentration of the BAC filtration effluent is below 6 mg-O₂/l, typically when the water temperature is above 15°C. The second largest contributor is softening; within softening 60.7% of the financial impact is from the costs of NaOH dosage. In ozonation the financial impact is mainly due to energy (53.6%). For coagulation the main contributor is the purchase of FeCl₃, which amounts to 44.1% of the impact of coagulation. The total financial impact of the chemical dosages NaOH, HCl, FeCl₃ and O₂ is 0.0454 €/m³; this is 36.0% of the total financial impact. Energy accounts for 17.1% (0.0216 €/m³) of the total financial impact, labor and maintenance account for 22.1% (0.0279 €/m³). The remainder 24.7% is due to new activated carbon, regeneration of activated carbon and garnet sand for pellet softening.

When investment costs and demolition costs are also considered, the distribution of the financial impact over the treatment processes will change because of the differences in these costs for the different treatment processes.

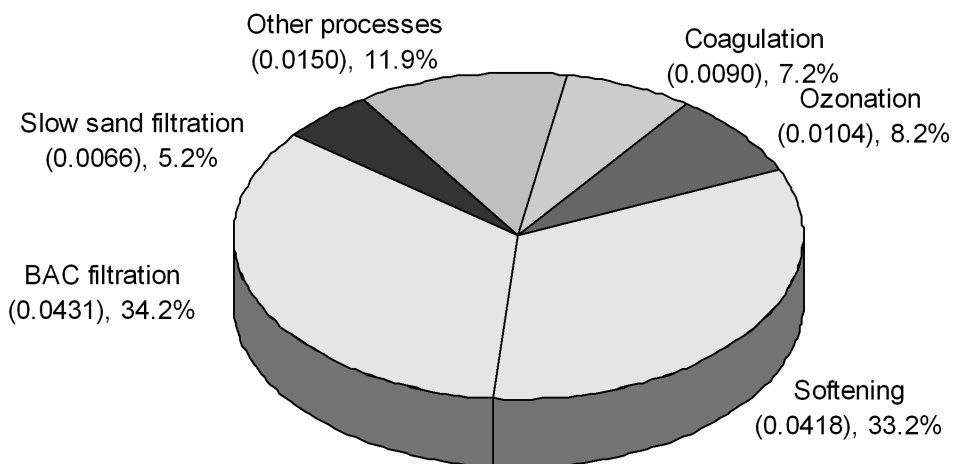


Figure 7 Contributions to financial impact from processes at WPK: (as €/m³), as percentage of the total financial impact

Table 3 Selection of the inventory data for the LCC study

Parameter	Value	Unit
Raw water intake		
Energy used	0.0012	€/m ³
Coagulation and settling		
FeCl ₃ used (as 100% concentration)	0.0039	€/m ³
Maintenance	0.0025	€/m ³
Lake-water reservoir		
HCl used (as 100% concentration)	0.0023	€/m ³
Labor time	0.0015	€/m ³
Pumping from lake		
Energy used	0.0025	€/m ³
Rapid sand filtration		
Labor time	0.0015	€/m ³
Maintenance	0.0014	€/m ³
Pumping to WPK		
Energy used	0.0031	€/m ³
Ozonation		
Energy used	0.0056	€/m ³
Labor time	0.0024	€/m ³
Maintenance	0.0024	€/m ³
Softening		
Energy used	0.0057	€/m ³
Garnet sand used	0.0024	€/m ³
NaOH used (as 100% concentration)	0.0254	€/m ³
HCl used (as 100% concentration)	0.0014	€/m ³
Labor time	0.0036	€/m ³
Maintenance	0.0034	€/m ³
BAC filtration		
Purchase of Activated Carbon	0.0072	€/m ³
Regeneration Activated Carbon	0.0195	€/m ³
NaOH used (as 100% concentration)	0.0045	€/m ³
Liquid O ₂ used	0.0078	€/m ³
Labor time	0.0030	€/m ³
Slow sand filtration		
Energy used	0.0027	€/m ³
Maintenance	0.0016	€/m ³
Storage and distribution	Not considered	
Total volume of drinking water produced	27,873,000	m ³ /year

Discussion

Objectives for integrated optimization of operation

Considering quality, environmental, and financial impact of drinking water on global scale, the greatest social, environmental, and economical threat is the use of bottled water for drinking instead of tap water. Bottled water will be used when tap water quality cannot be guaranteed or consumers do not trust the tap water quality or bottled water has a better image. In 2005 the global bottled water consumption

was 163.9 billions of liters, with an increase of 52% from 2000 to 2005 (Rodwan, 2006) and is consumed mainly in developed countries where tap water is of good quality and complies with stringent regulations. In Figure 8 the 15 countries with the greatest consumption of bottled water per person per year and the Netherlands are presented. The global annual consumer expenditure for bottled water approaches 100 billion USD (Gleick, 2004), so the mean price for a liter of bottled water is approximately 0.60 USD. According to Komives et al. (2005), the mean price of tap water in developed countries is 1.04 USD per m³. Bottled water costs on average almost 600 times more than tap water. The difference varies per country due to differences in the price of tap water and differences in the price of bottled water, which is, for a large part, determined by the travel distance from the water bottling site to the consumer. In the Netherlands for example, bottled water is on average approximately 150 to 200 times more expensive than tap water (CBS, 2007). In the USA this is a few thousand times (Franklin, 2006) up to 10,000 times (Maxwell, 2005) more expensive.

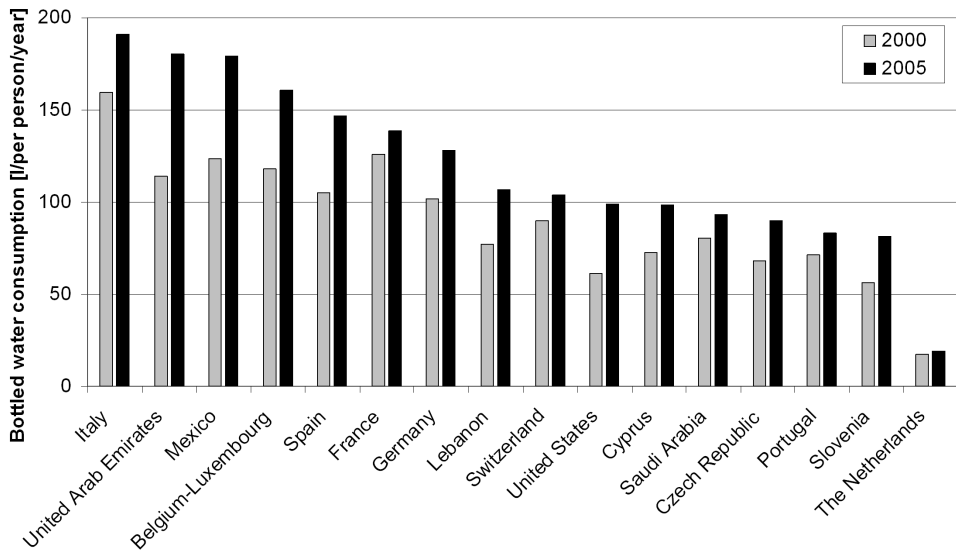


Figure 8 Bottled water consumption per person in 2000 and 2005 for the 15 countries with the greatest consumption per person (Rodwan, 2006) and the Netherlands (CBS, 2007)

One of the targets of the United Nations Millennium Development Goals (MDG) is to halve the proportion of people without sustainable access to safe drinking water by 2015 (Annan, 2000). The current investment in safe drinking water in the

developing world is 14 to 16 billion USD annually. To meet the MDG target, a doubling of this investment would be required (Toubkiss, 2006). This is in contrast with the annual 100 billion USD expenditure for bottled water in developed countries, which have access to safe tap water. When tap water was consumed instead of bottled water, the costs would have been only 0.2 billion USD per year.

Jungbluth (2006) assessed the environmental impact of tap water and bottled water. In that study the entire life cycle of tap and bottled water was traced from water extraction to consumption. This included water extraction, treatment, bottling including packaging, distribution via wholesale and retail channels, transportation to consumers' homes, distribution via water pipes including the requisite infrastructure and treatment at the consumption site (e.g., soda water maker). From a direct comparison of tap water with bottled water, Jungbluth found that the environmental impact of bottled water was 90 to more than a 1000 times greater than the environmental impact of tap water. The difference became more pronounced when the transport distance of the bottled water to the customer increased. When comparing carbonated water, Jungbluth found that carbonated bottled water had an environmental impact that was 5 to 8 times greater than that of "home" carbonated tap water. The number of plastic bottles thrown away in the US alone is more than 60 million per day of which 17% was recycled in 2004 (Franklin, 2006).

Based on these social, environmental and economical considerations, governments and drinking water supply companies should aim for an impeccable tap water quality and a reliable, healthy, and environmentally sound image of tap water in order to at least stop the increase in bottled water use. This determines the objectives for the optimization for operation of drinking water treatment plants.

The drinking water consumption in Amsterdam is 156 liters per person per day, so the environmental impact from drinking water production is 0.490 Eco-points per person per year. A one-way car trip from the Delft University of Technology to Amsterdam city center, which is 64 km, generates 0.960 Eco-points, almost twice as much (Barrios et al., 2006). A decrease of 10% in environmental impact due to optimization of the operation is equivalent to a decrease in car mileage of approximately 3 km per drinking water consumer in Amsterdam per year. Total costs of drinking water at Waternet are approximately 1.50 €/m³. The operational costs for production were determined to be 0.1259 €/m³. This is less than 10% of

the total costs that include also water distribution, investment costs, taxes, salaries of office personnel etc. A decrease in operational costs of 10% due to optimization would thus lead to a decrease in costs of less than 1% for consumers. When taking water quality, environmental impact and costs into account, it can be concluded that emphasis must be laid on maintaining a high drinking water quality; improvement of water quality is the most important objective for optimization of the operation of drinking water treatment plants. In addition, environmental and financial impacts will benefit from improvements in water quality since improvement of water quality also involves the optimal use of chemical dosages at minimum levels, and chemical dosages are the main contributors to the environmental impact and, for a large part, also to the financial impact.

However, there are technical and political constraints to the degree of optimization. For instance, in theory regrowth in the distribution system could be minimized by totally removing the NOM. A decrease in NOM can be achieved by more frequent regeneration of the activated carbon in the BAC filters. But, due to technical constraints, BAC filtration cannot remove all NOM, not even when it would be regenerated every day. There is a point when it would be more practical, economical and environmentally friendly to make changes to the design or treatment concept of the drinking water treatment plant instead of further optimizing it. The maximum price for drinking water is a political constraint.

At WPK, chemical stability, biological stability, and disinfection are the most important water quality objectives for integrated optimization. Toxicity (e.g. bromate) is in the current operation not a problem but should be a point of constant attention. For chemical stability the SI should be used as a parameter for optimization. The pH will change throughout the year, mainly due to changes in the water temperature and should be within preset boundaries for the different processes. For biological stability the water quality parameters for optimization should be AOC and DOC. For disinfection the water quality parameters for optimization should include selected indicators for pathogens.

Because the SI, AOC, DOC, and pathogen concentrations are influenced by multiple processes and influence multiple processes, an integrated approach to these parameters is necessary. Because of the complexity of the relationships and the effects on these parameters by changes in the operational settings, the settings can best be evaluated by an integrated model. For SI, an integrated pH model is

built including all chemical dosages influencing SI. For AOC, DOC, and pathogens, ozonation plays a key role in integrated optimization. Ozonation is influenced by coagulation, the reservoir with HCl dosage and the rapid sand filtration by changes in pH and DOC concentration. Ozonation also influences the softening and the BAC filtration by producing AOC. Ozonation is the only process in which disinfection can be actively influenced by means of the ozone dosage. Ozonation has effects on the toxicity because bromate can be formed. Therefore, research on integrated optimization and modeling with respect to disinfection, biological stability, and toxicity is focused on ozonation.

Conclusions

The environmental impact of the operation of drinking water production is relatively low compared to other activities, such as driving a car. Decreasing environmental impact of operation is possible without impact on water quality, for instance by changing from conventional energy sources to green energy. The operational costs of drinking water production are relatively low compared to the total costs of drinking water that include also water distribution, investment costs, taxes, salaries of office personnel etc. Therefore, the possible reduction of the total costs by changes in the operation of drinking water production is small. Based on social, environmental and economical considerations, governments and drinking water supply companies should aim for an impeccable tap water quality and a reliable, healthy, and environmentally sound image of tap water in order to at least stop the increase in bottled water use. Based on these considerations it is concluded that the objective for integrated optimization for the operation of drinking water treatment plants should be the improvement of water quality and not a priori reduction of environmental impact or costs of production of drinking water.

Acknowledgement

This research was carried out as part of the Promicit project, a cooperation of Waternet, Delft University of Technology, DHV B.V., and ABB B.V. and was subsidized by SenterNovem, agency of the Dutch Ministry of Economic Affairs. The aim of the project was to achieve a breakthrough in drinking water quality control by developing an integrated model of the total water treatment and using this model as a basis for operation.

Nomenclature

AOC	assimilable organic carbon
BAC	biological activated carbon
CO ₂	carbon dioxide
CT	ozone exposure ((mg-O ₃ /l)*min)
DOC	dissolved organic carbon
FeCl ₃	ferric chloride
HCl	hydrogen chloride
LCA	life cycle assessment
LCC	life cycle costing
LNV	pre-treatment plant Loenderveen of Waternet
MW	molecular weight
NaOH	sodium hydroxide
NOM	natural organic matter
SI	saturation index
SUVA	specific UV absorbance defined as UVA ₂₅₄ divided by DOC concentration ((1/m)/(mg-C/l))
UVA ₂₅₄	UV absorbance at 254 nm (1/m)
Waternet	water cycle company for Amsterdam and surrounding areas
WPK	drinking water treatment plant Weesperkarspel of Waternet

References

- Annan, K.A. (2000). *We the peoples : The role of the United Nations in the 21st century*. United Nations, New York, USA.
- Barrios, R., Siebel, M.A., van der Helm, A.W.C., Bosklopper, Th.G.J. and Gijzen, H.J. (2006). Environmental and financial life cycle impact assessment of drinking water production at Waternet. *J. Clean. Prod.*, doi:10.1016/j.jclepro.2006.07.052.
- Bosklopper, Th.G.J., Rietveld, L.C., Babuška, R., Smaal, B. and Timmer, J. (2004). Integrated operation of drinking water treatment plant at Amsterdam Water Supply. *Water Sci. Technol.: Water Supply*, 4(5-6), 263-270.
- Broo, A.E., Berghult, B. and Hedberg, T. (1998). Copper corrosion in water distribution systems-the influence of natural organic matter (NOM) on the solubility of copper corrosion products. *Corros. Sci.*, 40(9), 1479-1489.

- Carlson, K. and Amy, G. (1997). The formation of filter-removable biodegradable organic matter during ozonation. *Ozone Sci. Eng.*, 19(2), 179-199.
- CBS (2007). *Centraal Bureau voor de statistiek (Statistics Netherlands)*. <http://www.cbs.nl>, CBS, Voorburg/Heerlen, the Netherlands (accessed 7 March 2007).
- DPWS-NSW (2001). *Life Cycle Costing : Guideline*. New South Wales Department of Public Works and Services, Government Asset Management Committee, Sydney, Australia.
- Dullemont, Y.J. (2006a). *QMRA Enterovirussen locatie Weesperkarspel over de jaren 2003 en 2004 (QMRA Enteroviruses location Weesperkarspel for the years 2003 and 2004)*. Report Waternet, Amsterdam, the Netherlands.
- Dullemont, Y.J. (2006b). *QMRA Cryptosporidium en Giardia locatie Weesperkarspel over de jaren 2003 en 2004 (QMRA Cryptosporidium and Giardia location Weesperkarspel for the years 2003 and 2004)*. Report Waternet, Amsterdam, the Netherlands.
- Dullemont, Y.J. (2006c). *QMRA Campylobacter locatie Weesperkarspel over de jaren 2003 en 2004 (QMRA Campylobacter location Weesperkarspel for the years 2003 and 2004)*. Report Waternet, Amsterdam, the Netherlands.
- Edzwald, J.K. and Tobiasson, J.E. (1999). Enhanced coagulation: US requirements and a broader view. *Water Sci. Technol.*, 40(9), 63-70.
- Franklin, P. (2006). Down the drain. *Waste Manag. World*, 7(5), 62-65.
- Glaze, W. H., Koga, M., Cancilla, D., Wang, K., McGuire, M. J., Liang, S., Davis, M. K., Tate, C. H. and Aieta, E. M. (1989). Evaluation of ozonation by-products from two California surface waters. *Am. Water Works Assoc. J.*, 81(8), 66-73.
- Gleick, P.H. (2004). *The World's Water 2004-2005 : The Biennial Report on Freshwater Resources*. Island Press, Washington DC, USA.
- Goedkoop, M. and Spriensma, R. (2000). *The Eco-indicator 99 : A damage oriented method for Life Cycle Impact Assessment*. Ministry of Housing, Spatial Planning and the Environment (VROM)/Pré Consultants, Amersfoort, the Netherlands.
- Graveland, A., van Dijk, J.C., Moel, P.J. de and Oomen, J.H.C.M. (1983). Developments in water softening by means of pellet reactors. *Am. Water Works Assoc. J.*, 75(12), 619-625.
- Graveland, A. (1996). Application of biological activated carbon filtration at Amsterdam Water Supply. *Water Supply*, 14(2), 233-241.

- Hammes, F., Salhi, E., Köster, O., Kaiser, H.P., Egli, T. and von Gunten, U. (2006). Mechanistic and kinetic evaluation of organic disinfection by-product and assimilable organic carbon (AOC) formation during the ozonation of drinking water. *Water Res.*, 40(12), 2275-2286.
- ISO (2000). *Environmental management – Life cycle assessment – Principles and framework*. International standard ISO14040:1997(E).
- Jungbluth, N. (2006). Vergleich der Umweltbelastungen von Hahnenwasser und Mineralwasser (Comparison of the environmental impact of drinking water versus bottled mineral water). *Gas Wasser Abwasser*, 2006(3), 215-219.
- Komives, K., Foster, V., Halpern, J. and Wodon, Q. (2005). *Water, electricity and the poor : Who benefits from utility subsidies?* The International Bank for Reconstruction and Development / The World Bank, Washington DC, USA.
- Korshin, G.V., Ferguson, J.F. and Lancaster, A.C. (2005). Influence of natural organic matter on the morphology of corroding lead surfaces and behaviour of lead-containing particles. *Water Res.*, 39, 811-818.
- Maxwell, S. (2005). Market outlook - water is cheap – ridiculously cheap! *Am. Water Works Assoc. J.*, 97(6), 38-41.
- Melin, E. S., and Ødegaard, H. (2000). The effect of biofilter loading rate on the removal of organic ozonation by-products. *Water Res.*, 34(18), 4464-4476.
- Mohapatra, P., Siebel, M.A., Gijzen, H.J., van der Hoek, J.P. and Groot, C. (2002). Improving eco-efficiency of Amsterdam Water Supply – a LCA approach. *J. Water Supply Res. Technol. AQUA*, 51(4), 217-227.
- Richardson, S.D., Simmons, J.E. and Rice, G (2002). Disinfection byproducts: The next generation. *Environ. Sci. Technol.*, 36(9), pp. 198A-205A
- Rodwan, J.G.Jr. (2006). Bottled water 2005: U.S. and international developments and statistics. *Bottled Water Reporter*, 2006(April/May), 18-25.
- Rook, J.J., Graveland, A. and Schultink, L.J. (1982). Considerations on organic matter in drinking water treatment. *Water Res.*, 16(1), 113-122.
- Schulten, H.-R. and Schnitzer, M. (1993). A state of the art structural concept for humic substances. *Naturwissen.*, 80(1), 29-30.
- Stevenson, F.J. (1982). *Humus chemistry*. Wiley, New York, USA.
- Toubkiss, J. (2006). *Costing MDG target 10: on water supply and sanitation: comparative analysis obstacles and recommendations*. Report World Water Council, 4th World Water Forum Mexico 2006.
- van der Hoek, J.P., Hofman, J.A.M.H. and Graveland, A. (2000). Benefits of ozone-activated carbon filtration in integrated treatment processes, including membrane systems. *J. Water Supply Res. Technol. AQUA*, 49(6), 341-356.

- van der Kooij, D., Hijnen, W.A.M. and Kruithof J.C. (1989). The effects of ozonation, biological filtration and distribution on the concentration of easily assimilable organic carbon (AOC) in drinking water. *Ozone Sci. Eng.*, 11, 297-311.
- van der Kooij, D., van Lieverloo, J.H.M., Schellart, J. and Hiemstra, P. (1999). Maintaining quality without a disinfectant residual. *Am. Water Works Assoc. J.*, 91(1), 55-63.
- van der Veen, C., Graveland, A. and Kats, W. (1987). Coagulation of two different kinds of surface water before inlet into lakes to improve the self-purification process. *Water Sci. Technol.*, 19(5/6), 803-812.
- van Dijk, J.C. and van der Kooij, D. (2004). Water Quality 21 research programme for water supplies in The Netherlands. *Water Sci. Technol.: Water Supply*, 4(5-6), 181-188.
- von Gunten, U. (2003). Ozonation of drinking water: Part II. Disinfection and by-product formation in presence of bromide, iodide or chlorine. *Water Res.* 37(7), 1469-1487.

3. Modeling of ozonation for dissolved ozone dosing¹

Experimental research was carried out for calibration and validation of a model describing ozone decay and ozone exposure (CT), decrease in UV absorbance at 254 nm (UVA_{254}), increase in assimilable organic carbon concentration and bromate formation. The model proved to be able to predict these parameters on the basis of the applied ozone dosage. The experimental ozone dosages ranged from 0.4 mg- O_3 /l to 0.9 mg- O_3 /l for natural water with a dissolved organic carbon concentration of 2.4 mg-C/l. The UVA_{254} was found to be an effective parameter for estimation of rapid ozone consumption for natural water under experimental conditions tested. The experimental setup consisted of a bench-scale plug flow reactor (approximately 100 l/h) with dissolved ozone dosing.

Introduction

Ozonation is applied in drinking water treatment plants for disinfection, oxidation of natural organic matter (NOM), degradation of organic micro pollutants and for color, taste and odor improvement. During ozonation the disinfection by-product bromate can be formed in bromide-containing waters (von Gunten, 2003). In many cases the legal standard for bromate limits the ozone dosage, thus limiting the efficacy of disinfection. In addition, during ozonation biological degradable organic matter is formed, which has a positive influence on NOM removal in biological filtration and a negative influence on the biological stability of water and on clogging of biological filters.

In order to be able to predict disinfection, bromate formation and assimilable organic carbon (AOC) formation, as a measure for biological degradable organic

¹ This chapter is based on: van der Helm, A.W.C., Smeets, P.W.M.H., Baars, E.T., Rietveld, L.C. and van Dijk, J.C. (2007). Modeling of ozonation for dissolved ozone dosing. *Ozone Sci. Eng.*, accepted for publication, February 2007.

matter, an ozonation model was developed. The purpose of the ozone model is to use it in integrated optimization and to use it for process control at drinking water treatment plants of Waternet (the water cycle company for Amsterdam and surrounding areas). For calibration and validation of the model parameters experimental research was carried out.

For the experiments water from Leiduin was used. Leiduin is one of two drinking water treatment plants of Waternet with a drinking water production of 70 million m³/y. At Leiduin pre-treated surface water is infiltrated in the dunes and subsequently treated by aeration, rapid sand filtration, ozonation, softening, biological activated carbon filtration and slow sand filtration.

Materials and methods

Bench-scale dissolved ozone plug flow reactor

Experiments were performed in a bench-scale dissolved ozone plug flow reactor (DOPFR) with a flow of approximately 100 l/h. The DOPFR concept is based on two flows, one small side stream with dissolved ozone that is mixed with a larger main stream. Subsequently contact time is created in a plug flow reactor. The side stream was pre-treated and consisted of Milli-Q[®] demineralised water, with a conductivity of around $5.5 \cdot 10^{-3}$ mS/m, produced with a Milli-Q[®] Academic A10. Milli-Q[®] was bromide free and had DOC concentrations in the order of 5 µg-C/l. Ozone for the side stream was produced from medical grade air using a Fisher ozone generator model 503. A counter current glass bubble column with a diameter of 40 mm and a height of 1.0 m was operated at 4 l/h to 10 l/h, 0.5 bar and 5°C to dissolve ozone in Milli-Q[®] water. High ozone concentrations up to 40 mg-O₃/l were reached without bromate formation. The dissolved ozone side stream was dosed through Teflon tubing by a flow-controlled pump to the main stream just before a static mixer, which provided instantaneous mixing. The main stream was fed by water from the effluent of the rapid sand filters of Leiduin with a flow of 96.7 l/h to 100.3 l/h. The plug flow reactor consisted of a 63.9 m PTFE tube of 8 mm internal diameter with 14 sampling points at different distances. During sampling the total flow was directed through the sampling point through a three-way valve. Figure 1 shows the experimental setup of the installation and Table 1 presents the tube dimensions.

Analysis methods

For the DOPFR experiments ozone was analyzed according to the indigo method described by Kiwa method LAM-062 v1.0 (Kiwa, 1999). Bromate and physical parameters were analyzed according to Dutch standard drinking water methods described in NEN standards. The UV absorbance measured at 254 nm is expressed as the absorbance per meter of cell length.

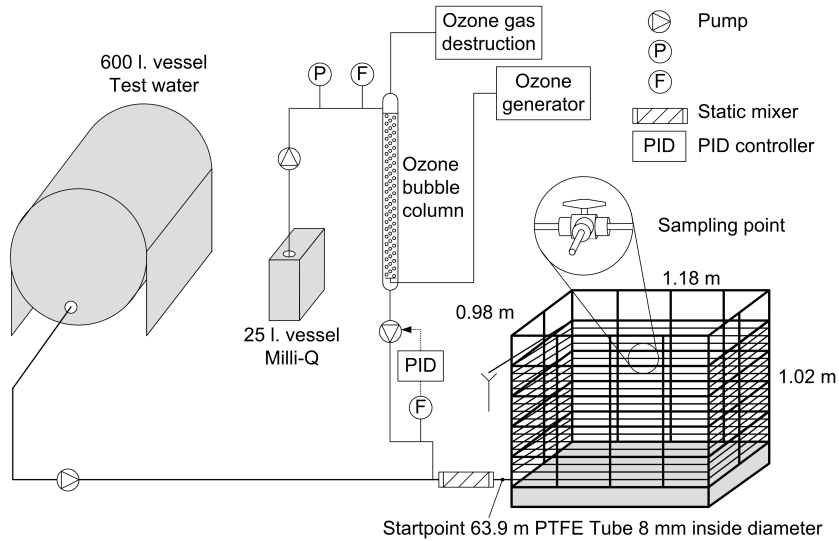


Figure 1 Experimental setup of the DOPFR

Table 1 Tube dimensions of the DOPFR

Sampling Point	Tube length (m)	Volume* (ml)	Hydraulic residence time based on volume** (s)
1	0.1	47	1.7
2	0.8	106	3.8
3	1.7	179	6.5
4	2.7	252	9.1
5	3.7	325	11.7
6	4.6	398	14.3
7	7.2	555	20.0
8	9.8	711	25.6
9	12.5	868	31.2
10	15.1	1024	36.9
11	23.2	1458	52.5
12	31.3	1892	68.1
13	47.4	2726	98.1
14	63.9	3576	128.7

* The volumes include the volumes of the sampling points

** Hydraulic residence times for a flow of 100 l/h

Experimental procedures for the DOPFR

The dissolved ozone production in Milli-Q[®] was run for one hour to reach steady state conditions in the bubble column. The effluent ozone in water concentration was set to the desired level by changing the ozone in gas concentration. Subsequently the side stream with high ozone concentrations was connected to the DOPFR. A sampling point, representing a chosen contact time, was opened and the system was allowed to refresh at least 3 times before taking samples. After sampling the DOPFR was switched to the next sampling point, and again a period of 3 times the residence time was allowed before taking samples. The maximum residence time in the DOPFR was approximately 2 minutes. To investigate longer contact times a 2 liter Erlenmeyer was completely filled at the last sampling point. Samples were taken from the Erlenmeyer after the required contact time. The Milli-Q[®] flow and the flow of the combined test water plus Milli-Q[®] water were determined regularly by volume measurements. Cooling in a refrigerator or heating in a warm bath prior to the experiments regulated temperature of the test water. During the experiments the water temperature was measured in the test water vessel (DOPFR inlet) and at the sampling points. Temperature changes during the experiments were limited to 2°C.

Experiments

Experiments were carried out for different ozone dosages and different temperatures. The water quality parameters of the test water, the ozone dosages and the temperatures are presented in Table 2.

Table 2 Experimental conditions and water quality parameters for the test water

Experiment	Ozone dosage (mg-O ₃ /l)	Temperature (°C)	pH (-)	Bromide (µg-Br/l)	DOC (mg-C/l)	UVA ₂₅₄ (1/m)
1	0.43	12	8.0	158	2.4	6.1
2	0.52	12	8.0	158	2.4	6.1
3	0.82	11	8.1	152	2.4	6.2
4	0.88	7	8.1	152	2.4	6.2
5	0.90	10	8.0	152	2.7	6.4
6	0.90	12	8.0	158	2.4	6.1
7	0.90	20	8.1	152	2.4	6.2

Modeling of the hydraulic properties of the DOPFR

The residence time distribution (RTD) of the plug flow reactor was determined for each sampling point by step-tracer experiments using a salt solution. The conductivity was simultaneously recorded every 0.1 s just before the static mixer

and at a sampling point to determine the RTD between these two points. A completely stirred tank reactor (CSTR) in series model was selected to describe the hydraulic characteristics of the plug flow reactor. The number of CSTRs and the hydraulic residence time between sampling points were determined from the measured RTD curves by parameter estimation through numerical integration of advection described by Taylor expansion (Peyret and Taylor, 1983):

$$\left. \frac{dc}{dt} \right|_i^n = -v \frac{c_{i+1}^n - c_i^n}{\Delta x} \quad [1]$$

with

$$\Delta x = \frac{L}{n} \quad [2]$$

$$v = \frac{L}{t_h} \quad [3]$$

where c is the tracer concentration (g/m^3), t is the time (s), n is the number of CSTRs (-), v is the water velocity (m/s), Δx is the length of one CSTR (m), L is the length of the DOPFR (m) and t_h is the hydraulic residence time between sampling points (s).

The discretization error (numerical dispersion) is assumed to be equal to the hydrodynamic dispersion. The relation between the dispersion coefficient, the number of CSTRs and the hydraulic residence time is:

$$D = v \frac{\Delta x}{2} = \frac{vL}{2n} = \frac{L^2}{2t_h n} \quad [4]$$

where D is the hydrodynamic dispersion coefficient (m^2/s).

Modeling of ozone decay and UV absorbance

Several researchers have investigated ozone decay in water. According to Park et al. (2001), ozone, added to natural water, is consumed in two steps: the rapid

ozone consumption step and the rather slow decay step. The rapid ozone consumption is mainly due to reactions with NOM and Westerhoff et al. (1999) found that ozone reacts preferentially with the aromatic constituents of NOM giving a decrease in UVA_{254} . Duguet et al. (1985, 1986) performed research with on-line monitoring of UVA_{254} during ozonation and concluded it is a parameter very well suited for control of ozonation. Therefore, Rietveld (2005) described rapid ozone consumption as a function of the degradation of UVA_{254} . Assuming instantaneous mixing in the static mixer, the ozone concentration and the UVA_{254} in the DOPFR can be described by the following equations:

$$\frac{\partial c_{O_3}}{\partial t} = -\frac{Q}{A} \frac{\partial c_{O_3}}{\partial x} - k_{UVA} (UVA - UVA_0) Y - k_{O_3} c_{O_3} \quad [5]$$

$$\frac{\partial (UVA)}{\partial t} = -\frac{Q}{A} \frac{\partial (UVA)}{\partial x} - k_{UVA} (UVA - UVA_0) \quad [6]$$

where c_{O_3} is the concentration of ozone in water (mg- O_3 /l), Q is the water flow (m^3 /s), A is the surface area of the reactor (m^2), x is the length of the reactor (m), k_{O_3} is the slow ozone decay rate (1/s), k_{UVA} is the UVA_{254} decay rate (1/s), Y is the yield for ozone consumed per UVA_{254} decrease ((mg- O_3 /l)/(1/m)), UVA is the UVA_{254} in water (1/m) and UVA_0 is the stable UVA_{254} after completion of the ozonation process (1/m).

The first term of Equation [5] for the ozone concentration in water describes transport of ozone in water. The second term describes the rapid ozone consumption in water as a function of the UVA_{254} decrease. After rapid ozone consumption the UVA_{254} is considered stable therefore the UVA_0 is incorporated in Equation [5] and Equation [6]. As the ozonation progresses, the rate of ozone decay is shifted to the slow kinetic regime (Zhou et al., 1994). The third term describes slow ozone decay by first-order kinetics.

The first term of Equation [6] for the UVA_{254} in water describes transport of UVA_{254} in water. The second term describes the UVA_{254} decrease by first-order kinetics.

Modeling of bromate formation

The formation of bromate from naturally occurring bromide involves numerous reactions, which have been described in detail by von Gunten and Hoigné (1994). It has been shown that bromate formation consists of an initial fast increase after which the bromate concentration increases linearly with ozone exposure (CT) (von Gunten and Hoigné, 1994; von Gunten et al., 2001). This relation was applied in a model for describing bromate formation in the DOPFR.

Modeling of AOC formation

The increase of the AOC concentration during ozonation is related linearly with the decrease of UVA₂₅₄ (van der Kooij et al., 1989). The relation is derived from AOC en UVA₂₅₄ measurements of influent and effluent of the Leiduin full-scale ozonation plant and is applied on the DOPFR experiments.

Modeling of disinfection efficacy

The hydraulic model used is a CSTR in series model that calculates the ozone concentration and the residence time in every CSTR and thus a CT profile can be calculated. With the CT profile the disinfection can be determined with the USEPA CT10 method (USEPA, 2003). However, a CSTR in series model is also well suited for inactivation calculation with the USEPA CSTR method (USEPA, 2003). Smeets et al. (2006) found that the CSTR method should be preferred over the CT10 method when calculating inactivation for ozone-sensitive pathogens such as viruses and *Campylobacter*, which are the pathogens of main interest for drinking water treatment plant Leiduin. CT is calculated with:

$$CT = \sum_{i=0}^n c_{O_3,i} (t_i / 60 - t_{i-1} / 60) \quad [7]$$

where CT is the ozone exposure ((mg-O₃/l)*min).

Calibration and validation

Prior to calibration of the model, a sensitivity analysis was performed on slow ozone decay rate, UVA₂₅₄ decay rate and yield factor. On basis of the sensitivity analysis a calibration methodology was designed in which first slow ozone decay was calibrated and subsequently fast ozone decay. Calibration was done on

measured ozone concentrations and on the measured stable UVA_{254} after completion of the ozonation process.

Part of the experiments was used for model calibration and part of the experiments was used for model validation. Assumptions made for the validation runs were:

- slow ozone decay rate k_{O_3} and UVA_{254} decay rate k_{UVA} decreases with increasing ozone dosage. Assuming a constant contribution of the ozone decomposition cycle, this can be explained by the various types of sites within NOM that have different reactivity with ozone. For low ozone dosages only the fast-reacting sites consume ozone. When higher ozone dosages are applied, the rate of ozone consumption decreases since slowly reacting sites are oxidized as well (Hoigné and Bader, 1994; Gallard et al., 2003);
- yield for consumed ozone per UVA_{254} decrease is not influenced by the ozone dosage since it has the properties of a stoichiometric coefficient;
- UVA_{254} decrease during ozonation increases with ozone dosage;
- initial fast bromate formation and bromate formation in the linear phase both increase with the total CT.

Results and discussion

The hydraulic properties of the DOPFR, ozone decay and UVA_{254} , bromate formation and AOC formation were separately calibrated and are separately discussed. For validation all processes were combined and the results are presented accordingly.

Calibration of the hydraulic properties of the DOPFR

In Figure 2 the results of three tracer experiments for three different sampling points with their respective calibrated hydraulic properties are presented, demonstrating a CSTR in series model can be applied for the DOPFR. In Table 3 the number of CSTRs and the hydraulic residence time for all sampling points of the plug flow reactor are given. Linear regression shows that the static mixer represents 10 CSTRs and that the number of CSTRs in the plug flow reactor is linear with the increase of the hydraulic residence time, so the hydraulic properties are the same over the total length of the plug flow reactor. However, the tracer experiment at sampling point 1 resulted in a unlikely high number of CSTRs, higher than at the second sampling point which is physically not possible. On basis of the

linear regression, the number of CSTRs on sampling point 1 was estimated equal to 19. The calculated number of CSTRs was used in the model to describe the hydraulic properties. The high number of CSTRs demonstrates the tube has good plug flow characteristics.

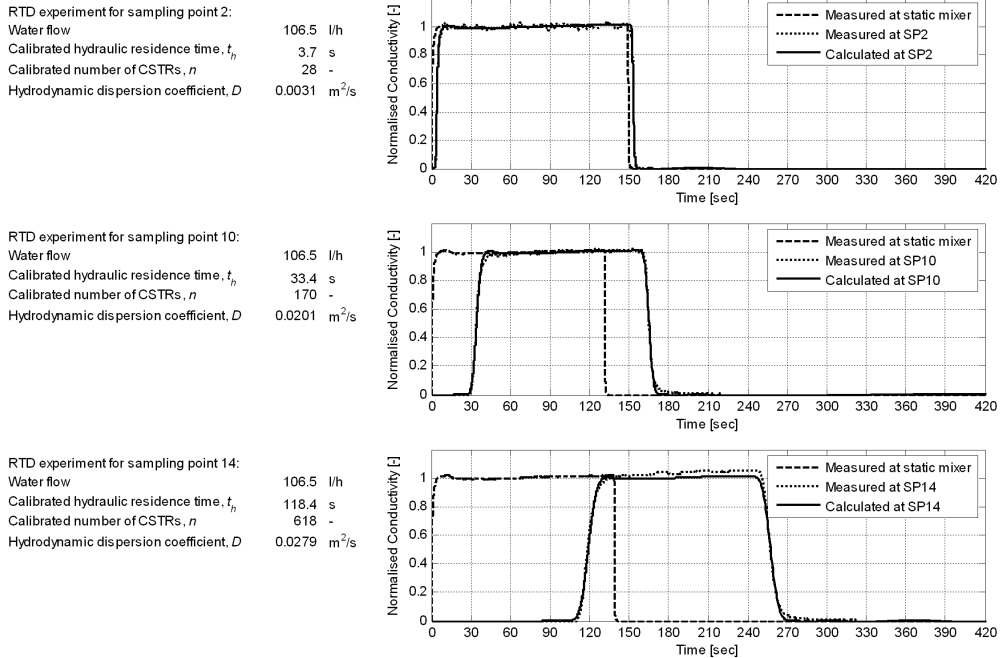


Figure 2 Calibration results for the number of CSTRs and the hydraulic residence time at three different sampling points for a water flow of 106.5 l/h through the DOPFR

Table 3 Number of CSTRs and the hydraulic residence time determined from tracer experiments for a flow of 106.5 l/h through the DOPFR

Sampling point	1	2	3	4	5	6	7
CSTRs (-)	30	28	40	51	57	70	104
t_h (s)	1.9	3.7	5.9	8.3	10.5	12.9	17.9
Sampling point	8	9	10	11	12	13	14
CSTRs (-)	121	141	170	243	323	460	618
t_h (s)	23.2	28.4	33.4	47.9	62.2	90.7	118.4

Calibration of ozone decay and UV absorbance

Model calibration runs were carried out for the experiments 1, 2, 5 and 6 at a water temperature of approximately 12°C, and for experiment 7 at a water temperature of 20°C. These experiments were selected in order to cover the range of applied ozone dosages and different water temperatures. Calibration was performed on the measured ozone concentrations and the stable UVA₂₅₄ after completion of the ozonation process. The calibration results for experiments 1, 6 and 7 are shown in Figure 3 and all calibrated parameters are summarized in Table 4. In Figure 3 the difference in the ozone profile and thus CT between different ozone dosages can be observed from experiment 1 and 6. The ozone profiles of experiment 6 and 7 demonstrate the influence of temperature; a higher temperature gives higher decay rate constants and thus a lower CT.

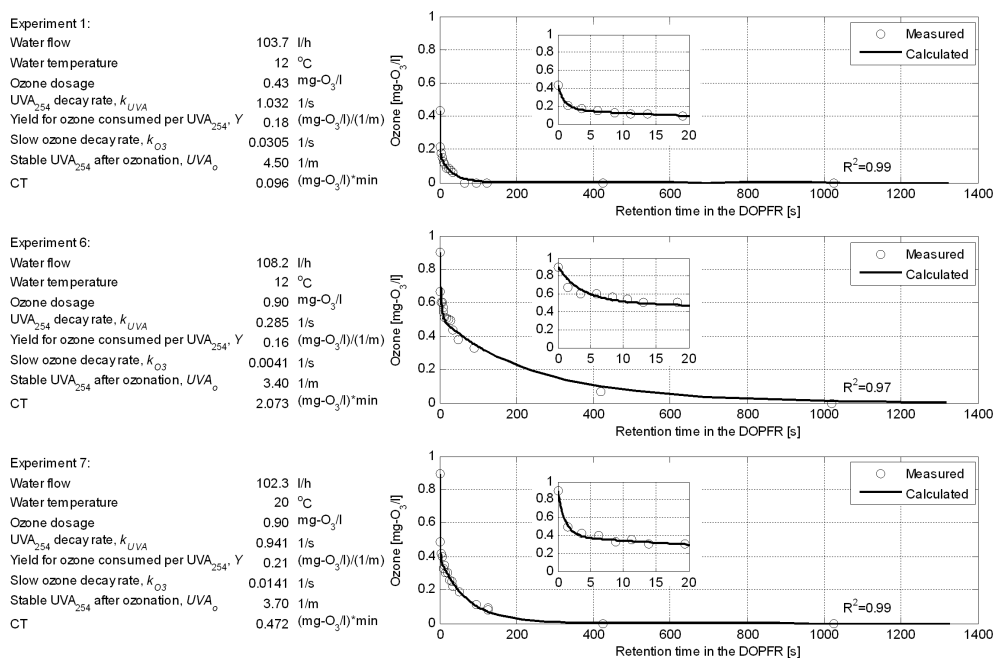


Figure 3 Calibration results for experiments 1, 6 and 7

From the calibrated parameters and measurements of experiments 1, 2, 5 and 6 for a temperature of approximately 12°C, the k_{O_3} , k_{UVA} , Y and $(UVA_{in}-UVA_0)$ were determined as a function of the ozone dosage:

$$k_{O_3} = 0.1653e^{-4.093C_{O_3,DOS}} \quad [8]$$

$$k_{UVA} = 3.95e^{-3.005C_{O_3,DOS}} \quad [9]$$

$$Y = 0.063c_{O_3,DOS} + 0.140 \quad [10]$$

$$(UVA_{in} - UVA_0) = 1.319c_{O_3,DOS} + 0.995 \quad [11]$$

where $c_{O_3,DOS}$ is the ozone dosage (mg-O₃/l) and UVA_{in} is the influent UVA_{254} (1/m).

In Figure 4 the Equations [8], [9], [10] and [11] are shown with 90% confidence intervals. The k_{O_3} and k_{UVA} appear to be an exponential function of the ozone dosage rather than linear. Since the yield factor has the properties of a stoichiometric coefficient it was expected to be constant for different ozone dosages. However Figure 4 shows that the yield increases slightly with increasing ozone dosage but taking into account the confidence interval the yield factor can be assumed to be independent of the ozone dosage. The correlation is poor which is to be expected since there is no correlation if the yield factor is independent of the ozone dosage. From the calibrated data the total decrease in UVA_{254} is assumed to be linear with increasing ozone dosage, however the correlation is not very good (Figure 4 lower right). The k_{O_3} and k_{UVA} for 20°C are higher as would be expected since chemical rate coefficients increase with increasing temperature. The Y for 20°C does not appear to be different from the Y for 12°C, which is to be expected since it has the properties of a stoichiometric coefficient. The $UVA_{in}-UVA_0$ does not seem to be dependent on temperature, however it should be noted that with only one experiment at 20°C the dataset is rather small.

Table 4 Calibration results for ozone decay and UVA_{254} for experiments 1, 2, 5, 6 and 7

Experiment	Temperature (°C)	Ozone dosage (mg-O ₃ /l)	k_{O_3} (1/s)	k_{UVA} (1/s)	Y ((mg-O ₃ /l)/(1/m))
1	12	0.43	0.0305	1.032	0.18
2	12	0.52	0.0159	0.914	0.16
5	10	0.90	0.0078	0.192	0.22
6	12	0.90	0.0041	0.285	0.16
7	20	0.90	0.0141	0.941	0.21

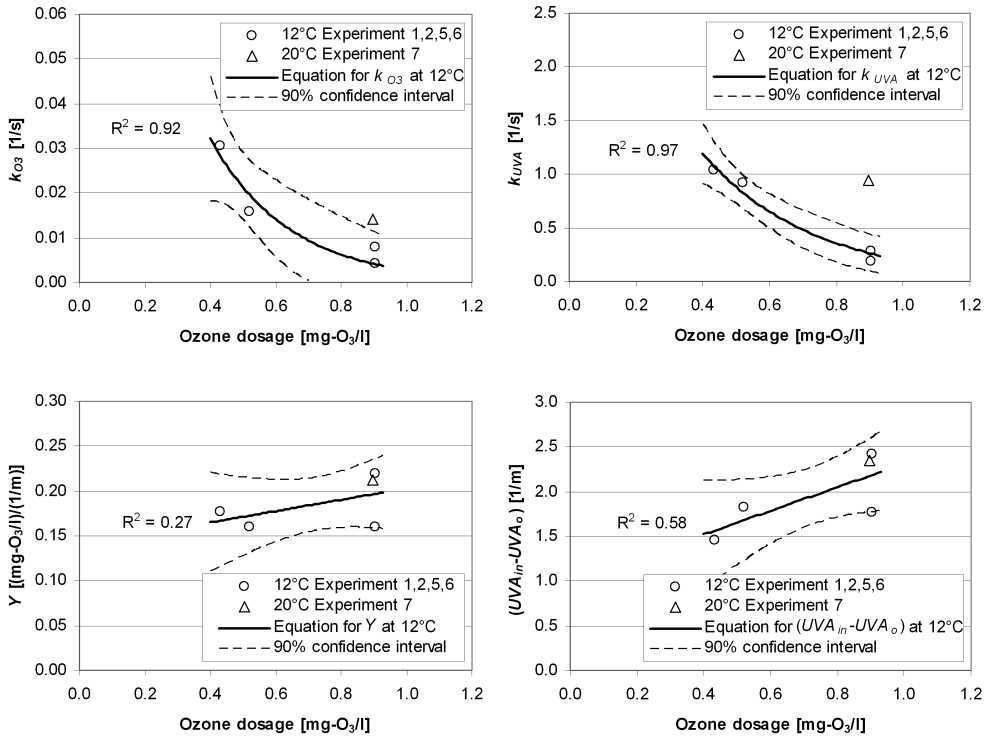


Figure 4 k_{O_3} , k_{UVA} , Y and $(UVA_{in}-UVA_o)$ as a function of the ozone dosage with their 90% confidence intervals for experiments 1, 2, 5, 6 and 7

Calibration of bromate formation

As for ozone decay and UVA_{254} , model calibration for bromate formation was also carried out for the experiments 1, 2, 5, 6 and 7. Bromate formation was modeled as a linear function of CT after an initial fast bromate formation. From calibrating a linear equation on the experimental data the amount of bromate formed in the DOPFR in the initial phase, $\Delta C_{BrO_3,ini}$, and the amount of bromate formed in the linear phase, $\Delta C_{BrO_3,lin}$, were determined. The results for experiment 7 are presented graphically in Figure 5 and all calibration results are given in Table 5. The CT in the DOPFR in Figure 5 is calculated from the calibrated ozone profile in the DOPFR (see Figure 3).

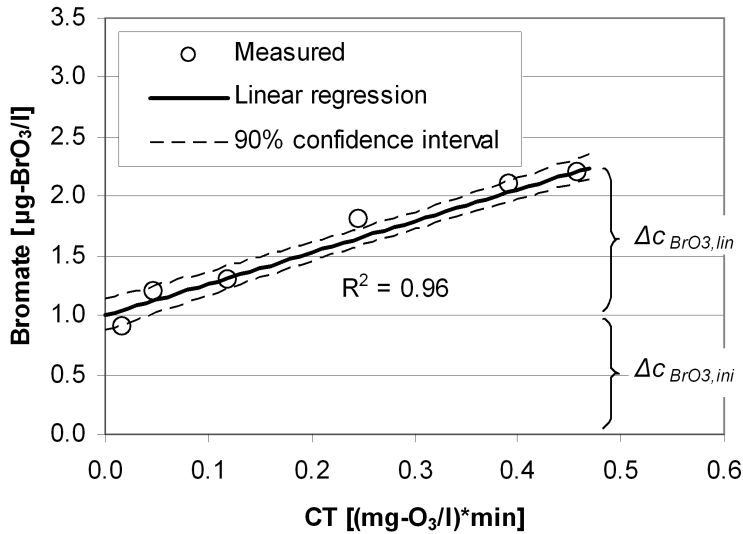


Figure 5 Bromate formation in the DOPFR for experiment 7

Table 5 Calibration results of bromate formation for experiments 1, 2, 5, 6 and 7

Experiment	$\Delta c_{BrO_3,ini}$ ($\mu\text{g-BrO}_3/\text{l}$)	$\Delta c_{BrO_3,lin}$ ($\mu\text{g-BrO}_3/\text{l}$)
1	0.5	0.4
2	1.0	0.4
5	1.9	1.6
6	3.6	3.1
7	1.0	1.2

From the calibration results in Table 5 equations were determined for prediction of the initial fast bromate formation and the bromate formation in the linear phase based on the total CT after ozonation:

$$\Delta c_{BrO_3,ini} = 1.5CT_{TOT} + 0.5 \quad [12]$$

$$\Delta c_{BrO_3,lin} = 1.4CT_{TOT} + 0.2 \quad [13]$$

where $\Delta c_{BrO_3,ini}$ is the bromate formation in the initial phase ($\mu\text{g-BrO}_3/\text{l}$), $\Delta c_{BrO_3,lin}$ is the bromate formation in the linear phase ($\mu\text{g-BrO}_3/\text{l}$) and CT_{TOT} is the CT after completion of the ozonation process ($(\text{mg-O}_3/\text{l})\cdot\text{min}$).

Equations [12] and [13] are presented in Figure 6 with their respective 90% confidence intervals. The initial bromate formation as well as the bromate formation in the linear phase has a little deviation from the origin of respectively 0.5 and 0.2 $\mu\text{g-BrO}_3/\text{l}$. This can be explained by either non-linear behavior at very low CT values or by uncertainty in as well the bromate measurement at very low concentrations as the calculation of CT values after very short contact times.

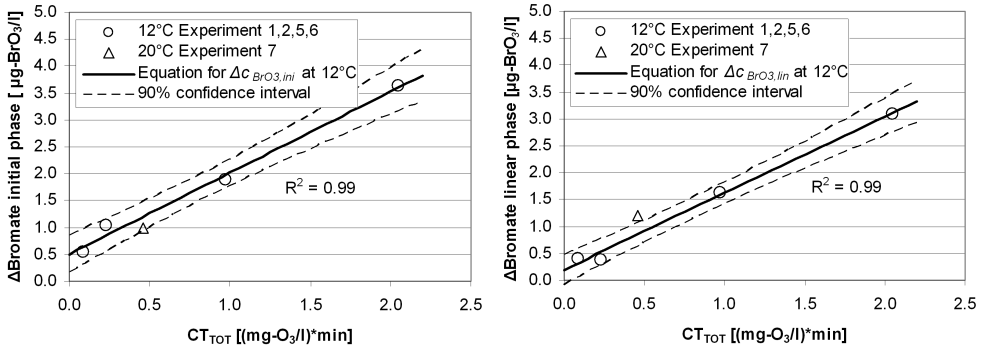


Figure 6 Initial bromate formation (left) and bromate formation in the linear phase (right) both as a function of the total CT with 90% confidence intervals for experiments 1, 2, 5, 6 and 7.

Calibration of AOC formation

The number of data for AOC concentration and UVA_{254} of influent and effluent of ozonation at the full-scale Leiduin treatment plant at the same day is limited. In Figure 7 the available data are plotted with a linear regression line. The relation is given by:

$$\Delta c_{\text{AOC}} = 25.48 (\text{UVA}_{\text{in}} - \text{UVA}_0) \quad [14]$$

where Δc_{AOC} is the increase in AOC after completion of the ozonation process ($\mu\text{g-C/l}$).

Even though the Pearson R-square is low and a number of observations are outside the 90% confidence interval, this relation was used for calculation of the AOC formation during ozonation in the DOPFR and thus will only give an indication of the actual AOC formed.

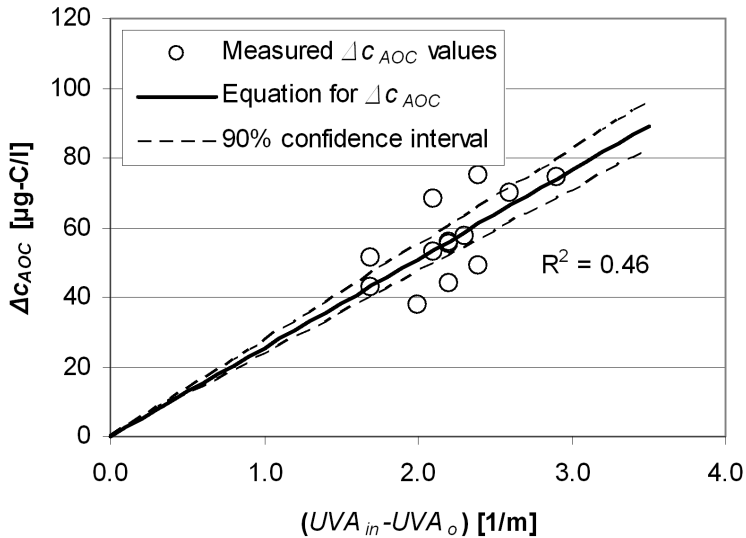


Figure 7 Increase of AOC as a function of the decrease of UVA_{254} for Leiduin full-scale ozonation plant (data from 2001-2002)

Model validation

In Figure 8 and Figure 9 the results of the validation runs of experiment 3 and 4 are presented. The validation runs presented here show that the model was able to predict ozone decay, UVA_{254} decrease, AOC formation and bromate formation for other ozone dosages than the dosages used in the calibration experiments. The prediction for experiment 4 with a slightly lower temperature of 7°C also gave good results for ozone decay and UVA_{254} , however bromate formation is a little over estimated. With incorporation of OH radical formation during ozonation, bromate formation can be predicted more accurate. But since the model was developed for on-line control with possible further on-line calibration the choice was made to discard the involvement of OH radicals and test whether it was possible to model bromate formation based on just the CT. From these experiments this seems feasible.

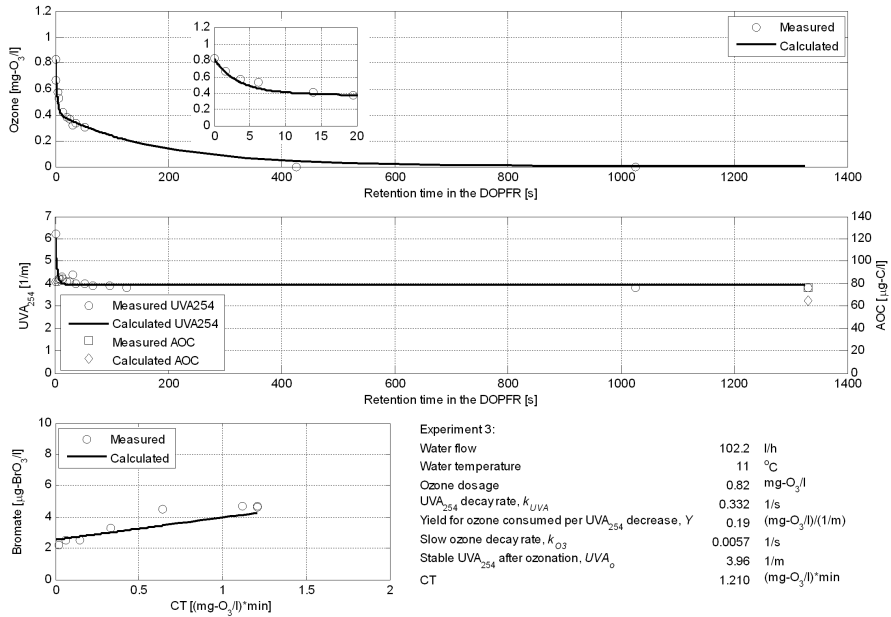


Figure 8 Results of the validation run for experiment 3

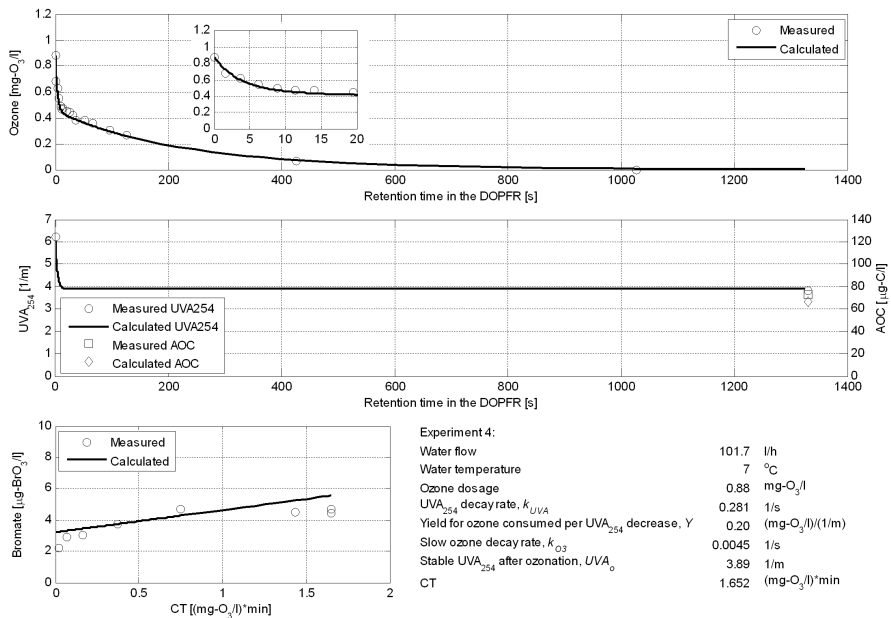


Figure 9 Results of the validation run for experiment 4

Conclusions

From the model runs it was shown that the proposed model was capable of predicting ozone decay and CT, decrease in UVA_{254} , increase in AOC concentration and bromate formation on the basis of the applied ozone dosage for the water tested. The UVA_{254} was found to be an effective parameter for estimation of rapid ozone consumption for natural waters under experimental conditions tested in this research. Since UVA_{254} can be measured on-line it is a parameter well suited for use in operation of ozonation. The relation between CT and bromate formation will depend on the OH radical reaction and will be different for different water types. After establishing the relation for a different water type the CT can be used as a good indicator for prediction of bromate formation. With relations between CT and pathogen removal it is possible to directly predict the disinfection capacity of ozonation. This makes the model a valuable tool for managing the balance between disinfection, bromate formation and AOC formation.

The model was only validated with one type of water in a limited time span. As Duguet et al. (1986) have shown it is important to evaluate the validity of the equations derived for the calibrated parameters and the use of the model during the year and for different natural waters. Therefore it is necessary to perform experiments on different waters and in different periods of the year since the quality of the surface water varies.

The ozonation model was developed for integrated optimization and use in control of ozonation, softening and biological activated carbon filtration at drinking water treatment plants of Waternet. The model will be combined with a gas transfer model and used at drinking water treatment plants Leiduin and Weesperkarspel of Waternet for operational support of the current ozonation processes. The model will also be used for on-line model-based control of the ozonation pilot plant at Weesperkarspel (15 m³/h) with conventional bubble and contact columns. For this purpose the pilot plant at Weesperkarspel is fully automated and equipped with on-line ozone and UVA_{254} monitors. In this installation the model can be further calibrated and validated during different times of the year.

Acknowledgement

This research was carried out as part of the project 'Promicit', a cooperation of Waternet, Delft University of Technology, DHV B.V. and ABB B.V. and was subsidized by SenterNovem, agency of the Dutch Ministry of Economic Affairs. The aim of the project was to achieve a breakthrough in drinking water quality control by developing an integrated model of the total water treatment and using this model as a basis for operation. The DOPFR experiments were performed in cooperation with Kiwa Water Research Nieuwegein, the Netherlands.

Nomenclature

AOC	assimilable organic carbon
CSTR	completely stirred tank reactor
DOPFR	dissolved ozone plug flow reactor
NOM	natural organic matter
RTD	residence time distribution
UVA_{254}	UV absorbance at 254 nm
Waternet	water cycle company for Amsterdam and surrounding areas
A	surface area of the reactor (m^2)
c	tracer concentration (g/m^3)
ΔC_{AOC}	increase of AOC after completion of the ozonation process ($\mu g-C/l$)
$\Delta C_{BrO_3,ini}$	bromate formation in the initial phase ($\mu g-BrO_3/l$)
$\Delta C_{BrO_3,lin}$	bromate formation in the linear phase ($\mu g-BrO_3/l$)
C_{O_3}	concentration of ozone in water ($mg-O_3/l$)
$C_{O_3,DOS}$	ozone dosage ($mg-O_3/l$)
CT	ozone exposure ($(mg-O_3/l)*min$)
CT_{TOT}	CT after completion of the ozonation process ($(mg-O_3/l)*min$)
D	hydrodynamic dispersion coefficient (m^2/s)
k_{O_3}	slow ozone decay rate (1/s)
k_{UVA}	UVA_{254} decay rate (1/s)
L	length of the DOPFR (m)
n	number of CSTRs (-)
Q	water flow (m^3/s)
t	time (s)
t_h	hydraulic residence time between sampling points (s).
UVA	UVA_{254} in water (1/m)

UVA_o	stable UVA_{254} after completion of the ozonation process (1/m)
UVA_{in}	influent UVA_{254} (1/m)
v	water velocity (m/s)
x	length of the reactor (m)
Δx	length of one CSTR (m)
Y	yield for ozone consumed per UVA_{254} decrease ((mg-O ₃ /l)/(1/m))

References

- Duguet, J.P., Brodard, E., Dussert, B. and Mallevalle, J. (1985). Improvement in the effectiveness of ozonation of drinking water through the use of hydrogen peroxide. *Ozone Sci. Eng.*, 7(3), 241-258.
- Duguet, J.P., Brodard, E., Roustan, M. and Mallevalle, J. (1986). An automated procedure for monitoring the effectiveness of ozonation processes. *Ozone Sci. Eng.*, 8(4), 321-338.
- Gallard, H., von Gunten, U. and Kaiser, H.P. (2003). Prediction of the disinfection and oxidation efficiency of full-scale ozone reactors. *J. Water Supply Res. Technol. AQUA*, 52(4), 277-290.
- Hoigné, J. and Bader, H. (1994). Characterization of water quality criteria for ozonation processes. Part II: Lifetime of added ozone. *Ozone Sci. Eng.*, 16(2), 121–134.
- Kiwa (1999). *Bepaling van ozon in water met behulp van spectrofotometrie conform Kiwa-voorschrift 1-07-1 (1999), LAM-062 v1.0. (Determination of ozone in water with spectrophotometry in accordance with Kiwa-regulation 1-07-1 (1999), LAM-062 v1.1)*. Kiwa Water Research, Nieuwegein, the Netherlands.
- Park, H., Hwang, T., Kang, J., Choi, H. and Oh, H. (2001). Characterization of raw water for the ozone application measuring ozone consumption rate. *Water Res.*, 35(11), 2607-2614.
- Peyret, R. and Taylor, T.D. (1983). *Computational Methods for Fluid Flow*. Springer series in computational physics, Springer-Verlag, New York, USA.
- Rietveld, L.C. (2005). *Improving operation of drinking water treatment through modelling*. PhD Thesis, Faculty of Civil Engineering and Geosciences, Delft University of Technology.

- Smeets, P.W.M.H., van der Helm, A.W.C., Dullemont, Y., Rietveld, L.C., van Dijk, J.C. and Medema, G.J. (2006). Inactivation of *Escherichia coli* by ozone under bench scale plug flow and full scale hydraulic conditions. *Water Res.*, 40(17), 3239-3248.
- USEPA (2003). *LT2ESWTR Long Term Second Enhanced Surface Water Treatment Rule and Draft Toolbox Guidance Manual*. USEPA, Cincinnati, USA.
- van der Kooij, D., Hijnen, W.A.M. and Kruithof, J.C. (1989). The effects of ozonation, biological filtration and distribution on the concentration of easily assimilable organic carbon (AOC) in drinking water. *Ozone Sci. Eng.*, 11(3), 297-311.
- von Gunten, U. and Hoigné, J. (1994). Bromate formation during ozonation of bromide-containing waters: Interaction of ozone and hydroxyl radical reactions. *Environ. Sci. Technol.*, 28(7), 1234-1242.
- von Gunten, U., Driedger, A., Gallard, H. and Salhi, E. (2001). By-products formation during drinking water disinfection: a tool to assess disinfection efficiency? *Water Res.*, 35(8), 2095-2099.
- von Gunten, U. (2003). Ozonation of drinking water: Part II. Disinfection and by-product formation in presence of bromide, iodide or chlorine. *Water Res.*, 37(7), 1469-1487.
- Westerhoff, P., Aiken, G., Amy, G. and Debroux, J. (1999). Relationships between the structure of Natural Organic Matter and its reactivity towards molecular ozone and hydroxyl radicals. *Water Res.*, 33(10), 2265-2276.
- Zhou, H., Smith, D.W. and Stanley, S.J. (1994). Modeling of dissolved ozone concentration profiles in bubble columns. *J. Environ. Eng.*, 120(4), 821-840.

4. Disinfection and by-product formation during ozonation in a pilot-scale plug flow reactor and CSTR

Pilot-scale ozonation experiments (2.5-5 m³/h) were performed with dosing of dissolved ozone and subsequently contact time was created in a pipe with plug flow reactor (PFR) characteristics and a vessel with completely stirred tank reactor (CSTR) characteristics. From the experimental data it was concluded that (i) the rate of rapid ozone consumption in the first 20 seconds of contact time follows diffusion-limited kinetics; (ii) at low ozone dosages a major part of the inactivation of ozone-sensitive organisms takes place during rapid ozone consumption; and, (iii) the disinfection capacity for the ozone sensitive-organism *E. coli* is 3 to 5 times higher in a PFR compared to a CSTR for the same amount of ozone dosed. Therefore, plug flow conditions should be established from the first contact between ozone and water. From the experimental data a semi-empirical dynamic model for describing ozone decay, *E. coli* disinfection, bromate and AOC formation in natural water was developed.

Introduction

Ozonation is widely used for treatment of drinking water. It is employed for disinfection, oxidation of micro pollutants, formation of biodegradable organic matter for removal by biological (activated carbon) filtration, and for improvement of color, taste and odor. Ozonation can also be applied in wastewater treatment for oxidation of emerging substances such as endocrine-disrupting chemicals and pharmaceuticals and personal care products (von Gunten et al., 2005). An undesired effect of ozonation in drinking water treatment is the formation of the by-product bromate that is formed in bromide-containing waters (von Gunten, 2003).

Ozonation systems usually consist of an ozone dosage section, where gaseous ozone is dissolved in water, and a contactor, where contact time is created between dissolved ozone and water. For dosing ozone, different systems can be

distinguished. The most applied system is fine bubble diffusion, where ozone gas is added through a number of diffuser plates or a network of perforated pipes in so-called 'bubble chambers'. Bubble chambers can be co-current with water flowing in an upward direction or counter current with water flowing in a downward direction (see Figure 1). Bubble chambers can also be applied in series. Other systems for the dosing of ozone are injection with a Venturi mixer (Jackson et al., 1999, Rakness, 2005), injection just before a static mixer (Chandranth et al., 2003) or injection in the deep U tube (Roustan et al., 1992; Muroyama et al., 2005). The ozone contactor after the ozone dosage section usually consists of a number of contact tanks in series, divided by baffles (see Figure 1). All these systems applied at full-scale have different hydraulic properties and mixing characteristics. Van der Helm et al. (2007b) and Smeets et al. (2006) showed the importance of hydraulic properties and mixing characteristics in bench-scale ozonation experiments with the dosing of dissolved ozone and contact time in a plug flow reactor; the concept was named dissolved ozone plug flow reactor (DOPFR). From these experiments it was concluded that improving plug flow conditions should be considered instead of increasing ozone dosage to improve the disinfection capacity for ozone-sensitive organisms in a conventional ozone contactor (Smeets et al., 2006). A precondition is that the ozone is mixed properly with the entire water flow.

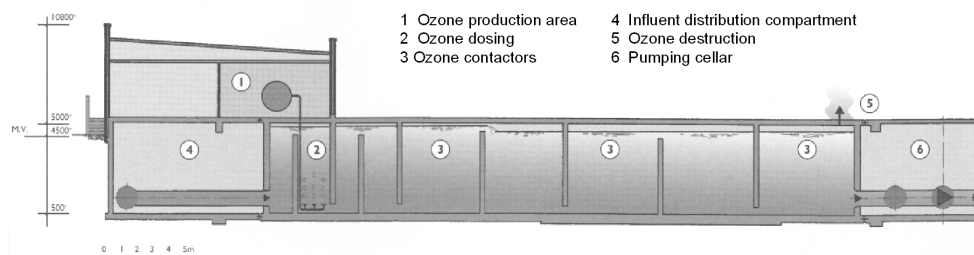


Figure 1 Example of a fine bubble diffusion ozone process

Ozone is an unstable oxidant in water. In general, when ozone is added to natural water, it is consumed in two steps: the initial rapid ozone consumption step followed by a subsequent, slow ozone decay step. The rapid ozone consumption is mainly due to reactions with natural organic matter (NOM). As a result of direct ozone consumption by unsaturated bonds in NOM, larger organic components are oxidatively transformed into smaller organic components, and a decrease in UV absorbance at 254 nm (UVA_{254}) occurs. Westerhoff et al. (1999) found, from extensive research on physical and chemical properties of NOM isolates, that

ozone reacts preferentially with the aromatic constituents of NOM, and specifically electron-enriched aromatics. For describing rapid ozone consumption, a number of different semi-empirical models can be found in the literature. One group of semi-empirical models is based on fundamental chemical reactions for ozone decay (Staehelin and Hoigné, 1982; Bühler et al., 1984; Staehelin et al., 1984), containing empirical relations between NOM and ozone and NOM and hydroxyl radicals (Gilligly et al., 2001). Another group of semi-empirical models describes rapid ozone consumption as an instantaneous ozone demand (Park et al., 2001), as a zero-order reaction in the first minute of contact time (Westerhoff et al., 1999; Sohn et al., 2004) or up to the first 3 minutes of contact time (Gilligly et al., 2001), as an instantaneous ozone demand followed by a first-order rapid ozone consumption until approximately 2 minutes of contact time (Westerhoff, 2002), and as a function of the decrease in UVA_{254} (Rietveld, 2005; van der Helm et al., 2007b). Models for rapid ozone consumption are generally based on research on ozone kinetics in batch experiments. In these experiments the first sample is normally taken after half a minute or one minute, the major part of rapid ozone consumption has then already taken place (Buffle et al., 2006; van der Helm et al., 2007a,b).

The objectives of this research are fourfold. The first part is assessing different semi-empirical models for rapid ozone consumption based on ozone measurements in the first seconds of contact time. The second part is assessing the differences in disinfection capacity between two extremes for hydraulic properties of ozone contactors, those being the plug flow reactor (PFR) and the completely stirred tank reactor (CSTR) at low ozone dosages. The assessment includes modeling of the disinfection capacity using different disinfection models. The third part is modeling of the formation of the disinfection by-products bromate and assimilable organic carbon (AOC) using different (semi-) empirical models. The fourth part is assessing the effects of upscaling the DOPFR concept from bench-scale to pilot-scale on the model parameters for ozone decay determined in a bench-scale DOPFR (van der Helm et al., 2007b). The developed models will be combined in an integrated dynamic model for the DOPFR concept.

Materials and methods

Experimental setup and experiments

Pilot-plant experiments were carried out at Leiduin, one of two drinking water treatment plants of Waternet (water cycle company for Amsterdam and surrounding

areas). The water used in the experiments was pre-treated surface water that was infiltrated in the dunes and subsequently treated by aeration and rapid sand filtration. The pilot plant consisted of a dissolved ozone plug flow reactor (DOPFR) with parallel to the plug flow reactor a vessel for contact time (see Figure 2).

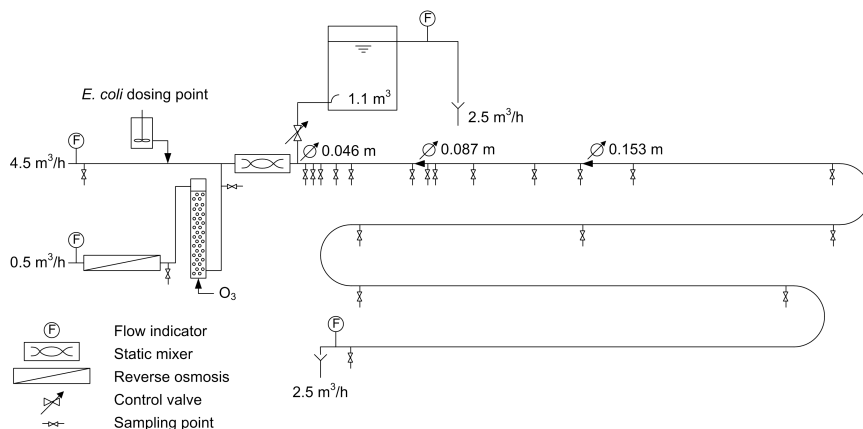


Figure 2 Experimental setup of the pilot plant, with flow through a pipe and flow through a vessel

Ozone was dissolved in a side stream that was pre-treated with reverse osmosis (Hydronautics ESPA2 membrane) for removal of dissolved organic carbon (DOC) and bromide. The dissolved ozone was added to the main stream and mixed in a static mixer, after which the water stream was split. One stream entered a pipe with the hydraulic properties of a PFR, and one stream entered a vessel with the hydraulic properties of a CSTR. The pipe starts with a diameter of 0.046 m, after a length of 5 m it changed to 0.087 m and after another length of 5 m it changed to 0.153 m. The total length of the pipe was 63.5 m and it had 19 sampling points. In the installation, rapid ozone consumption as well as slow ozone decay was determined in one experiment. The retention times at the sampling points were 1.3 / 1.8 / 2.3 / 3.3 / 4.3 / 8.3 / 13.9 / 15.9 / 23.5 / 37.9 / 48.9 / 96 / 248 / 355 / 608 / 829 / 904 / 1129 / 1460 seconds for a flow of 2.5 m³/h. The water entered the vessel through a tangential inlet at the bottom of the vessel in order to create a circulation stream for mixing. The water left the vessel at the top. The volume was 1.1 m³, with a flow of 2.5 m³/h, the theoretical retention time in the vessel was 1584 seconds. In the influent *Escherichia coli* (*E. coli*) were dosed from a vessel with a concentration ranging from $2.2 \cdot 10^4$ to $4.8 \cdot 10^5$ CFU/ml. Because dissolved ozone was dosed, the transferred ozone was equal to the ozone dosage, which was determined by the

ozone concentration in the dissolved ozone side stream and the dilution ratio with the main stream. The pilot plant was operated at low ozone dosages 0.25-1.0 mg-O₃/l in order to obtain similarities with the full-scale Leiduin treatment plant and to be able to measure *E. coli* at the sampling points. The conditions for the experiments are given in Table 1. In all experiments listed in Table 1, the pipe was tested. For a limited number of experiments the vessel was tested. The bromate concentration in the influent of the DOPFR (see Table 1) was caused by bromate formation in the bubble column because not all bromide was removed by reverse osmosis. The experimental setup for experiments 1 to 4 and 9 to 11 differed from data in Figure 2. The flow through the pipe was 5 m³/h instead of 2.5 m³/h and the first part of the pipe had a diameter of 0.087 m instead of 0.046 m.

Table 1 Conditions and influent water quality parameters for the experiments

Parameter	Unit	Experiment number						
		1	2	3	4	5	6	7
Ozone dosage	mg-O ₃ /l	0.37	0.86	0.97	1.91	0.24	0.58	0.77
<i>E. coli</i>	CFU/100 ml	-	-	-	-	23000	13000	8200
pH	-	7.9	7.9	7.9	7.8	8.1	8.0	8.0
Bicarbonate	mg-HCO ₃ /l	168	164	162	167	169	172	169
UVA ₂₅₄	1/m	4.7	4.9	4.7	4.9	5.2	5.3	5.2
Bromide	µg/l	147	149	150	147	158*	158*	158*
Bromate	µg-BrO ₃ /l	-	-	-	<0.5	0.6	0.5	0.6
AOC-total	µg-C/l	7.7	7.8	8.8	7.5	12.6*	12.6*	12.6*
DOC	mg-C/l	1.8	2.2	2.1	1.9	1.9	1.8	2.1
Temperature	°C	12.6	12.3	12.5	12.0	15.6	16.0	16.7
Vessel tested	-	No	No	No	No	Yes	No	No
Parameter	Unit	Experiment number						
		8	9	10	11	12	13	14
Ozone dosage	mg-O ₃ /l	0.99	0.51	0.69	0.83	1.02	-	-
<i>E. coli</i>	CFU/100 ml	800	-	-	-	-	5100	7200
pH	-	8.0	7.9	7.9	7.8	7.8	8.0	8.0
Bicarbonate	mg-HCO ₃ /l	170	164	160	162	162	192	176
UVA ₂₅₄	1/m	5.2	5.0	5.0	4.8	4.9	5.3	5.4
Bromide	µg/l	158*	140	141	142	142	187	-
Bromate	µg-BrO ₃ /l	0.6	0.6	0.6	0.6	<0.5	<0.5	<0.5
AOC-total	µg-C/l	12.6*	8.8**	8.8**	8.8**	11.3	13.0	12.0
DOC	mg-C/l	2.2	2.0	1.9	1.8	1.7	2.2	2.2
Temperature	°C	16.0	18.5	18.4	19.1	17.8	12.6	11.5
Vessel tested	-	No	No	No	No	No	Yes	Yes

* measured at experiment 5 and assumed to be constant

** measured at experiment 9 and assumed to be constant

The ammonia concentration was always below the detection limit of 0.02 mg-N/l. For experiments 1 to 4, the average temperature was 12.4°C, for experiments 5 to 8 it was 16.1°C, and for experiments 9 to 12 it was 18.5°C. These average

temperatures were used to determine the dependency of model parameters on temperature.

Analysis methods

For experiments 5 to 8 ozone was analyzed according to the indigo method described by Bader and Hoigné (1982). For experiments 1 to 4 and 9 to 12, ozone was analyzed according to the DPD method described by Gilbert (1981). Both methods give consistent results (Gilbert and Hoigné, 1983). Bromate samples were concentrated on two Ionpac AG9-SC columns and analyzed using a Dionex ICS3000 ion chromatograph, with an anion micro membrane suppressor, UV detection (200 nm) and a conductivity meter. Dionex Ionpac AG9-SC, and AS9-SC columns were used with a 0.7 mM NaHCO₃ eluent. The detection limit was 0.5 µg-BrO₃/l (Orlandini et al., 1997; Smeenk et al., 1994). Bromide samples were analyzed using a Dionex DX120 ion chromatograph, with a chemical suppressor (12.5 mM H₂SO₄), UV detection (200 nm), and a conductivity meter. A Dionex Ionpac AS9-SC column was used with a 0.2 mM NaHCO₃ / 1.4 mM Na₂CO₃ eluent (Orlandini et al., 1997). AOC was measured in duplicate, applying the simultaneous incubation of strains P17 and NOX (van der Kooij et al., 1982). DOC, pH, bicarbonate and UVA₂₅₄ expressed as the absorbance per meter of cell length were determined using standard procedures (Standard Methods, 2005). *E. coli* WR1 strain was cultured on a low substrate as described in Smeets et al. (2006). Microbiological samples were taken in 1 liter sterile bottles containing sodiumthiosulfate to immediately quench any remaining ozone. Samples were analyzed either by direct filtration and inoculation of the filter or by dilution and direct inoculation of 0.1 ml on agar. The CT value for ozonation was calculated using:

$$CT = \sum_{i=0}^{n_{SP}} c_{O_3,i} (t_i / 60 - t_{i-1} / 60) \quad [1]$$

where CT is the ozone exposure ((mg-O₃/l)*min), n_{SP} is the number of sampling points (-), c_{O_3} is the concentration of ozone in water (mg-O₃/l) and t is time (s).

Rapid ozone consumption

Three different approaches for describing rapid ozone consumption with semi-empirical models were assessed. For the first approach the model of Westerhoff

(2002) was selected where rapid ozone consumption is modeled as an instantaneous ozone demand followed by first-order rapid ozone consumption until approximately 2 minutes of contact time:

$$\frac{dc_{O_3}}{dt} = -k_{O_3R}c_{O_3} \quad [2]$$

where k_{O_3R} is the first-order rapid ozone consumption rate (1/s). The amount of ozone consumed during instantaneous ozone demand is determined by the difference in the applied ozone dosage and the intercept of the first-order rapid ozone consumption with the ordinate. Within this approach the model parameters are not related to NOM.

The second approach is an adapted version of the model of Rietveld (2005) and describes rapid ozone consumption in relation to NOM by means of the UVA_{254} decrease:

$$\frac{dc_{O_3}}{dt} = -k_{UVA}(UVA-UVA_o)Y \quad [3]$$

$$\frac{d(UVA)}{dt} = -k_{UVA}(UVA-UVA_o) \quad [4]$$

where k_{UVA} is the UVA_{254} decay rate (1/s), UVA is the UVA_{254} in water (1/m), UVA_o is the stable UVA_{254} after completion of the ozonation process (1/m) and Y is the yield for ozone consumed per UVA_{254} decrease ((mg- O_3 /l)/(1/m)). This model is calibrated and validated on bench-scale DOPFR (100 l/h) experiments (van der Helm et al., 2007b).

The third approach is a new approach, describing rapid ozone consumption assuming diffusion-limited kinetics. From Higbie's penetration theory (Higbie, 1935) follows that displacement (L) of particles due to diffusion increases with the square root of diffusion (D) times time ($L \propto \sqrt{Dt}$). Due to the tortuous path, the displacement of particles by diffusion is not linear in time, as would be for a straight trajectory. This means for rapid ozone consumption that it is a function of the reciprocal value of the square root of time. Rapid ozone consumption following

diffusion-limited kinetics, where the diffusion coefficient is incorporated in the rapid ozone consumption rate coefficient, can be expressed as:

$$\frac{dc_{O_3}}{dt} = -k_{O_3DL} c_{O_3} \frac{1}{2\sqrt{t}} \quad 0 \leq t \leq t_{DL} \quad [5]$$

where k_{O_3DL} is the diffusion-limited rate constant for rapid ozone consumption ($1/\sqrt{s}$) and t_{DL} gives the duration of diffusion limitation (s). For all three approaches a first-order rate reaction was used for describing slow ozone decay to ensure a good transition from rapid ozone consumption to slow ozone decay. For the first-order rapid ozone consumption model the transition occurs after two minutes, for the UVA₂₅₄ decrease model the transition occurs gradually and for the diffusion limitation model the transition occurs at t_{DL} .

The diffusion-limitation model is a general model that should be applicable for different types of water and different scales of experimental setup. In order to investigate the general validity of the diffusion-limitation model data were also used from bench-scale experiments with water from drinking water treatment plant Weesperkarspel of Waternet (van der Helm et al., 2007a) and data from lab-scale experiments with lake Zurich water (Buffle et al., 2006). The tested Weesperkarspel water is seepage water treated by coagulation, self-purification in a lake and rapid sand filtration and optionally treated by ion exchange (IEX) or granular activated carbon (GAC).

Hydraulics of pipe (PFR) and vessel (CSTR)

Before assessing disinfection and by-product formation during ozonation in the pipe and in the vessel, hydraulics were determined by step-tracer experiments using a salt solution. For the pipe the conductivity was simultaneously recorded at multiple sampling points with a maximum of 6, to determine the residence time distributions (RTD) between the sampling points. From the differences in the measured RTD curves, the Peclet number (Pe) was determined by Taylor approximation (Taylor, 1954; Wols et al., 2006). The number of CSTR's was approximated from the Pe number by dividing it by two. The influent and effluent conductivity of the vessel was simultaneously recorded for determination of the RTD of the vessel. The RTD curve was compared to the analytical RTD curves of a single CSTR and two CSTRs in series.

Disinfection in pipe (PFR) and vessel (CSTR)

Disinfection in the pipe was determined by dosing *E. coli* to the tested water and measuring *E. coli* concentration at multiple sampling points in the pipe. For the vessel *E. coli* concentration was measured at the influent and effluent of the vessel. The inactivation was modeled using different semi empirical models. Gyürék and Finch (1998) assessed a great number of disinfection models and concluded that the incomplete gamma Hom model, incorporating first-order ozone decay, described best the inactivation of heterotrophic plate count bacteria. However, for inactivation models that make use of ozone concentrations calculated by separate equations the incomplete gamma Hom model incorporating first-order ozone decay cannot be used. The Hom model without incorporation of ozone decay is given by:

$$\frac{dN}{dt} = -\frac{k}{60} m N c_{O_3}^n t^{m-1} \quad [6]$$

Integration of Equation [6] gives:

$$\log \frac{N}{N_0} = -\frac{k}{60} c_{O_3}^n t^m \quad [7]$$

where N is the number concentration of organisms (CFU/100 ml), N_0 is the number concentration of organisms at time 0 seconds (CFU/100 ml), k is the inactivation rate coefficient ($l/(mg-O_3 \cdot \text{min})$) for $n=1$ and $m=1$ on a \log_{10} base and n and m are empirical constants (-). The Hom model is based on the commonly applied semi empirical Chick-Watson model (Hunt and Mariñas, 1997; Craik et al., 2003; Hijnen et al., 2004). The Chick-Watson model describes the rate of disinfection as first-order in time. Hom (1972) introduced the empirical constants n and m after observing that for chlorine disinfection of natural algal-bacterial systems the inactivation was not linear on a log scale but curvilinear. With the Hom model an initial slow inactivation or a tailing-off effect can be described. When $n=1$ and $m=1$ the Hom model simplifies to the Chick-Watson model. Haas (1980) theorized an inactivation model and found it was a function of the disinfectant concentration and t^2 , so $n=1$ and $m=2$. The influence of temperature on rate constants is normally modeled with Arrhenius' equation, given by:

$$k = A e^{(-E_a / RT_a)} \quad [8]$$

where A is the frequency factor (unit depending on the unit of k), E_a is the activation energy (J/mol), $R = 8.314$ J/(mol*K) is the ideal gas constant and T_a is the absolute temperature of the water (K).

Another model with slow initial inactivation was described by Rennecker et al. (1999). He proposed the delayed Chick-Watson model with a lag-phase for a minimum required ozone dosage:

$$\frac{N}{N_0} = \begin{cases} 1 & \text{if } CT \leq CT_{lag} = \frac{1}{k} \ln \left(\frac{N_1}{N_0} \right) \\ \frac{N_1}{N_0} \exp(-kCT) = \exp(-k \{CT - CT_{lag}\}) & \text{if } CT > CT_{lag} = \frac{1}{k} \ln \left(\frac{N_1}{N_0} \right) \end{cases} \quad [9]$$

where N_1/N_0 is the extrapolated intercept of the first-order line with the ordinate (-), CT is ozone exposure ((mg-O₃/l)*min), and CT_{lag} is the minimum CT value required for obtaining disinfection ((mg-O₃/l)*min). Note that k is at lognormal units here. The Hom model and the delayed Chick-Watson model were assessed on the experimental data measured in the DOPFR.

Disinfection by-product formation

The disinfection by-products of ozonation assessed in this research are bromate and AOC. Bromate was measured at multiple sampling points in the pipe. For modeling of bromate formation two different empirical models were applied. The first model was a multiple linear regression model (Carlson et al., 2001, Sohn et al., 2004):

$$c_{BrO_3} = 1.55 \cdot 10^{-6} (c_{DOC,in})^{-1.26} (pH_{in})^{5.82} (c_{O_3,DOS})^{1.57} (c_{Br,in})^{0.73} \left(\frac{t}{60}\right)^{0.28} (1.035)^{T-20} \quad [10]$$

where c_{BrO_3} is the bromate concentration ($\mu\text{g-BrO}_3/\text{l}$), $c_{DOC,in}$ is the influent dissolved organic carbon concentration (mg-C/l), $1.1 \leq c_{DOC,in} \leq 8.4$, pH_{in} is the influent pH, $6.5 \leq pH_{in} \leq 8.5$, $c_{O_3,DOS}$ is the ozone dosage (mg-O₃/l), $1.1 \leq c_{O_3,DOS} \leq 10.0$, $c_{Br,in}$ is the influent bromide concentration ($\mu\text{g-Br/l}$), $70 \leq c_{Br,in} \leq 440$, t is time (s), $1 \leq t/60 \leq 120$ and T is the temperature of the water ($^{\circ}\text{C}$), $2 \leq T \leq 24$.

The second model is a regression model dedicated to one treatment plant (van der Helm et al., 2007b), using the observation that bromate formation consists of an initial fast increase after which the bromate concentration increases linearly with the CT value (von Gunten and Hoigné, 1994; von Gunten et al., 2001):

$$c_{BrO_3} = c_{BrO_3,ini} + k_{BrO_3}CT \quad [11]$$

$$c_{BrO_3,ini} = F_{BrO_3,ini}c_{O_3,DOS} + c_{BrO_3,in} \quad [12]$$

where $c_{BrO_3,ini}$ is the initial bromate formation ($\mu\text{g-BrO}_3/\text{l}$), k_{BrO_3} is the bromate formation rate constant ($(\mu\text{g-BrO}_3/\text{l})/((\text{mg-O}_3/\text{l})\cdot\text{min})$), $F_{BrO_3,ini}$ is the constant for initial bromate formation ($(\mu\text{g-BrO}_3/\text{l})/(\text{mg-O}_3/\text{l})$), and $c_{BrO_3,in}$ is the influent bromate concentration ($\mu\text{g-BrO}_3/\text{l}$). Both models were assessed on the experimental data measured in the DOPFR.

Models for AOC formation are also usually empirical linear regression models. The model used describes AOC formation per DOC as a function of the ozone dosage (van der Helm et al., 2007a), resulting in the following equation:

$$c_{AOC} = F_{AOC}c_{O_3,DOS}c_{DOC,in} + c_{AOC,in} \quad [13]$$

where c_{AOC} is the AOC concentration ($\mu\text{g-C/l}$), F_{AOC} is the constant for AOC formation per DOC ($(\mu\text{g-C/l})/(\text{mg-O}_3/\text{l}\cdot\text{mg-C/l})$) and $c_{AOC,in}$ is the influent AOC concentration ($\mu\text{g-C/l}$).

Effects of upscaling on ozone decay model parameters for DOPFR concept

The rapid ozone consumption model described by Equations [3] and [4] was calibrated and validated on bench-scale DOPFR (100 l/h) experiments (van der Helm et al., 2007b) including slow ozone decay. Slow ozone decay was modeled by first-order kinetics (Hoigné and Bader, 1994). Expanding Equation [3] with slow ozone decay gives:

$$\frac{dc_{O_3}}{dt} = -k_{UVA}(UVA-UVA_o)Y - k_{O_3}c_{O_3} \quad [14]$$

where k_{O_3} is the slow ozone decay rate (1/s). The experimental data measured in the pilot-scale DOPFR were fitted on Equation [14] and [4]. The fitted model parameters were compared to the model parameters determined in the bench-scale DOPFR to assess the effects of upscaling of the DOPFR concept.

Results and discussion

Rapid ozone consumption

The results of the model fits for the three different approaches for modeling rapid ozone consumption in experiments 5 to 8 are presented in Figure 3. The model where instantaneous ozone demand is followed by first-order rapid ozone consumption was not specifically developed for describing rapid ozone consumption and was based on batch experiments with the first ozone measurement after half a minute or one minute. Consequently, it can be observed from Figure 3 (upper left) that an instantaneous ozone demand followed by first-order rapid ozone consumption does not give an accurate description of rapid ozone consumption for the first 20 seconds. The approaches where rapid ozone consumption is a function of the UVA_{254} decrease (Figure 3, upper right) and where rapid ozone consumption is assumed to follow diffusion-limited kinetics (Figure 3, lower left) give good results for describing rapid ozone consumption.

Table 2 Diffusion-limited rate constants for rapid ozone consumption for different water types and experimental setup

Experimental setup	Water type	Temp [°C]	DOC [mg-C/l]	O ₃ dosage [mg-O ₃ /l]	k_{O_3DL} [1/√s]	Correlation R ² [-]
Pilot plant*	Dune filtered water	16	2.4	0.24	0.647	0.95
Pilot plant*	Dune filtered water	16	2.4	0.58	0.207	0.88
Pilot plant*	Dune filtered water	17	2.4	0.77	0.111	0.98
Pilot plant*	Dune filtered water	16	2.4	0.99	0.085	0.84
Bench-scale**	Seepage (SP) water	12	6.3	1.43	0.387	0.99
Bench-scale**	SP water IEX treated	12	3.1	1.39	0.060	0.81
Bench-scale**	SP water GAC treated	13	2.8	1.48	0.097	0.80
Bench-scale**	Dune filtered water	12	2.4	0.52	0.222	0.97
Bench-scale**	Dune filtered water	12	2.4	0.90	0.087	0.97
Lab-scale***	Lake Zurich water	22	1.4	2.4	0.128	0.99

* installation capacity 2.5 m³/h (experiments 5 to 8 this research)

** installation capacity 100 l/h (van der Helm et al., 2007a)

*** installation capacity 660 ml/h (Buffle et al., 2006)

In Table 2 the fitted diffusion-limited rate coefficients for rapid ozone consumption and the correlation coefficients for the model fit of the first 20 seconds of ozone

contact time are shown for water from different locations and for different scales of the experimental setup. The good fits for the diffusion-limitation model are an indication that rapid ozone consumption follows diffusion-limited kinetics.

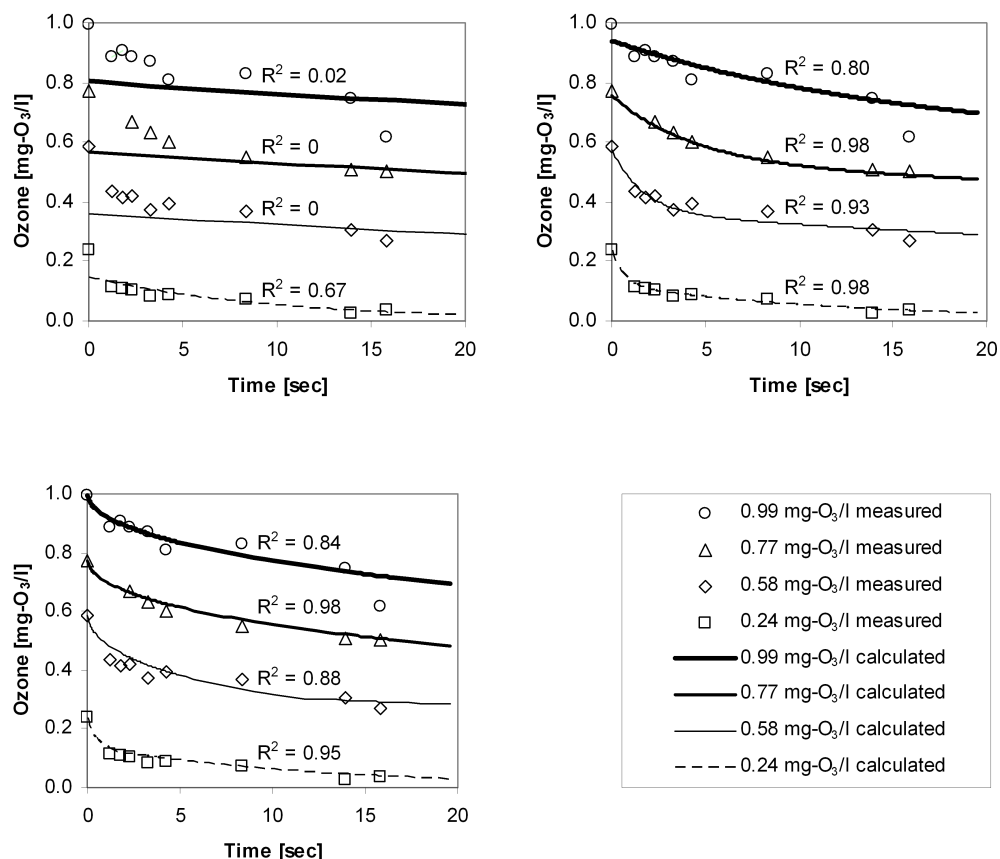


Figure 3 Rapid ozone consumption for experiments 5 to 8 modeled by (i) instantaneous ozone demand with first-order rapid ozone consumption, Equation [2] (upper left); (ii) UVA₂₅₄ decrease, Equations [3] and [4] (upper right); (iii) diffusion limitation, Equation [5] (lower left)

When ozone decay follows diffusion-limited kinetics, it would be expected that the diffusion-limited rate constants are equal for the same water in the same installation for the same temperature, since the diffusion coefficient is then regarded as a constant. In Table 2 it can be observed that this is not the case. The values for the diffusion-limited rate constant, k_{O_3DL} , decrease for increasing ozone dosage (per DOC). This is possibly caused by ozone concentration dependency of

the diffusion coefficient (Loulou et al., 2006; van der Zanden, 1998). Differences in k_{O_3DL} values between different ozone installations may be caused by differences in Reynolds numbers, which influence the turbulent diffusion. In Figure 4 the results for the diffusion-limited kinetics calculations and the measured values for experiments 5 to 8, are plotted against the square root of time. It can be observed that the rapid ozone consumption is a first order reaction on a square root time scale as described by Equation [5].

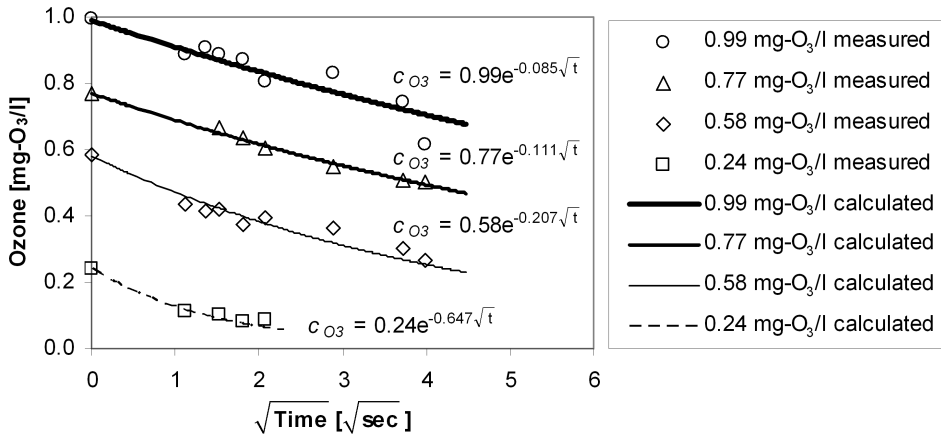


Figure 4 Rapid ozone consumption for experiments 5 to 8 modeled by diffusion limitation on a square root time scale

Hydraulics of pipe (PFR) and vessel (CSTR)

From the step-tracer experiments it was concluded that the pipe can be modeled as 250 CSTRs in series and can thus be seen as a plug flow reactor (Wols et al., 2006). In Figure 5, results of a step-tracer experiment are shown for the vessel. The measured influent and effluent are shown together with the analytical solution for 1 CSTR and for 2 CSTRs in series. From Figure 5, it can be observed that the hydraulic conditions in the vessel approach the hydraulic properties of 1 CSTR and the vessel can thus be modeled as a CSTR.

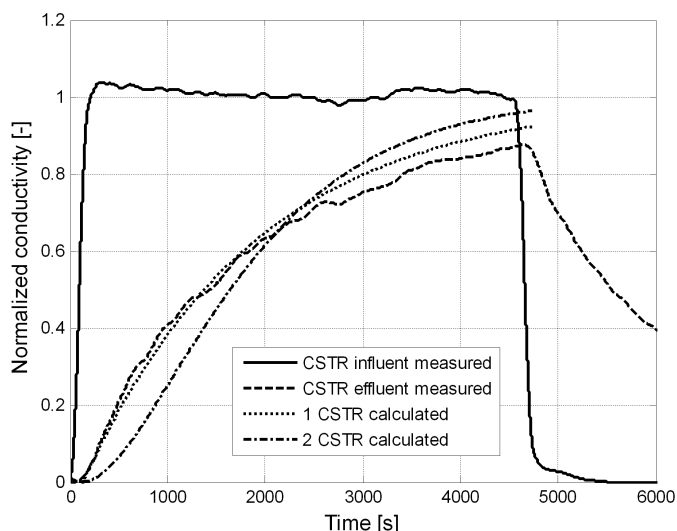


Figure 5 Results of the step-tracer experiment measured at the influent and effluent of the vessel and the analytical solutions for 1 CSTR and 2 CSTRs in series

Disinfection in pipe (PFR) and vessel (CSTR)

In the experiments 5 to 8 *E. coli* were dosed. The Hom model, Equation [7], and the delayed Chick-Watson model, Equation [9], were fitted on the experimental data. The results are shown in Figure 6. In accordance with the findings of Haas (1980), best fits with the Hom model were obtained with $n=1$ and $m=2$ for experiments 6, 7, and 8. By applying $m=2$, the lag phase or shoulder at low t values and high c_{O_3} values disappears. However the model does not fit the data from experiment 5 with a low ozone dosage. The inactivation rate coefficient is the same for different ozone concentrations when plotted on a C times t^2 axis (see Figure 6, left). If plotted on a normal time axis, the inactivation rate coefficient will be different for different ozone dosages. The inactivation rate coefficients fitted on a normal time scale for different ozone dosages are presented in Figure 7 and are found to be an exponential function of the ozone dosage:

$$k = 4.49e^{3.305C_{O_3,DOS}} \quad [15]$$

Because k is calculated for $m=2$, the unit for k on a \log_{10} base becomes $l/(mg-O_3 \cdot \min) \cdot 1/s$ (see Equations [6] and [7]). The best results with the delayed Chick-Watson model were achieved with an inactivation rate coefficient of 316 $l/(mg-$

$O_3 \cdot \text{min}$) and CT_{lag} of 0.010 (mg- O_3 /l)*min (Figure 6, right). For an ozone dosage of 0.58 and 0.77 mg- O_3 /l tailing is observed. For an ozone dosage of 0.24 mg- O_3 /l ozone is depleted before inactivation reaches the point for tailing, and for an ozone dosage of 0.99 mg- O_3 /l tailing is not observed because all samples from experiment 8 with a higher CT value than 0.06 mg- O_3 /l*min had a count of 0 CFU per liter. The model predictions do not account for tailing, only for the lag phase. This means that the predictions for *E. coli* inactivation are valid until an inactivation of 4 log units. Therefore, the correlation coefficients are calculated until an inactivation of 4 log units. The values from the experiment with an ozone dosage of 0.24 mg- O_3 /l are not included in the correlation coefficient for inactivation with the Hom model.

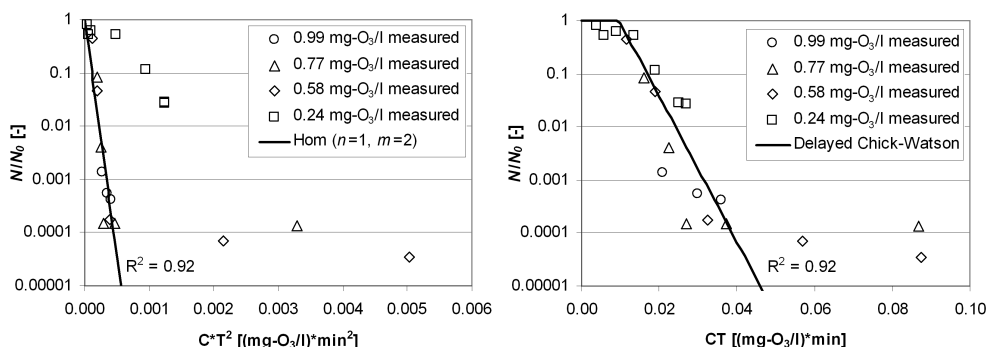


Figure 6 Modeling inactivation of *E. coli* with the Hom model (left) and the delayed Chick-Watson model (right) for experiments 5 to 8; in both graphs the same data is plotted on different abscissas

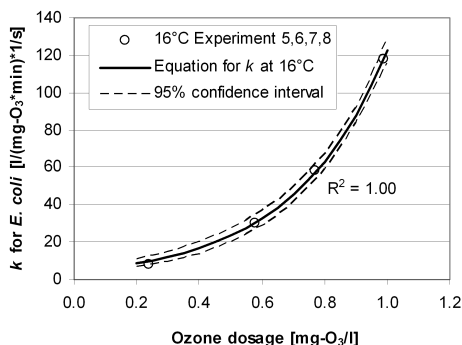


Figure 7 *E. coli* inactivation rate coefficients on a \log_{10} base for Hom model, with $n=1$ and $m=2$ fitted on a normal time scale, as a function of the ozone dosage

In Table 3 the results for *E. coli* inactivation and bromate formation are presented for the pipe that has the hydraulic properties of a PFR and the vessel that has the hydraulic properties of a CSTR. A comparison between the pipe and the vessel was possible since contact time and ozone dose were identical. The comparison was performed for experiments with low ozone dosages resulting in low CT values. It was not possible to measure *E. coli* concentrations in the effluent of the vessel at higher CT values. From Table 3 it can be observed that the PFR has an inactivation capacity of 3 to 5 times more, up to 3 log units difference, than the CSTR for the same amount of ozone dosed. The CT value for the CSTR could not be determined since the effluent ozone concentration of the vessel was 0 mg-O₃/l.

Table 3 Results from the experiments 5, 13 and 14 for the comparison of inactivation and bromate formation between the pipe and the vessel

Experiment	Contactors	CT value [(mg-O ₃ /l)*min]	<i>E. coli</i> [log inactivation]	Bromate formation [µg-BrO ₃ /l]
5	Pipe (PFR)	0.02	1.58	<0.50
5	Vessel (CSTR)	-	0.58	<0.50
13	Pipe (PFR)	0.08	3.71	0.70
13	Vessel (CSTR)	-	0.90	<0.50
14	Pipe (PFR)	0.08	3.58	<0.50
14	Vessel (CSTR)	-	0.67	<0.50

Disinfection by-product formation

Prediction of bromate formation with the multiple linear regression model given by Equation [10] was done for experiments 5 to 8 (see Figure 8). However, the linear regression model is valid for the ozone dosage range of 1.1-10.0 mg-O₃/l, so it cannot be used for experiments 5, 6 and 7, and the correlation coefficient is calculated only for experiment 8. Bromate formation in the first 60 seconds was not calculated because the model is only valid after 60 seconds of contact time.

Results of modeling bromate formation during the ozonation process in the DOPFR with an initial fast increase followed by a linear increase with the CT value as described by Equations [11] and [12], are shown in Figure 9 for experiments 5 to 8. For all experiments the bromate formation rate constant used was 1.66 (µg-BrO₃/l)/((mg-O₃/l)*min) and the constant for initial bromate formation used was 2.17 (µg-BrO₃/l)/(mg-O₃/l). The usage of the same rate constant gave an overestimation of 30% for experiment 5, however the absolute overestimation was less than 0.3 µg-BrO₃/l and the bromate concentrations were very near the detection limit of 0.5 µg- BrO₃/l (see inset Figure 9).

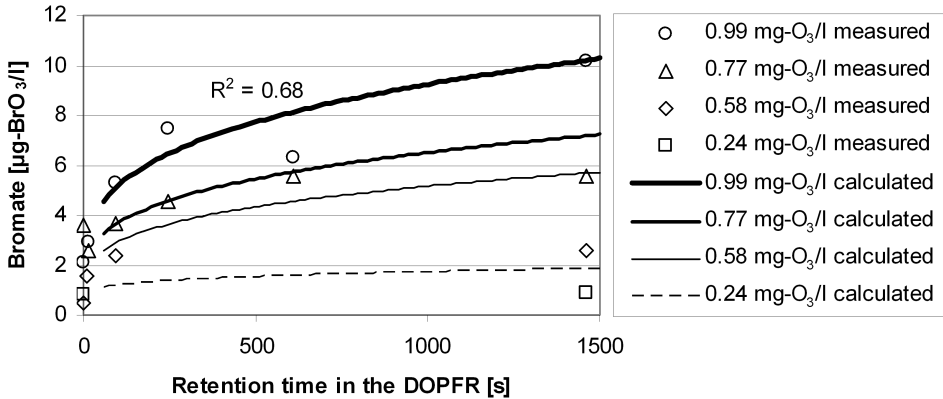


Figure 8 Bromate formation measured and calculated with the multiple linear regression model for experiments 5 to 8

In Figure 10 the final bromate concentrations after depletion of ozone are plotted versus the total CT value for experiments 1 to 12. The lower right inset shows all values, including an experiment with a high CT value, and the upper left inset is the Arrhenius' plot for the dependency of the final bromate concentrations on temperature.

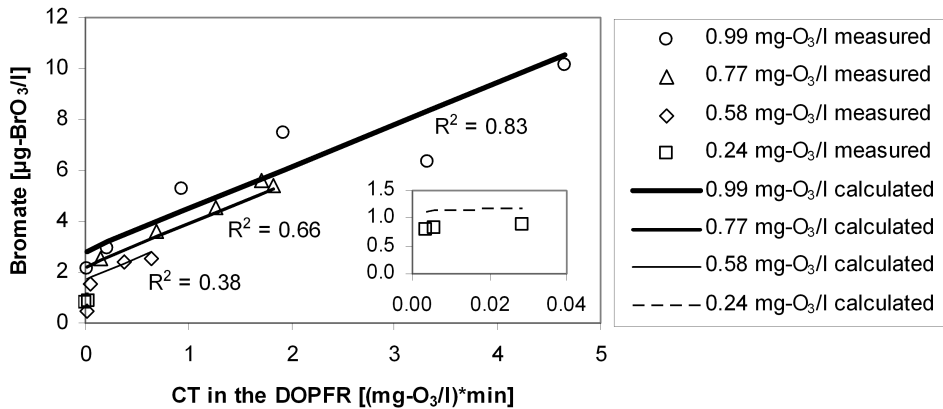


Figure 9 Bromate formation measured and calculated in the DOPFR, with the model describing bromate formation as an initial fast increase depending on the ozone dosage followed by a linear increase with the CT value for experiments 5 to 8

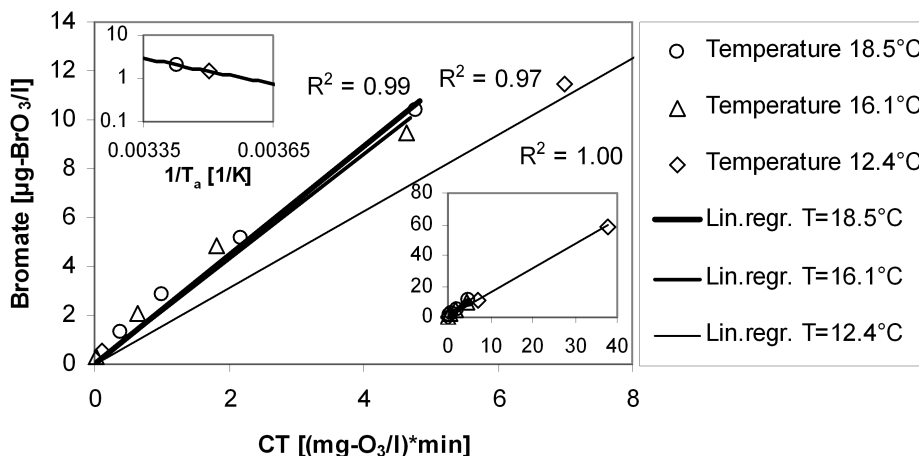


Figure 10 Bromate concentrations after completion of the ozonation process versus the total CT value for experiments 1 to 12; inset upper left is the Arrhenius' plot for the bromate formation, all data are in inset lower right

It can be observed that bromate formation in the pipe modeled as a linear function of the CT value can be applied at low ozone dosages. However, the correlation is lower for lower ozone dosages. The correlations for the total amount of bromate formed after ozonation plotted versus the total CT value are high and show a clear linear relationship (see Figure 10).

Results for AOC formation per DOC modeled as a function of the ozone dosage are presented in Figure 11. The constant for AOC formation is plotted in the Arrhenius' plot (inset in Figure 11) for the different temperatures and was 45 ($\mu\text{g-C/l}/(\text{mg-O}_3/\text{l} \cdot \text{mg-C/l})$) for experiments 5 to 8 at 16.1°C. This regression of AOC formation per DOC as a function of the ozone dosage can thus be used to give an indication of the AOC formation during ozonation.

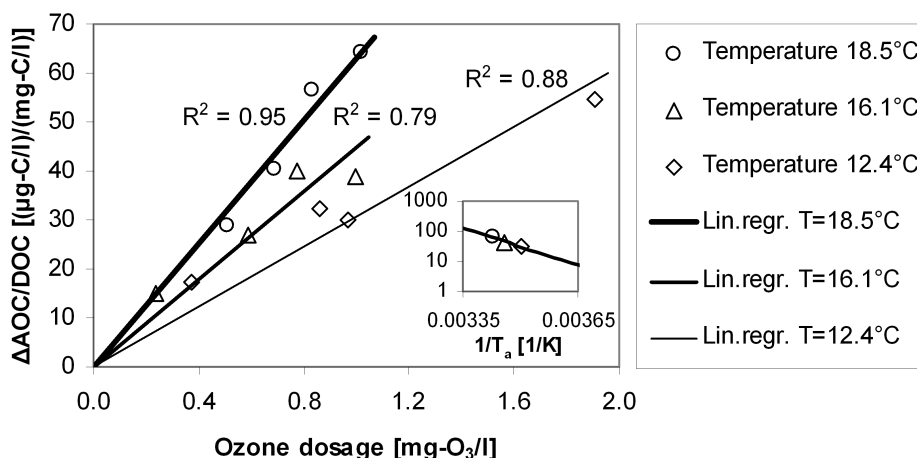


Figure 11 AOC formation per DOC as a function of the ozone dosage for experiments 1 to 12; the dependency of the temperature is shown in the Arrhenius' plot (inset)

Effects of upscaling on ozone decay model parameters for the DOPFR concept

The model given by Equations [14] and [4] has proven to adequately describe ozone decay in bench-scale DOPFR (100 l/h) ozonation experiments (van der Helm et al., 2007b). Some of the data from the bench-scale experiments were used for calibration of the model parameters, k_{O_3} , k_{UVA} , Y and UVA_0 , and some for validation of the model. In Figure 12 the calibrated equations for the model parameters based on the bench-scale experiments with their respective confidence intervals are shown. Within these graphs the fitted parameters from the pilot-scale experiments 1 to 12 are plotted. It is observed that the data from the pilot-scale experiments are within the confidence intervals of the data of the bench-scale experiments for k_{O_3} , k_{UVA} and $(UVA_{in} - UVA_0)$. The values for the Y are more scattered and partly outside the confidence interval. However, the average of the data including the pilot-scale data gives a horizontal line instead of the increasing line in Figure 12 (lower left). This was to be expected since the yield for consumed ozone per UVA_{254} decrease should be independent of the ozone dosage and the temperature because it has the properties of a stoichiometric coefficient. The k_{O_3} and k_{UVA} are temperature dependent, however, the dependency of k_{O_3} and k_{UVA} on temperature in the pilot-plant experiments is not as pronounced as from the bench-scale experiments. If it is assumed that the model parameters from the bench-scale

experiment at 20°C are outliers and taking into account that all pilot-scale experiments with temperatures ranging from 12°C to 19°C are within the confidence intervals determined for 12°C in the bench-scale experiments, no distinction can be made for the model parameters for different temperatures based on these experiments. For determination of a temperature dependency a larger number of experiments are needed for a larger temperature range.

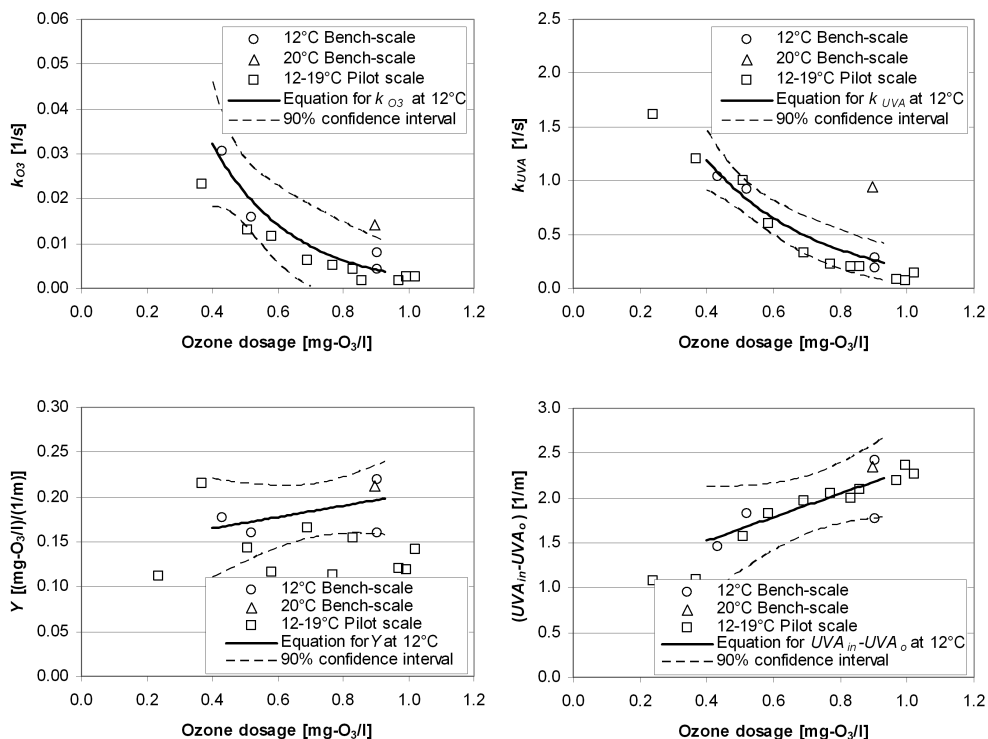


Figure 12 k_{O_3} , k_{UVA} , Y and $(UVA_{in}-UVA_0)$ as a function of the ozone dosage with their 90% confidence intervals for bench-scale experiments (van der Helm et al., 2007b) and for pilot-scale experiments 1 to 12

In Figure 12, upper left, it is observed that the rate of slow ozone decay decreased with increasing ozone dosage. Assuming a constant contribution of the ozone decomposition cycle, this can be explained by the various types of sites within NOM that have different reactivity with ozone. For low ozone dosages only the fast-reacting sites consume ozone. When higher ozone dosages were applied, the rate of ozone consumption decreased when slowly reacting sites were oxidized as well (Hoigné and Bader, 1994; Gallard et al., 2003). In Figure 12, upper right, it is

observed that the rate of rapid ozone consumption also decreases with increasing ozone dosage. Because k_{UVA} describes a process that follows diffusion-limited kinetics, this is possibly caused by ozone concentration dependency of the diffusion coefficient as discussed before.

Based on the data from experiments 1 to 12, the functions for k_{O_3} , k_{UVA} , Y and $(UVA_{in}-UVA_0)$ are:

$$k_{O_3} = 0.1454e^{-4.372C_{O_3,DOS}} \quad [16]$$

$$k_{UVA} = 3.75e^{-3.443C_{O_3,DOS}} \quad [17]$$

$$Y = -0.0042C_{O_3,DOS} + 0.137 \approx 0.137 \quad [18]$$

$$UVA_0 = UVA_{in} - (1.261C_{O_3,DOS} + 1.0237) \quad [19]$$

where UVA_{in} is the influent UVA_{254} (1/m).

Dynamic model for dissolved ozone dosing

In order to simulate the discussed processes simultaneously with regard to changes in the influent water quality over time, the models were incorporated into Stimela. Stimela is an environment where different drinking water treatment processes can dynamically be modeled. The Stimela models are developed in Matlab/Simulink[®]. Partial differential equations are numerically integrated so variations in time and space can be followed (van der Helm and Rietveld, 2002). For rapid ozone consumption the model using UVA_{254} decrease was selected and not the diffusion-limitation model. The main reason for this selection was that this model relates rapid ozone consumption to reactions with NOM, and with on-line UVA_{254} measurement an extra parameter is available for on-line calibration and validation. To describe disinfection, the Hom model was selected with $n=1$ and $m=2$. Reasons for this were its consistency with the inactivation model theorized by Haas (1980) and the fact that it has one parameter less to fit than the delayed Chick-Watson model where both k and CT_{lag} have to be fitted. For bromate formation the model based on linearity with CT values was selected because it is able to predict bromate concentrations at low ozone dosages, contrary to the

general multiple linear regression model for bromate formation that is not valid for low ozone dosages. Applying bromate formation as a function of the CT value has an extra advantage in a dynamic modeling environment such as Stimela: a partial differential equation for the CT value can be formulated so that the CT development during the ozonation process is simultaneously calculated. Summarizing, the partial differential equations for the ozonation model of the DOPFR were:

$$\frac{\partial c_{O_3}}{\partial t} = -u \frac{\partial c_{O_3}}{\partial x} - k_{UVA}(UVA - UVA_o)Y - k_{O_3} c_{O_3} \quad [20]$$

$$\frac{\partial c_{UVA}}{\partial t} = -u \frac{\partial c_{UVA}}{\partial x} - k_{UVA}(UVA - UVA_o) \quad [21]$$

$$\frac{\partial c_{BrO_3}}{\partial t} = -u \frac{\partial c_{BrO_3}}{\partial x} + k_{BrO_3} c_{O_3} \quad c_{BrO_3,ini} = F_{BrO_3,ini} c_{O_3,DOS} + c_{in,BrO_3} \quad [22]$$

$$\frac{\partial N}{\partial t} = -u \frac{\partial N}{\partial x} - kmNc_{O_3}^n (t/60)^{m-1} \quad [23]$$

$$\frac{\partial CT}{\partial t} = -u \frac{\partial CT}{\partial x} + c_{O_3} \quad [24]$$

where u is the water velocity (m/s) and x is the length of the reactor (m). The AOC concentration was not modeled as a partial differential equation but as a regression according to Equation [13]. The temperature range from 12°C to 19°C was not wide enough to determine temperature dependency for k_{UVA} , k_{O_3} and UVA_o in the pilot-plant experiments. For the temperature dependency on the F_{AOC} the derived Arrhenius' plot was used in the model. The k_{BrO_3} and $F_{BrO_3,ini}$ for the formation of bromate during ozonation could not be derived from the Arrhenius' relation, only the end value of bromate concentration after complete depletion of ozone could. In order to calculate the bromate formation during ozonation the $k_{BrO_3} = 1.66$ ($\mu\text{g-BrO}_3/\text{l})/((\text{mg-O}_3/\text{l})\cdot\text{min})$ and $F_{BrO_3,ini} = 2.17$ ($\mu\text{g-BrO}_3/\text{l})/(\text{mg-O}_3/\text{l})$ were used. The temperature dependency on the inactivation rate of *E. coli* could not be derived from experiments 1 to 12 since *E. coli* dosing was only performed in experiments 5 to 8 with approximately the same temperatures.

An example of the results of the Stimela ozone model for experiment 7 is given in Figure 13. All parameters used for the calculations in Figure 13 were determined from the derived relationships. From Figure 13 the differences in time scales for the different processes during ozonation can be observed. It shows that *E. coli* inactivation is 4 log units after 5 seconds, that the major part of the rapid ozone consumption is finished after 20 seconds (UVA_{254} decrease has stopped) and that bromate formation stops after approximately 700 seconds. On the basis of the model calculation, the total CT in the pipe can be accurately estimated and is 1.65 (mg-O₃/l)*min. With the model, effects of changes in the operation or changes in the influent water quality can be evaluated.

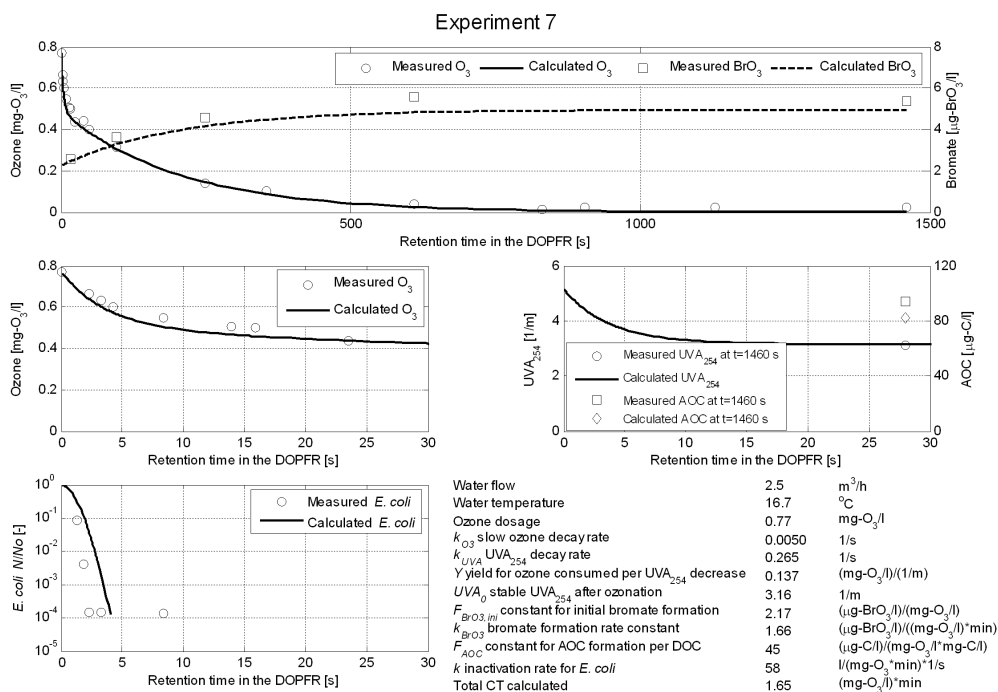


Figure 13 Results of the dynamic Stimela ozonation model for experiment 7

Conclusions

From experiments where ozone decay was measured from 1.3 seconds to 1450 seconds and literature data describing ozone decay in the first 20 seconds of contact time, it has been concluded that the rate of rapid ozone consumption followed diffusion-limited kinetics. For the water tested, a majority of ozone-

sensitive organisms were inactivated during rapid ozone consumption. From the experiments it can be concluded that the disinfection capacity for the ozone-sensitive organism *E. coli* is 3 to 5 times higher in a PFR compared to a CSTR. Therefore, focus should be on establishing plug flow conditions from the first contact between ozone and water. This can be achieved by instant mixing of ozone in water with a static mixer, followed by a contactor approaching plug flow characteristics. If ozone is not properly mixed over the total water flow and for instance 1% is not ozonated, then, the disinfection capacity is limited to 2 log units. From comparison of different bromate formation models, it can be concluded that modeling bromate formation as an initial fast increase after which the concentration increases linearly with the CT value gave good results for prediction of bromate formation. From comparison of model parameters for ozone decay based on bench-scale experiments and pilot-scale experiments, it can be concluded that upscaling of the DOPFR concept gives consistent results and upscaling to a full-scale installation would therefore be possible from the bench-scale and pilot-scale experiments. From pilot-plant experiments a dynamic model was developed for describing ozonation in a DOPFR. It is concluded that semi-empirical models are suited for modeling of ozone decay, disinfection, bromate and AOC formation in natural water.

Acknowledgement

This research was carried out as part of the project 'Promicit', a cooperation of Waternet, Delft University of Technology, DHV B.V. and ABB B.V. and was subsidized by SenterNovem, agency of the Dutch Ministry of Economic Affairs. The aim of the project was to achieve a breakthrough in drinking water quality control by developing an integrated model of the total water treatment and using this model as a basis for operation.

Nomenclature

AOC	assimilable organic carbon
CSTR	completely stirred tank reactor
DOC	dissolved organic carbon
DOPFR	dissolved ozone plug flow reactor
<i>E. coli</i>	<i>Escherichia coli</i>
NOM	natural organic matter
PFR	plug flow reactor

RTD	residence time distribution
UVA_{254}	UV absorbance at 254 nm
Waternet	water cycle company for Amsterdam and surrounding areas
A	frequency factor (unit depending on the unit of k)
C_{AOC}	AOC concentration ($\mu\text{g-C/l}$)
$C_{AOC,in}$	influent AOC concentration ($\mu\text{g-C/l}$)
$C_{Br,in}$	influent bromide concentration ($\mu\text{g-Br/l}$)
C_{BrO_3}	bromate concentration ($\mu\text{g-BrO}_3/\text{l}$)
$C_{BrO_3,in}$	influent bromate concentration ($\mu\text{g-BrO}_3/\text{l}$)
$C_{BrO_3,ini}$	initial bromate formation ($\mu\text{g-BrO}_3/\text{l}$)
$C_{DOC,in}$	influent dissolved organic carbon concentration (mg-C/l)
C_{O_3}	concentration of ozone in water ($\text{mg-O}_3/\text{l}$)
$C_{O_3,DOS}$	ozone dosage ($\text{mg-O}_3/\text{l}$)
CT	ozone exposure ($(\text{mg-O}_3/\text{l}) \cdot \text{min}$)
CT_{lag}	minimum CT required for obtaining disinfection ($(\text{mg-O}_3/\text{l}) \cdot \text{min}$)
E_a	activation energy (J/mol)
F_{AOC}	constant for AOC formation per DOC ($(\mu\text{g-C/l})/(\text{mg-O}_3/\text{l} \cdot \text{mg-C/l})$)
$F_{BrO_3,ini}$	constant for initial bromate formation ($(\mu\text{g-BrO}_3/\text{l})/(\text{mg-O}_3/\text{l})$)
k	inactivation rate coefficient ($1/(\text{mg-O}_3 \cdot \text{min})$ for $n=1$ and $m=1$)
k_{BrO_3}	bromate formation rate constant ($(\mu\text{g-BrO}_3/\text{l})/((\text{mg-O}_3/\text{l}) \cdot \text{min})$)
k_{O_3}	slow ozone decay rate ($1/\text{s}$)
k_{O_3DL}	diffusion-limited rate constant for rapid ozone consumption ($1/\sqrt{\text{s}}$)
k_{O_3R}	first-order rapid ozone consumption rate ($1/\text{s}$)
k_{UVA}	UVA_{254} decay rate ($1/\text{s}$)
n_{SP}	number of sampling points (-)
n, m	empirical constants (-)
N	number concentration of organisms (CFU/100 ml)
N_0	number concentration of organisms at time 0 (CFU/100 ml)
N_1/N_0	extrapolated intercept of the first-order line with the ordinate (-)
Pe	Peclet number
pH_{in}	influent pH
R	ideal gas constant ($8.314 \text{ J}/(\text{mol} \cdot \text{K})$)
t	time (s)
T_a	absolute temperature of the water (K)
T	temperature of the water ($^{\circ}\text{C}$)
t_{DL}	duration of diffusion limitation (s)
UVA	UVA_{254} in water ($1/\text{m}$)

UVA_o	stable UVA_{254} after completion of the ozonation process (1/m)
UVA_{in}	influent UVA_{254} (1/m)
Y	yield for ozone consumed per UVA_{254} decrease ((mg- O_3 /l)/(1/m))
u	water velocity (m/s)
x	length of the reactor (m)

References

- Bader, H. and Hoigné, J. (1982). Determination of ozone in water by the indigo method; a submitted standard method. *Ozone Sci. Eng.*, 4(4), 169-176.
- Buffle, M., Schumacher, J., Salhi, E., Jekel, M. and von Gunten, U. (2006). Measurement of the initial phase of ozone decomposition in water and wastewater by means of a continuous quench-flow system: Application to disinfection and pharmaceutical oxidation. *Water Res.*, 40(9), 1884-1894.
- Bühler, R.E., Staehelin, J. and Hoigné, J. (1984). Ozone decomposition in water studied by pulse radiolysis. 1. HO₂/O₂- and HO₃/O₃- as intermediates. *J Phys. Chem.*, 88, 2560-2564.
- Carlson, K.H., Bellamy, W., Ducoste, J. and Amy, G.L. (2001). *Implementation of the Integrated Disinfection Design Framework*. AWWARF, Denver, USA.
- Chandrananth, M., Leparc, J., Smith, D.W., Craik, S., Finch, G., Lake, R., Agutter, P., Traversay, C. de, Wolbert, D. and Amy, G.L. (2003). *Improvement of the ozonation process through the use of static mixers*. AWWARF/IWA Publishing, London, UK.
- Craik, S.A., Smith, D.W., Chandrananth, M.S. and Belosevic, M. (2003). Efficient inactivation of *Cryptosporidium parvum* in static mixer ozone contactor. *Ozone Sci. Eng.*, 25(4), 295-306.
- Gallard, H., von Gunten, U. and Kaiser, H.P. (2003). Prediction of the disinfection and oxidation efficiency of full-scale ozone reactors. *J. Water Supply Res. Technol. AQUA*, 52(4), 277-290.
- Gilbert, E. (1981). Photometrische bestimmung niedriger ozonkonzentrationen in wasser mit hilfe von Diäthyl-p-phenylendiamin (DPD) (Photometric determination of low ozone concentrations in water using Diethyl-p-phenylenediamine (DPD)). *GWF Wasser Abwasser*, 122(9), 410-416.
- Gilbert, E. and Hoigné, J. (1983). Messung von ozon in wasserwerken; Vergleich der DPD- und indigo-methode (Measurement of ozone in water treatment; Comparison of the DPD and indigo method). *GWF Wasser Abwasser*, 124(11), 527-531.

- Gillogly, T., Najm, I., Minear, R., Mariñas, B., Urban, M., Kim, J.H., Echigo, S., Amy, G., Douville, C., Daw, B., Andrews, R., Hofmann, R. and Croué, J.P. (2001). *Bromate formation and control during ozonation of low bromide waters*. AWWARF/AWWA, Denver, USA.
- Gyürék, L.L and Finch, G.R. (1998). Modeling water treatment chemical disinfection kinetics. *J. Environ. Eng.-ASCE*, 124(9), 783-793.
- Haas, C.N. (1980). A mechanistic kinetic model for chlorine disinfection. *Environ. Sci. Technol.*, 14(3), 339-340.
- Higbie, R. (1935). The rate of absorption of a pure gas into a still liquid during a short time of exposure. *Trans. Am. Inst. Chem. Eng.*, 31, 365–389.
- Hijnen, W.A.M., Baars, E.T., Bosklopper, Th.G.J., van der Veer, A.J., Meijers, R.T. and Medema, G.J. (2004). Influence of DOC on the inactivation efficiency of ozonation assessed with *Clostridium perfringens* and a lab-scale continuous flow system. *Ozone Sci. Eng.*, 26(5), 465-473.
- Hoigné, J. and Bader, H. (1994). Characterization of water quality criteria for ozonation processes. Part II: Lifetime of added ozone. *Ozone Sci. Eng.*, 16(2), 121–134.
- Hom, L.W. (1972). Kinetics of chlorine disinfection in an ecosystem. *J. Sanit. Eng. Div.*, 98(SA1), 183-194.
- Hunt, N.K. and Mariñas, B.J. (1997). Kinetics of *Escherichia coli* inactivation with ozone. *Water Res.*, 31(6), 1355-1362
- Jackson, J.R., Overbeck, P.K. and Overby, J.M. (1999). Dissolved oxygen control by pressurized side stream ozone contacting and degassing. *Proceedings of the IOA-EA3G 14th world congress and exhibition*, Dearborn, USA, 1999.
- Loulou, T., Adhikari, B. and Lecomte, D. (2006). Estimation of concentration-dependent diffusion coefficient in drying process from the space-averaged concentration versus time with experimental data. *Chem. Eng. Sci.*, 61(22), 7185-7198.
- Muroyama, K., Yamasaki, M., Shimizu, M., Shibutani, E. and Tsuji, T. (2005). Modeling and scale-up simulation of U-tube ozone oxidation reactor for treating drinking water. *Chem. Eng. Sci.*, 60(22), 6360-6370.
- Orlandini, E., Kruithof, J., van der Hoek, J.P., Siebel, M. and Schippers, J. (1997). Impact of ozonation on disinfection and formation of biodegradable organic matter and bromate. *J. Water Supply Res. Technol. AQUA*, 46(1), 20-30.
- Park, H., Hwang, T., Kang, J., Choi, H. and Oh, H. (2001). Characterization of raw water for the ozone application measuring ozone consumption rate. *Water Res.*, 35(11), 2607-2614.

- Rakness, K.L. (2005). *Ozone in drinking water treatment: Process design, operation, and optimization*. AWWA, Denver, USA.
- Rennecker, J.L., Mariñas, B.J., Owens, J.H. and Rice, E.W. (1999). Inactivation of *Cryptosporidium parvum* oocysts with ozone. *Water Res.*, 33(11), 2481-2488.
- Rietveld, L.C. (2005). *Improving operation of drinking water treatment through modelling*. PhD Thesis, Faculty of Civil Engineering and Geosciences, Delft University of Technology.
- Roustan, M., Liné, A. and Wable, O. (1992). Modeling of vertical downward gas-liquid flow for the design of a new contactor. *Chem. Eng. Sci.*, 47(13-14), 3681-3688.
- Smeenck, J.G.M.M., van Rossum, W.J.M., Gademan, W.J.H. and Bruggink, C. (1994). Trace level determination of bromate and chlorite in drinking and surface water by ion chromatography with automated preconcentration. *Proceedings of the International Ion Chromatography Symposium*, Torino, Italy, 1994.
- Smeets, P.W.M.H., van der Helm, A.W.C., Dullemont, Y.J., Rietveld, L.C., van Dijk, J.C. and Medema, G.J. (2006). Inactivation of *Escherichia coli* by ozone under bench-scale plug flow and full-scale hydraulic conditions. *Water Res.*, 40(17), 3239-3248.
- Sohn, J., Amy, G., Cho, J., Lee, Y. and Yoon, Y. (2004). Disinfectant decay and disinfection by-products formation model development: chlorination and ozonation by-products. *Water Res.*, 38(10), 2461-2478.
- Staehelin, J. and Hoigné, J. (1982). Decomposition of ozone in water: rate of initiation by hydroxide ions and hydrogen peroxide. *Environ. Sci. Technol.*, 16(10), 676-681.
- Staehelin, J., Bühler, R.E. and Hoigné, J. (1984). Ozone decomposition in water studied by pulse radiolysis. 2. OH and HO₄ as chain intermediates. *J. Phys. Chem.*, 88(24), 5999-6004.
- Standard Methods (2005). *Standard Methods for the examination of water & wastewater 2005 21st edition*, American Public Health Association/American Water Works Association/Water Environment Federation, Baltimore, USA.
- Taylor, G. (1954). The dispersion of matter in turbulent flow through a pipe. *Proceedings of the Royal Society of London, Series A, Mathematical and Physical Sciences*, 223(1155), 446-468.
- van der Helm, A.W.C. and Rietveld, L.C. (2002). Modelling of drinking water treatment processes within the Stimela environment. *Water Sci. Technol.: Water Supply*, 2(1), 87-93.

- van der Helm, A.W.C., Grefte, A., Baars, E.T., Rietveld, L.C., van Dijk, J.C. and Amy, G.L. (2007a). Effects of natural organic matter (NOM) character and removal on efficiency of ozonation. *J. Water Supply Res. Technol. AQUA*, submitted for publication, April 2007.
- van der Helm, A.W.C., Smeets, P.W.M.H., Baars, E.T., Rietveld, L.C. and van Dijk, J.C. (2007b). Modelling of Ozonation for Dissolved Ozone Dosing. *Ozone Sci. Eng.*, accepted for publication, February 2007.
- van der Kooij, D., Visser, A. and Hijnen, W.A.M. (1982). Determining the concentration of easily assimilable organic carbon in drinking water. *Am. Water Works Assoc. J.*, 74(10), 540-545.
- van der Zanden, A.J.J. (1998). An iterative procedure to obtain the concentration dependency of the diffusion coefficient from the space-averaged concentration vs time. *Chem. Eng. Sci.*, 53(7), 1397-1404.
- von Gunten, U. and Hoigné, J. (1994). Bromate formation during ozonation of bromide-containing waters: Interaction of ozone and hydroxyl radical reactions. *Environ. Sci. Technol.*, 28(7), 1234-1242.
- von Gunten, U., Driedger, A., Gallard, H. and Salhi, E. (2001). By-products formation during drinking water disinfection: a tool to assess disinfection efficiency? *Water Res.*, 35(8), 2095-2099.
- von Gunten, U. (2003). Ozonation of drinking water: Part II. Disinfection and by-product formation in presence of bromide, iodide or chlorine. *Water Res.*, 37(7), 1469-1487.
- von Gunten, U., Huber, M.M., Göbel, A., Joss, A., Hermann, N., Löffler, D., McArdell, C.S., Ried, A., Siegrist, H. and Ternes, T.A. (2005). Oxidation of pharmaceuticals during ozonation of municipal wastewater effluents: a pilot study. *Proceedings of the IOA 17th World Ozone Congress*, Strasbourg, France, 2005.
- Westerhoff, P., Aiken, G., Amy, G. and Debroux, J. (1999). Relationships between the structure of Natural Organic Matter and its reactivity towards molecular ozone and hydroxyl radicals. *Water Res.*, 33(10), 2265-2276.
- Westerhoff, P. (2002). *Kinetic-based models for bromate formation in natural waters*. USEPA Washington, USA.
- Wols, B.A., Hofman, J.A.H.M., Uijtewaal, W.S.J. and van Dijk, J.C. (2006). The effect of turbulent diffusion on the performance of ozone systems. *Proceedings of the Workshop Developments in Drinking Water Treatment Modelling*, Delft University of Technology, Delft, the Netherlands, 2006.

5. Effects of natural organic matter (NOM) character and removal on efficiency of ozonation

The objective of this study was to evaluate the effects of the character and the removal of natural organic matter (NOM) on the formation of assimilable organic carbon (AOC) and bromate during ozone disinfection, in order to determine what amount and which part of the NOM should be removed prior to ozonation for improvement of ozonation efficiency. Natural waters from two locations with different dissolved organic carbon (DOC) concentrations were tested. In addition, the DOC concentration of one of the natural waters was reduced either by ion exchange (IEX) or by granular activated carbon (GAC) filtration. The resulting four water types were tested in conventional pilot-scale ozone bubble column reactors and in a bench-scale plug flow reactor with dissolved ozone dosing. For the tested waters UV absorbance at 254 nm (UVA_{254}), ozone, AOC, bromate, and DOC concentrations were measured. NOM fractions were determined with size exclusion chromatography with DOC and UVA_{254} detection. It is concluded that for the same ozone dosages the CT is higher when NOM is removed by IEX or GAC compared to the situation without NOM removal. In addition it is concluded that ozonation efficiency improved more with the removal of the humic substances fraction (MW ~ 1000 g/mol) of NOM as compared to the removal of the building blocks fraction (MW 300-500 g/mol) of NOM, because it led to less AOC formation and less bromate formation this could be achieved by NOM removal using IEX.

Introduction

Natural organic matter (NOM) can be quantified and characterized in different ways. The most basic quantification of NOM is measurement of total organic carbon (TOC), or dissolved organic carbon (DOC), after filtering the sample through a 0.45 μm filter. The difference between TOC and DOC is particulate

organic carbon (POC). NOM is a mixture of a range of organic components that can be further characterized by size, polarity, aromaticity, functionality, and biodegradability.

NOM characterization by size is possible with size exclusion chromatography combined with online dissolved organic carbon detection (SEC-DOC, also known as LC-OCD). With this method the chromatographic part of the DOC can be separated into groups of different molecular weight (MW), humic substances (~1000 g/mol), building blocks (breakdown products of humic substances, 300-500 g/mol), neutrals and amphiphilics (< 350 g/mol) and low molecular weight (LMW) acids (Huber and Frimmel, 1992, 1996). Characterization by humics and non-humics is also possible with SEC-DOC because it also detects non-humic components such as polysaccharides and proteins (MW \geq 20000 g/mol). With three-dimensional fluorescence excitation-emission matrices (FEEM) it is also possible to separately distinguish humic-like (humic and fulvic acids) and protein-like organic matter, but fluorescence detection is inappropriate for measuring polysaccharides (Amy and Her, 2004).

Characterization by polarity is possible with the XAD-8/4 resin adsorption chromatography method where DOC can be fractionated into hydrophobic and transphilic organic acids as the fractions that are retained on XAD-8 and XAD-4 resins, respectively. The XAD-8 adsorbable fraction also corresponds to the humic substances fraction, distinguished from non-humics or hydrophilic fraction (not adsorbed by XAD-8).

Characterization of NOM by its aromaticity is done by UV absorbance at 254 nm (UVA_{254}). UVA_{254} is sensitive to unsaturated bonds. In natural waters, most unsaturated bonds are present in NOM as aromatic carbon. The aromaticity per unit of DOC is expressed by the specific UV absorbance (SUVA), which is defined by UVA_{254} expressed as the absorbance per meter of path length (1/m) divided by the DOC concentration (mg-C/l). Edzwald and Tobiason (1999) developed a classification for NOM based on SUVA stating that, when SUVA is larger than 4 (1/m)/(mg-C/l), NOM consists mostly of aquatic humics with high hydrophobicity and high molecular weight; when SUVA is smaller than 2 (1/m)/(mg-C/l), NOM consists mostly of non-humics with low hydrophobicity and LMW; and, when SUVA is between 2 and 4 (1/m)/(mg-C/l), NOM is a mixture of humics and non-humics. From NOM characterization by SEC, XAD-8/4, solid state ^{13}C NMR, FEEM and

SUVA, Croué et al. (1999) also found positive correlations between higher hydrophilic character, lower C/O atomic ratio, lower SUVA, lower aromatic carbon content and lower molecular weight. Westerhoff et al. (1999) observed that SUVA, aromatic carbon content and molecular weight correlate well for NOM isolates.

The biodegradable part of NOM can be expressed by biodegradable DOC (BDOC) (Joret and Levy, 1986) or by assimilable organic carbon (AOC) (van der Kooij et al., 1982).

Several studies have been undertaken on the removal of NOM by ion exchange (IEX) and granular activated carbon (GAC) with respect to NOM character. Croué et al. (1999) did extensive research on two strong base anion exchange resins (macroporous matrix and gel matrix) and one weak base anion exchange resin. Croué et al. concluded that strong base resins are generally more efficient for removal of DOC, and the higher the molecular weight of the NOM fraction, the lower the affinity with the anion exchange resin. Hongve et al. (1999) performed tests with a macroporous polystyrene based anion exchange resin and found that the major removal was in DOC with a molecular weight of less than 5000 g/mol. Newcombe et al. (2002) studied NOM removal with 6 different GAC types using ¹³C NMR, high-performance size exclusion chromatography, UV-visible absorbance and elemental analysis for NOM characterization. From this research, it was concluded that adsorption of NOM isolates is controlled predominantly by the relationship between the molecular weight distribution of the NOM and the pore size distribution of the carbon. The LMW compounds were adsorbed to a greater extent compared to the larger compounds, due to size exclusion effects. These results were based on three NOM isolates with average molecular weights of 949, 1232, and 2647 g/mol.

Matilainen et al. (2006) conducted research on the performance and capacity of NOM removal by three different GAC types. These researchers using high-performance size exclusion chromatography measurements, concluded that GAC was most effective for DOC fractions with a molecular weight of 1000 – 4000 g/mol and that the removal efficiency for fractions with higher and lower molecular weights was very small. Chen (1999) and Fettig (2005) performed comparison studies between IEX and GAC for NOM removal without a focus on NOM character. Chen used water with TOC concentrations of 0.5 – 2.2 mg-C/l and Fettig used water with DOC concentrations of 10.2 – 42.5 mg-C/l. Both concluded that a

strong base anion exchange resin was more effective compared to GAC for removal of TOC and DOC. Fearing et al. (2004) compared GAC and MIEX[®] (magnetic IEX) with respect to three molecular weight ranges of DOC: smaller than 2000 g/mol, between 2000 and 5000 g/mol, and larger than 5000 g/mol. They found that there was no difference between GAC and MIEX[®] for the decrease in UVA₂₅₄ for DOC with a molecular weight higher than 2000 g/mol; for DOC with a molecular weight lower than 2000 g/mol, the UVA₂₅₄ decrease was higher for GAC than for MIEX[®].

Ozone is an unstable oxidant in water. In general, when ozone is added to natural water, it is consumed in two steps: an initial rapid ozone consumption step followed by a subsequent slow decay step (Park et al., 2001). The rapid ozone consumption is mainly due to reactions with NOM. Based on the reactivity of model compounds with ozone, it is known that ozone consumption is influenced by organic carbon structures and functionality. For example, unsaturated bonds can directly consume ozone, alkyl compounds can inhibit ozone consumption, and aryl compounds can promote or inhibit ozone consumption. Given its heterogeneous nature, NOM can be involved in any or all of these mechanisms (Westerhoff et al., 1999). As a result of direct ozone consumption by unsaturated bonds, larger organic components are oxidatively transformed into smaller organic components and, consequently, a decrease in UVA₂₅₄ occurs during ozonation. Westerhoff et al. (1999) found from extensive research on physical and chemical properties of NOM isolates that ozone reacts preferentially with the aromatic constituents of NOM, specifically electron enriched aromatics, and that the ozone decomposition rate parameters correlated best with SUVA. This indicated that a higher SUVA of NOM isolates results in a higher reactivity with ozone.

Siddiqui et al. (1997) performed research on biological removal of NOM in sand filters after ozonation. They found that increasing the ozone dosage per unit of DOC resulted in more conversion of DOC to BDOC, however, an ozone dosage per unit of DOC of higher than 1.0 (mg-O₃/l)/(mg-C/l) did not further increase DOC removal. Next to BDOC or AOC formation, during ozonation, bromate is also formed as a disinfection by-product in bromide-containing waters (von Gunten, 2003) and is the major constraint to application of ozonation.

The objective of this study was to evaluate the effects of the character of NOM and the removal of NOM on the formation of AOC and bromate during ozone

disinfection, in order to determine what amount and which part of the NOM should be removed for improvement of ozonation efficiency.

Materials and methods

Test waters

Natural waters were tested from the drinking water treatment plants Leiduin (LDN) and Weesperkarspel (WPK) of Waternet (the water cycle company for Amsterdam and surrounding areas), each with a different DOC concentration. In addition, the DOC concentration of the WPK water was reduced by IEX or by GAC filtration. At both plants the test water was taken before the ozonation steps. The LDN water before ozonation is Rhine River water treated by coagulation, rapid sand filtration, dune infiltration, aeration and rapid sand filtration. The WPK water before ozonation is seepage water treated by coagulation, self-purification in a lake and rapid sand filtration. For IEX treatment of the WPK water, PWA 958, a strong base anion exchange type 1 resin from Rohm & Haas, was used. PWA 958 is a macroreticular cross linked acrylic copolymer with an exchange capacity of 0.8 meq/ml (Cl⁻ form) or 4.3 meq/g. For GAC treatment of the WPK water fresh Chemviron F300 was used. The applied empty bed contact time (EBCT) was 15 seconds for IEX, and 5 minutes for GAC. These EBCTs were sufficient to reduce the DOC concentration by more than 50%.

Installations

Experiments were performed in three different installations:

1. Bench-scale dissolved ozone plug flow reactor (DOPFR). In the DOPFR a small side stream of Milli-Q[®] demineralized water containing dissolved ozone (approximately 10 l/h, with ozone concentrations up to 16 mg-O₃/l) was mixed with a larger main stream consisting of test water (approximately 100 l/h). Subsequently, contact time was created in a plug flow reactor that consisted of a 63.9 m long PTFE tube with an inner diameter of 8 mm with multiple sampling points (van der Helm et al., 2007). In this installation water from LDN and from WPK was treated.
2. Pilot-plant co-current ozone bubble column (5.10 m height, diameter of 0.10 m with 10 sampling points) followed by a counter current ozone bubble column (4.50 m height, diameter of 0.10 m with 10 sampling points) and two contact columns (4.40 m and 4.20 m height, diameter of 0.39 m with sampling points in

the effluent). The flow through the installation was approximately 1 m³/h. In the co-current bubble column, 40% of the ozone was dosed, and in the counter current bubble column 60% of the ozone was dosed. The water could be treated by either IEX or GAC before entering the ozonation. In this installation water from WPK was treated.

3. Pilot-plant counter current ozone bubble column (5.30 m water height, diameter of 0.22 m with 12 sampling points) followed by three contact columns (5.25 m water height, diameter of 0.22 m with 12 sampling points, 4.9 m water height and 4.7 m water height, both a diameter of 0.65 m with sampling points in the effluent). The flow through the installation was approximately 5 m³/h. In this installation water from LDN was treated.

Experiments

The ozone dosages, bromide concentrations and NOM related parameters for the experiments in the DOPFR and in the bubble column installations at WPK and LDN are presented in Table 1. The ozone dosage in the DOPFR was determined by measuring the ozone concentration in the side stream, the flow of the side stream and the flow of the main stream. The ozone dosage in the bubble column experiments was determined from the applied ozone gas concentration, ozone gas flow and the water flow. Since the transfer efficiency of ozone in the bubble columns was near 100%, based on measurements of the ozone gas concentration of the off-gas, the ozone dosage was regarded as the amount of ozone transferred to water.

The pH and bicarbonate of the tested WPK water ranged from 7.6 to 7.8 and from 201 mg-HCO₃/l to 212 mg-HCO₃/l, and that of the LDN water from 7.9 to 8.0 and from 186 mg-HCO₃/l to 200 mg-HCO₃/l. The temperature and AOC concentrations for all experiments ranged from 11°C to 16°C and 3 µg-C/l to 14 µg-C/l. From the full-scale plant data of WPK and LDN, it can be stated that both waters had a carbonate concentration of ~0 mg-CO₃/l, the LDN water had a nitrate concentration of 0.8 ± 0.4 mg-N/l and a sulfate concentration of 55 ± 6 mg-SO₄/l, and the WPK water had a nitrate concentration of 1.2 ± 0.4 mg-N/l and a sulfate concentration of 8 ± 2 mg-SO₄/l.

Table 1 Ozone dosages and water quality parameters for: (i) DOPFR experiments; (ii) WPK bubble column experiments at “low” ozone dosages and LDN bubble column experiment; (iii) WPK bubble column experiments at “high” ozone dosages

DOPFR experiments					
Parameter	Unit	WPK water	WPK IEX	WPK GAC	LDN water
O ₃ dosage	mg-O ₃ /l	1.43	1.39	1.48	0.90
UVA ₂₅₄	1/m	15.4	5.6	6.3	6.1
Bromide	µg-Br/l	97	99	110	158
DOC	mg-C/l	6.3	3.1	2.8	2.4
SUVA	$\frac{(1/m)}{(mg-C/l)}$	2.46	1.81	2.25	2.54
SEC-DOC	-	NO	NO	NO	NO
O ₃ /DOC	$\frac{(mg-O_3/l)}{(mg-C/l)}$	0.36	0.72	0.84	0.45

WPK bubble column experiments “low” ozone dosages and LDN bubble column experiment									
Parameter	Unit	WPK water	WPK water	WPK water	WPK IEX	WPK IEX	WPK GAC	WPK GAC	LDN water
O ₃ dosage	mg-O ₃ /l	0.85	0.85	0.85	0.85	0.85	0.85	0.85	0.93
UVA ₂₅₄	1/m	14.4	14.4	14.4	2.5	4.1	1.2	6.0	5.5
Bromide	µg-Br/l	99	94	90	-	98	-	-	170
DOC	mg-C/l	6.6	6.0	5.8	1.5	2.7	0.7	2.8	2.5
SUVA	$\frac{(1/m)}{(mg-C/l)}$	2.18	2.40	2.48	1.67	1.52	1.62	2.14	2.20
SEC-DOC	-	NO	NO	YES	NO	YES	NO	YES	NO
O ₃ /DOC	$\frac{(mg-O_3/l)}{(mg-C/l)}$	0.13	0.14	0.15	0.57	0.31	1.15	0.30	0.37

WPK bubble column experiments “high” ozone dosages									
Parameter	Unit	WPK water	WPK water	WPK water	WPK IEX	WPK IEX	WPK IEX	WPK GAC	WPK GAC
O ₃ dosage	mg-O ₃ /l	1.70	1.70	1.70	1.70	1.70	1.70	1.70	1.70
UVA ₂₅₄	1/m	14.2	13.8	14.6	1.4	3.0	3.4	0.3	6.7
Bromide	µg-Br/l	92	93	98	-	46	102	-	-
DOC	mg-C/l	5.7	5.5	5.6	1.4	1.8	2.2	0.2	3.3
SUVA	$\frac{(1/m)}{(mg-C/l)}$	2.49	2.51	2.61	1.00	1.67	1.55	1.36	2.03
SEC-DOC	-	NO	NO	NO	NO	NO	NO	NO	NO
O ₃ /DOC	$\frac{(mg-O_3/l)}{(mg-C/l)}$	0.30	0.31	0.30	1.21	0.94	0.77	7.73	0.52

Analysis methods

For the DOPFR experiments, ozone was analyzed with the indigo method based on Bader and Hoigné (1982). For the bubble column experiments ozone was analyzed with DPD method described by Gilbert (1981). Both methods give consistent results (Gilbert and Hoigné, 1983). AOC was measured in duplicate, applying the simultaneous incubation of strains P17 and NOX (van der Kooij et al.,

1982). DOC and UVA₂₅₄ expressed as the absorbance per meter of cell length were determined using standard procedures (Standard Methods, 2005). Bromate samples were concentrated on two Ionpac AG9-SC columns and analyzed using a Dionex ICS3000 ion chromatograph, with an anion micro membrane suppressor, UV detection (200 nm) and conductivity meter. Dionex Ionpac AG9-SC and AS9-SC columns were used with a 0.7 mM NaHCO₃ eluent. The minimum detection limit is 0.5 µg- BrO₃⁻/l (Orlandini et al., 1997; Smeenk et al., 1994). Bromide samples were analyzed using a Dionex DX120 ion chromatograph, with chemical suppressor (12.5 mM H₂SO₄), UV detection (200 nm), and conductivity meter. A Dionex Ionpac AS9-SC column was used with a 0.2 mM NaHCO₃ / 1.4 mM Na₂CO₃ eluent (Orlandini et al., 1997).

NOM characterization was performed by SEC-DOC (also known as LC-OCD) with on-line UVA₂₅₄ detection, described by Huber and Frimmel (1992, 1996). The result of an SEC-DOC measurement is a chromatogram with the relative signal response of organic carbon detection (OCD) and of UVA₂₅₄ detection (UVD). The various peaks of the chromatograms are proportional to the DOC concentration and UVA₂₅₄ measured in a bypass. From the OCD chromatogram, the DOC concentrations of NOM fractions with different molecular weights can be determined. The fractions of interest for this research are the humic substances fractions (quantified on the basis of Suwannee River Standard Stream humic substances, MW~1000 g/mol), the building blocks fraction (humic substances hydrolysates formed from the breakdown of humic substances, MW 300-500 g/mol), and the LMW acids fraction (free monoprotic and diprotic LMW organic acids). For analysis of the reactivity of NOM with ozone, the SUVA was determined from the SEC-DOC chromatograms for the humic substances fraction, for the building blocks fraction, and for the combined fractions of humic substances and building blocks together:

$$SUVA_{HS} = \frac{\text{relative signal response } UVD_{\text{at elution time HS peak}} \cdot f_{UVD}}{\text{relative signal response } OCD_{\text{at elution time HS peak}} \cdot f_{OCD}} \quad [1]$$

$$SUVA_{BB} = \frac{\text{relative signal response } UVD_{\text{at elution time BB peak}} \cdot f_{UVD}}{\text{relative signal response } OCD_{\text{at elution time BB peak}} \cdot f_{OCD}} \quad [2]$$

$$SUVA_{HS+BB} = \frac{(rel.sign.resp.UVD_{at\ el.\ time\ HS\ peak} + rel.sign.resp.UVD_{at\ el.\ time\ BB\ peak})f_{UVD}}{(rel.sign.resp.OCD_{at\ el.\ time\ HS\ peak} + rel.sign.resp.OCD_{at\ el.\ time\ BB\ peak})f_{OCD}} \quad [3]$$

where $SUVA_{HS}$ is the SUVA for the humic substances fraction ((1/m)/(mg-C/l)), $SUVA_{BB}$ is the SUVA for the building blocks fraction ((1/m)/(mg-C/l)), $SUVA_{HS+BB}$ is the SUVA for the humic substances fraction and the building blocks fraction together ((1/m)/(mg-C/l)), f_{UVD} is the conversion factor for calculation of UVA_{254} from the relative signal response of the UVD chromatogram (1/m), and f_{OCD} is the conversion factor for calculating the DOC concentration from the relative signal response of the OCD chromatogram (mg-C/l); f_{UVD} and f_{OCD} are determined from the integrated signal responses of the chromatograms and the measurements of UVA_{254} and DOC in the bypass.

CT calculation

The CT value (ozone in water concentration “C” times contact time “T”) is calculated using:

$$CT = \sum_{i=0}^{n_{SP}} \frac{c_{O_3,i} + c_{O_3,i-1}}{2} (t_i - t_{i-1}) \quad [4]$$

where CT is the ozone exposure ((mg-O₃/l)*min), c_{O_3} is the concentration of ozone in water (mg-O₃/l), t is the hydraulic residence time (min) defined by the reactor volume divided by the water flow, and n_{SP} is the number of sampling points. CT values calculated for the bubble column experiments include the contact columns as well as the bubble columns.

Ozone decay

Ozone decay consists of an initial rapid ozone consumption followed by a subsequent slow ozone decay step. van der Helm et al. (2007) described rapid ozone consumption as a function of the degradation of UVA_{254} with first-order kinetics, and slow ozone decay was described as first-order kinetics (Hoigné and Bader, 1994), resulting in the following equations:

$$\frac{dc_{O_3}}{dt} = -k_{UVA}(UVA - UVA_0)Y - k_{O_3}c_{O_3} \quad [5]$$

$$\frac{d(UVA)}{dt} = -k_{UVA}(UVA - UVA_0) \quad [6]$$

where k_{UVA} is the UVA_{254} decay rate (1/s), UVA is the UVA_{254} in water (1/m), UVA_0 is the stable UVA_{254} after completion of the ozonation process (1/m), Y is the yield for ozone consumed per UVA_{254} decrease ((mg- O_3 /l)/(1/m)), and k_{O_3} is the slow ozone decay rate (1/s).

The first term of Equation [5] for the ozone concentration in water describes the rapid ozone consumption in water as a function of the UVA_{254} decrease. The rate of ozone decay shifts from the rapid to the slow kinetic regime as the ozonation progresses (Zhou et al., 1994). The second term describes slow ozone decay by first-order kinetics. Equation [6] describes the UVA_{254} decrease by first-order kinetics.

The rate constants k_{O_3} and k_{UVA} and the yield Y are calculated from the ozone concentration profiles measured in the DOPFR. In the DOPFR ozone depletion can be measured for contact times of approximately 1.5 to 120 seconds. For contact times beyond 120 seconds, batch experiments were performed. A bottle was filled at the last sampling point of the DOPFR, and ozone concentration in the bottle was frequently measured up to a time of 1000 seconds.

Results and discussion

NOM characterization of test waters

On all four test waters a SEC-DOC analysis was performed. For these experiments the DOC concentration of the WPK water was 5.8 mg-C/l and the removal with IEX or GAC was around 50% resulting in 2.7 mg-C/l and 2.8 mg-C/l, respectively. The DOC concentration of the LDN water was 2.4 mg-C/l. In Table 1 the other water quality parameters for the four test waters are shown. The relevant parts of the OCD and the UVD chromatogram determined by SEC-DOC, as well as the relevant part of the SUVA (UVD divided by the OCD) chromatogram, are shown in Figure 1 for the WPK water. The concentrations of the DOC fractions calculated from the OCD chromatogram are shown in Figure 2. DOC recovery by the SEC-DOC measurements was 85% - 90% for the three WPK waters and 77% for the LDN water.

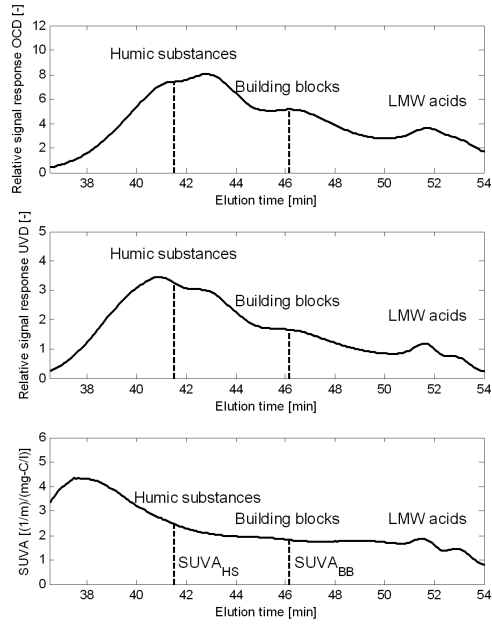


Figure 1 SEC-DOC chromatograms of the WPK water: (i) relative signal response of the organic carbon detection (top); (ii) relative signal response of the UVA₂₅₄ detection (middle); (iii) SUVA determined from the relative signal responses of the UVD and the OCD (bottom); the dotted lines indicate the elution time of the centroids of the humic substances peak and the building blocks peak of the OCD chromatogram (top)

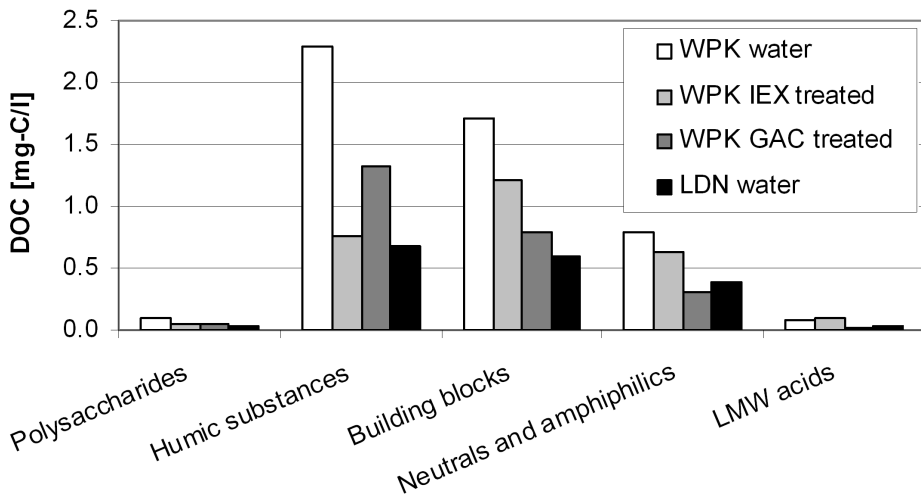


Figure 2 Concentrations of the DOC fractions of the test waters

The removal of the DOC fractions by IEX or GAC is shown in Table 2. From Figure 2 and Table 2, it can be concluded that IEX removes more humic substances than GAC, and GAC removes more building blocks, neutrals and LMW acids than IEX.

Table 2 Removal of DOC fractions by GAC or IEX for the WPK water

Fraction	Removal of DOC (%)	
	WPK IEX treated	WPK GAC treated
Polysaccharides	42	44
Humic substances	67	42
Building blocks	29	54
Neutrals and amphiphilics	20	61
LMW acids	0	78

The results for IEX in Figure 2 appear to be in contradiction with the conclusion reported by Croué et al. (1999) who stated that the higher the MW of the NOM fraction is, the lower the affinity with the anion exchange resin. However, Croué et al. based this conclusion on NOM fractions ranging from 1000-3000 g/mol. For fractions with an average MW of lower than 1000 g/mol, the data support the conclusion that the lower the MW is, the lower the removal efficiency of IEX.

In Table 3 the UVA_{254} , the DOC concentrations and the SUVA values are given for the ozone reactive DOC fractions. It is observed that even though the IEX treated WPK water and the GAC treated WPK water have differences in UVA_{254} , DOC concentration, and SUVA value for the separate humic substances and building blocks fractions, the summed values (HS+BB) are almost equal.

Table 3 UVA_{254} , DOC concentrations and SUVA values for the ozone reactive DOC fractions

	UVA_{254} (1/m)			DOC (mg-C/l)			SUVA ((1/m)/(mg-C/l))		
	HS	BB	HS+BB	HS	BB	HS+BB	HS	BB	HS+BB
WPK water	5.6	3.3	8.9	2.3	1.7	4.0	2.43	1.94	2.23
WPK IEX treated	1.9	2.0	3.9	0.8	1.2	2.0	2.38	1.67	1.95
WPK GAC treated	2.8	1.3	4.1	1.3	0.8	2.1	2.15	1.63	1.95
LDN water	1.7	1.1	2.8	0.7	0.6	1.3	2.43	1.83	2.15

Effect of ozonation on NOM fractions

In Figure 3 (left), the effect of an ozone dosage of 1.70 mg- O_3 /l on NOM is shown for the WPK water, and in Figure 3 (right), the effect of an ozone dosage of 1.04 mg- O_3 /l on NOM is shown for the LDN water for different ozone contact times. From the decrease in the UVD chromatograms in Figure 3, it is suggested that

ozone attacks unsaturated bonds in the humic substances and building blocks fractions, which results in smaller organic components since the OCD chromatograms show a small decrease in humic substances accompanied by a small net increase in building blocks and an increase in LMW acids. From Figure 3 (right) it is concluded that the largest part of the change in DOC in the LDN water takes place in the first 20 minutes of ozone exposure.

In Table 4 the decrease in SUVA due to ozonation is given for the four different test waters. The results shown in Table 4 indicate that the building blocks fraction is more ozone reactive than the humic substances fraction, since the decrease in $SUVA_{BB}$ is larger than the decrease in $SUVA_{HS}$. The IEX treated WPK water has a higher decrease in $SUVA_{BB}$ than the GAC treated WPK water. A possible explanation for the difference between GAC and IEX is that GAC may remove more building blocks with aromatic constituents than IEX does.

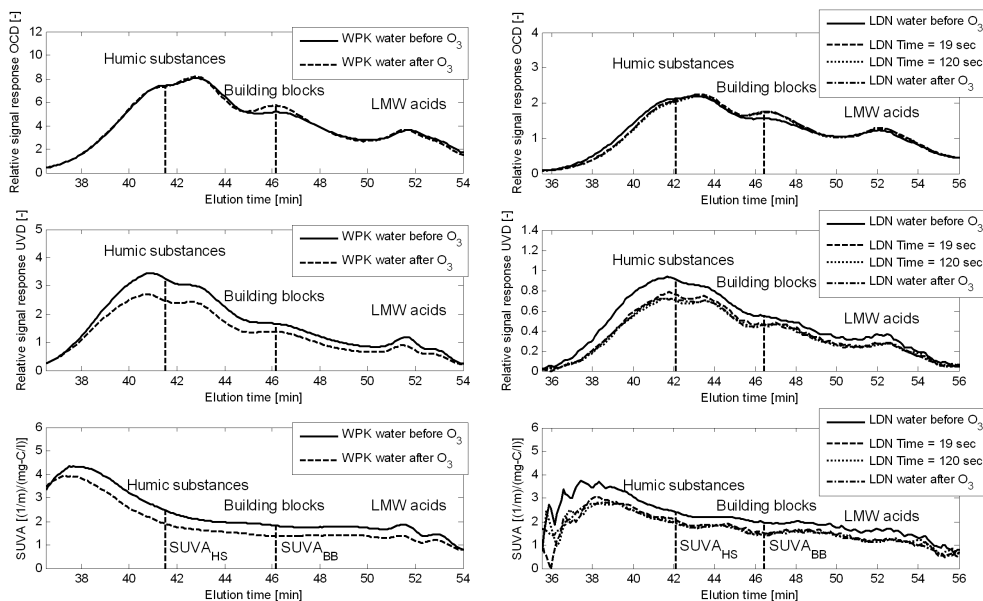


Figure 3 SEC-DOC chromatograms showing the effect of ozone on NOM: (i) WPK water before and after ozonation (left); (ii) LDN water before ozonation, during ozonation for 19 and 120 seconds and after ozonation (right); the dotted lines indicate the elution time of the centroids of the humic substances peak and the building blocks peak of the OCD chromatogram (top)

Table 4 *Decrease in SUVA in percentage due to ozonation*

	Ozone dosage (mg-O ₃ /l)	Δ SUVA (%)		
		HS	BB	HS+BB
WPK water	0.85	17	23	19
WPK IEX treated	0.85	18	27	23
WPK GAC treated	0.85	18	19	19
LDN water	1.04	17	28	23

Effect of NOM character and removal on AOC formation

In Figure 4 the incremental (Δ) AOC formation per unit of DOC, determined in the bubble column experiments for the four different test waters, is plotted against the ozone dosage, including regression lines and 95% confidence intervals. For the IEX treated WPK water, no correlation can be determined because there are only values for one ozone dosage. Although the GAC treated WPK water has a high Pearson R-square, the 95% confidence interval for the GAC treated WPK water is large because the regression is based on only two measurements. For this reason no statistically-based conclusions can be drawn from Figure 4. However, the figure shows a trend towards higher Δ AOC concentrations per unit of DOC for the IEX treated WPK water compared to the GAC treated WPK water and the WPK water. This trend could be explained by the differences in NOM character. Part of the oxidized humic substances and building blocks are transformed into AOC. From Table 4 it is suggested that the ozone reactivity of building blocks is higher compared to the ozone reactivity of humic substances. From the DOC concentrations shown in Table 3, it can be observed that the IEX treated WPK water contains relatively more building blocks compared to the GAC treated WPK water and the WPK water. This suggests that AOC formation from building blocks is higher compared to AOC formation from humic substances.

The LMW acids measured with SEC-DOC are small carboxylic acids, ketones and aldehydes. These small acids are biodegradable organic compounds such as formic acid and acetic acid (Huber and Frimmel, 1996). Biodegradable organic compounds can be measured as AOC so there should be a relation between LMW acids measured with SEC-DOC and the AOC concentration. In Figure 5 LMW acids concentrations from the SEC-DOC measurements are plotted against AOC concentrations for three ozonation experiments. There are three values for each experiment: the influent concentration before ozonation (white symbol), the effluent concentration after ozonation (grey symbol), and the Δ value which is the difference between the effluent and the influent concentration representing the

incremental increase due to ozonation (black symbol). Figure 5 shows no correlation between the measured LMW acids concentrations and the measured AOC concentrations (white and grey symbols), but there is a good correlation between the increase in the LMW acids concentration and the increase in the AOC concentration due to ozonation.

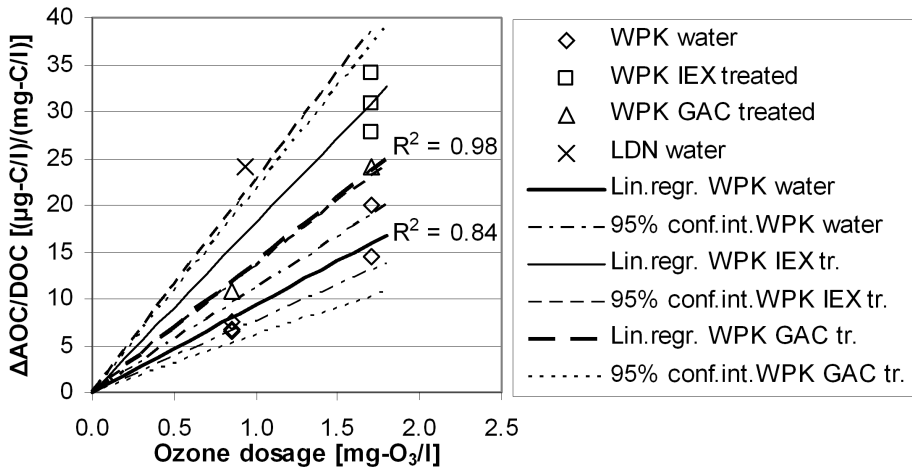


Figure 4 Effects of ozone on AOC formation per unit of DOC for the different test waters

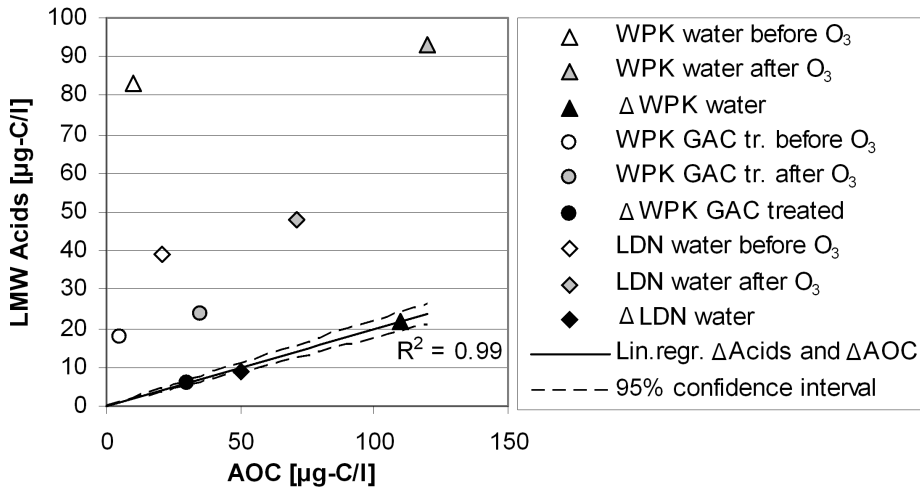


Figure 5 Absolute values LMW acids versus AOC (white and grey symbols) and Δ LMW acids versus Δ AOC (black symbols) for the WPK water with an ozone dosage of 1.70 mg-O₃/l, for the GAC treated WPK water with an ozone dosage of 0.85 mg-O₃/l and for the LDN water with an ozone dosage of 1.04 mg-O₃/l

Van der Kooij et al. (1989) reported a linear relationship through the origin between the decrease in UVA_{254} and AOC formation during ozonation, this can also be observed for the WPK water (see Figure 6, left). However, for the GAC treated WPK water the correlation is very low and for the WPK water treated by IEX there is no correlation for a linear regression line through the origin. Alternatively, when focusing on the decrease in UVA_{HS+BB} , in relation to the AOC formation, positive correlations are obtained for all water types (see Figure 6, right). From Figure 6 (right), it is concluded that the lower the $SUVA_{HS+BB}$ before ozonation is, the higher the AOC formation per unit of UVA_{HS+BB} decrease due to ozonation. Water types with the same $SUVA_{HS+BB}$ before ozonation, such as the IEX and the GAC treated WPK water (average $SUVA_{HS+BB} = 1.9$ (1/m)/(mg-C/l)), have the same AOC formation for the same decrease in UVA_{HS+BB} due to ozonation (see Figure 6, right).

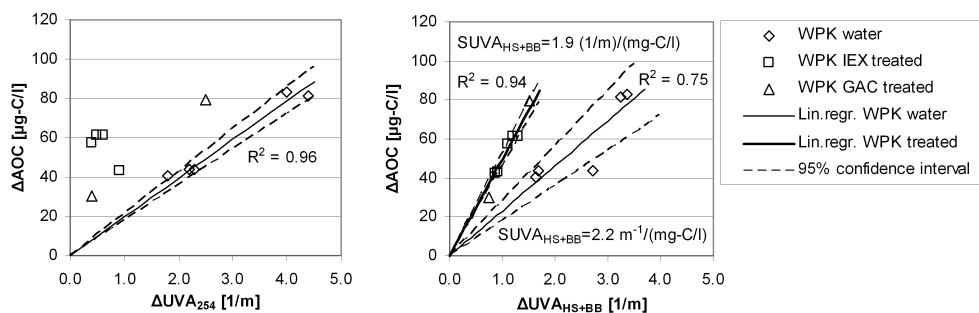


Figure 6 AOC formation: (i) ΔAOC vs. ΔUVA_{254} (left); (ii) ΔAOC vs. ΔUVA_{HS+BB} (right), for ozone bubble column pilot-plant experiments with the WPK water and the IEX and the GAC treated WPK water

Effect of NOM character and removal on the CT value

In Figure 7, the CT values are plotted against the DOC concentrations for different ozone dosages in the bubble column experiments. In the case of the WPK water, the total amount of ozone reacts with DOC and there is no measurable residual ozone for calculating a CT value. For decreasing DOC concentrations, residual ozone and, thus, CT values will first appear for the ozone dosage of 1.70 mg- O_3 /l and subsequently for the ozone dosage of 0.85 mg- O_3 /l. From Figure 7, it is observed that the relation between the CT value and DOC concentration for the IEX and GAC treated WPK water coincide. Thus, the CT value is not influenced by which fraction, i.e., the humic substances fraction or the building blocks fraction, is removed to a greater extent.

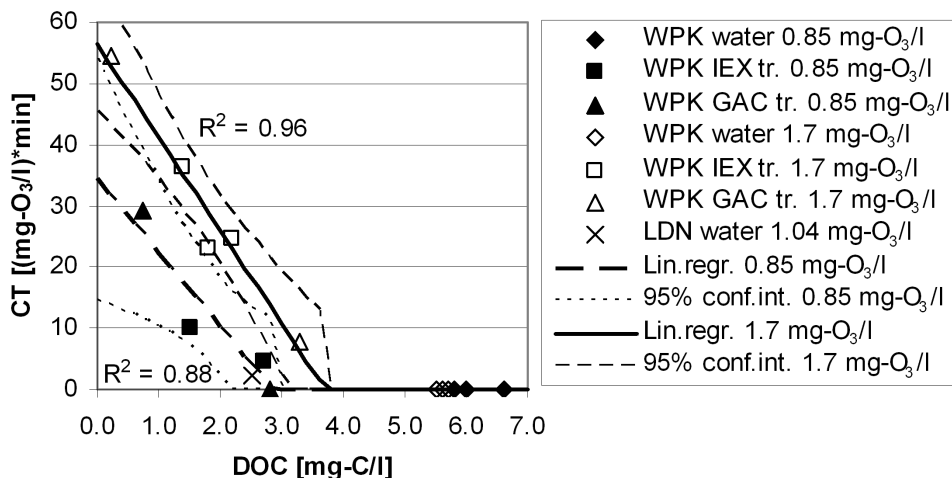


Figure 7 CT values at different DOC concentrations for the WPK and the LDN pilot-plant bubble column experiments

From the DOPFR experiments (see Table 1), rapid ozone consumption and slow ozone decay were determined without interference from ozone gas transfer. By fitting Equations 5 and 6 on the measured ozone profiles in the DOPFR experiments, the rate constants k_{O_3} and k_{UVA} , and the yield Y for the different test waters were determined. The results of the fits are presented in Table 5, with their respective Pearson R-square values (R^2).

Table 5 Rate coefficients for rapid ozone consumption (k_{UVA}) and slow ozone decay (k_{O_3}), and the yield factor (Y) determined from DOPFR experiments

	O ₃ dosage (mg-O ₃ /l)	Temp. (°C)	DOC (mg-C/l)	k_{O_3} (1/s)	k_{UVA} (1/s)	Y (mg-O ₃ /l)/(1/m)	R^2 (-)
WPK water	1.43	12	6.3	0.0687	2.201	0.25	0.99
WPK IEX tr.	1.39	12	3.1	0.0025	0.034	0.41	0.97
WPK GAC tr.	1.48	13	2.8	0.0027	0.153	0.51	0.99
LDN water	0.90	12	2.4	0.0041	0.285	0.16	0.97

From Table 5, it can be seen that the k_{O_3} for the IEX and GAC treated WPK water are nearly the same, and that the k_{UVA} for the GAC treated WPK water is more than 4 times greater than for the IEX treated WPK water. Since the GAC treated WPK water contains more humic substances and fewer building blocks than the IEX treated WPK water (see Table 3), this may indicate that humic substances react faster with ozone than building blocks. The Y for the GAC treated WPK water is higher than for the IEX treated WPK water, however the UVA₂₅₄ decrease for the

IEX treated WPK water is higher than that for the GAC treated WPK water, resulting in an ozone decrease due to rapid ozone consumption of 0.94 mg-O₃/l and 0.92 mg-O₃/l for the IEX and the GAC treated WPK water, respectively.

From Figure 7 data it is observed that for the same DOC concentrations, the CT values for the bubble column experiments with the IEX and GAC treated WPK water are the same, even though the k_{UVA} is more than 4 times greater for the GAC than for the IEX treated WPK water. This can be explained by the fact that in bubble column experiments the k_{UVA} is not the decisive parameter for the CT value. The main part of rapid ozone consumption will take place in the bubble column and therefore will be determined by the gas exchange rate, the k_La (Lewis and Whitman, 1924), between ozone gas and water, which is one or more orders slower than rapid ozone consumption. Values found in the literature for the k_La of ozone in bubble columns range from 0.0001 1/s to 0.0192 1/s depending on turbulence and the gas exchange area (Roustan et al., 1987; Roustan et al., 1996). The decisive parameters for the CT value in bubble column experiments are the amount of ozone consumed during the rapid ozone consumption step and the k_{O_3} . The first parameter determines the ozone concentration at the point where rapid ozone consumption shifts to slow ozone decay, and the second parameter determines the time for this ozone concentration to decrease to zero. Since the differences between both the amount of ozone consumed during rapid ozone consumption and the k_{O_3} for the IEX and the GAC treated WPK water are relatively small, the CT values for both waters in bubble column experiments are almost the same for the same DOC concentrations, as seen in Figure 7.

The k_{UVA} that was found for the LDN water was 0.285 1/s (see Table 5). This means that 99% of rapid ozone consumption occurs in the first 16 seconds. This is in agreement with Figure 3 (right) where it was observed that the largest part of the UVA₂₅₄ decrease for the LDN water took place within the first 20 seconds.

Effect of NOM character and removal on bromate formation

In Figure 8, bromate formation is plotted against the CT value for the bubble column experiments. For the WPK water with ozone dosages of 0.85 mg-O₃/l and 1.70 mg-O₃/l, the CT value is zero because of the high concentration of NOM in the water (see Figure 7); accordingly, the bromate formation is zero. Bromate formation for the LDN water is higher than for the WPK water due to higher bromide concentrations of around 170 µg-Br/l versus 90-100 µg-Br/l for the WPK

water. From the experimental data it can be concluded that the IEX resin does not remove bromide, but bromate formation for the IEX treated WPK water is lower than for the GAC treated WPK water. It should be noted that this observation is based on a limited number of data points and, as a consequence, the 95% confidence bounds are wide.

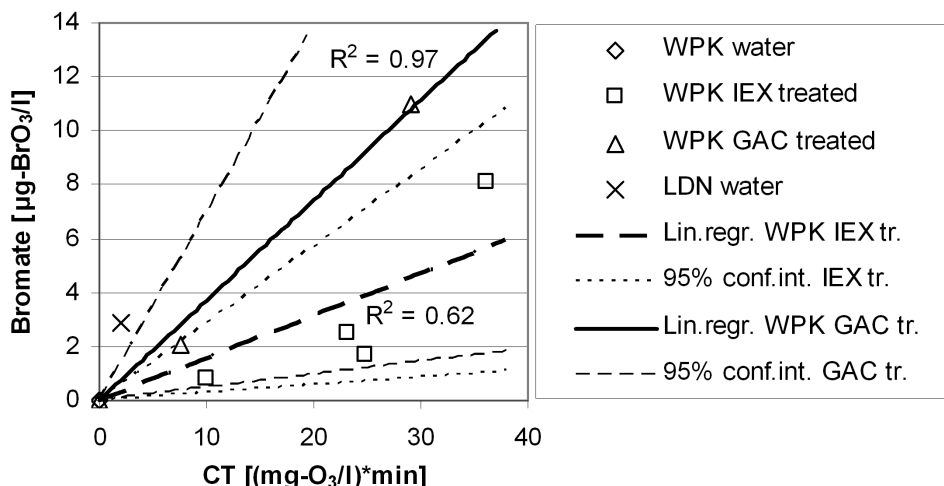


Figure 8 Bromate formation for the bubble column pilot-plant experiments

Conclusions

The humic substances fraction (MW ~ 1000 g/mol) and the building blocks fraction (MW 300-500 g/mol) of NOM, as determined by SEC-DOC, are the ozone reactive fractions and thus most important for assessment of ozonation efficiency. With respect to AOC formation during ozonation, it is concluded that AOC formation per unit of DOC is higher for NOM containing more building blocks than humic substances for the same ozone dosage. As a result of ozonation the LMW acids fraction of NOM, as determined by SEC-DOC, increased, and a good correlation was found between the increase in LMW acids and the AOC formation. Also, good correlations were found between the AOC increase and the UVA₂₅₄ decrease in the humic substances fraction and the building blocks fraction together. With respect to the CT value for disinfection during ozonation, it is concluded that removal of humic substances and building blocks leads to a higher CT value for the same ozone dosage. The rate of rapid ozone consumption is higher for NOM containing more humic substances than building blocks, however, the CT value is not influenced by

which fraction is removed to a greater extent. CT values in bubble column ozone reactors are not determined by the rate of rapid ozone consumption but by the amount of ozone consumed during rapid ozone consumption and by the slow ozone decay rate. With respect to bromate formation during ozonation, it is concluded that bromate formation is possibly higher for NOM containing more humic substances than building blocks.

From a water quality point of view, it is concluded that ozonation efficiency improved more with the removal of the humic substances fraction (MW ~ 1000 g/mol) of NOM as compared to the removal of the building blocks fraction (300-500 g/mol) of NOM. This led to less AOC formation and less bromate formation. When considering IEX (Rohm & Haas, PWA 958; strong base anion exchange type 1 resin) and GAC filtration (Chemviron, F300) for NOM removal, IEX is preferred, because from NOM characterization by SEC-DOC, it is concluded that IEX removed more humic substances than GAC filtration.

Acknowledgements

This research was carried out as part of the Promicit project, a cooperation of Waternet, Delft University of Technology, DHV B.V., and ABB B.V. and was subsidized by SenterNovem, agency of the Dutch Ministry of Economic Affairs. The aim of the project was to achieve a breakthrough in drinking water quality control by developing an integrated model of the total water treatment and using this model as a basis for operation. The DOPFR experiments were performed in cooperation with Kiwa Water Research Nieuwegein, the Netherlands. The authors want to thank M. van Leenen for performing the main part of the experiments.

Nomenclature

AOC	assimilable organic carbon
BB	building blocks (break down products of humic substances)
CT	ozone exposure ((mg-O ₃ /l)*min)
DOC	dissolved organic carbon (mg-C/l)
DOPFR	dissolved ozone plug flow reactor
FEEM	fluorescence excitation-emission matrices
GAC	granular activated carbon

HS	humic substances
IEX	ion exchange
LC-OCD	liquid chromatography combined with online organic carbon detection
LDN	drinking water treatment plant Leiduin of Waternet
LMW acids	low molecular weight acids
MW	molecular weight
NOM	natural organic matter
OCD	organic carbon detection
POC	particulate organic carbon
SEC-DOC	size exclusion chromatography combined with online dissolved organic carbon detection
SUVA	specific UV absorbance defined as UVA_{254} divided by DOC concentration $((1/m)/(mg-C/l))$
TOC	total organic carbon
UVA_{254}	UV absorbance at 254 nm
UVD	UV absorbance detection
Waternet	water cycle company for Amsterdam and surrounding areas
WPK	drinking water treatment plant Weesperkarspel of Waternet
c_{O_3}	concentration of ozone in water (mg- O_3/l)
f_{OCD}	conversion factor for calculation of the DOC concentration from the relative signal response of the OCD chromatogram measured with SEC-DOC (mg-C/l)
f_{UVD}	conversion factor for calculation of the UVA_{254} from the relative signal response of the UVD chromatogram measured with SEC-DOC (1/m)
k_{O_3}	slow ozone decay rate (1/s)
k_{UVA}	UVA_{254} decay rate (1/s)
n_{SP}	number of sampling points
$SUVA_{BB}$	SUVA for building blocks fraction from SEC-DOC $((1/m)/(mg-C/l))$
$SUVA_{HS}$	SUVA for humic substances fraction from SEC-DOC $(1/m)/(mg-C/l)$
$SUVA_{HS+BB}$	SUVA for the humic substances fraction and the building blocks fraction from SEC-DOC together $((1/m)/(mg-C/l))$
t	hydraulic residence time (min)
UVA	UVA_{254} in water (1/m)
UVA_0	stable UVA_{254} after completion of the ozonation process (1/m)
Y	yield for ozone consumed per UVA_{254} decrease $((mg-O_3/l)/(1/m))$

References

- Amy, G. and Her, N. (2004). Size exclusion chromatography (SEC) with multiple detectors: a powerful tool in treatment process selection and performance monitoring. *Water Sci. Technol.: Water Supply*, 4(4), 19-24.
- Bader, H. and Hoigné, J. (1982). Determination of ozone in water by the indigo method; a submitted standard method. *Ozone Sci. Eng.*, 4(4), 169-176.
- Chen, P.H. (1999). Removing aquatic organic substances by anion-exchange resin and activated carbon. *Environ. Int.*, 25(5), 655-662.
- Croué, J.P., Voilleau, D., Bodaire, C. and Legube, B. (1999). Removal of hydrophobic and hydrophilic constituents by anion exchange resin. *Wat. Sci. Technol.*, 40(9), 207-214.
- Edzwald, J.K. and Tobiasson, J.E. (1999). Enhanced coagulation: US requirements and a broader view. *Wat. Sci. Technol.*, 40(9), 63-70.
- Fearing, D.A., Banks, J., Wilson, D., Hillis, P.H., Campbell, A.T. and Parsons, S.A. (2004). NOM control options: the next generation. *Water Sci. Technol.: Water Supply*, 4(4), 139-145.
- Fettig, J. (2005). Modelling the uptake of natural organic matter (NOM) by different granular sorbent media. *J. Water Supply Res. Technol. AQUA*, 54(2), 83-93.
- Gilbert, E. (1981). Photometrische bestimmung niedriger ozonkonzentrationen in wasser mit hilfe von Diäthyl-p-phenylendiamin (DPD) (Photometric determination of low ozone concentrations in water using Diethyl-p-phenylenediamine (DPD)). *GWF Wasser Abwasser*, 122(9), 410-416.
- Gilbert, E. and Hoigné, J. (1983). Messung von ozon in wasserwerken; Vergleich der DPD- und indigo-methode (Measurement of ozone in water treatment; Comparison of the DPD and indigo method). *GWF Wasser Abwasser*, 124(11), 527-531.
- Hoigné, J. and Bader, H. (1994). Characterization of water quality criteria for ozonation processes. Part II: Lifetime of added ozone. *Ozone Sci. Eng.*, 16(2), 121-134.
- Hongve, D., Baann, J., Becher, G. and Beckmann, O.A. (1999). Experiences from operation and regeneration of an anionic exchanger for natural organic matter (NOM) removal. *Water Sci. Technol.*, 40(9), 215-221.
- Huber, S.A. and Frimmel, F.H. (1992). A new method for the characterization of organic carbon in aquatic systems. *Intern. J. Environ. Anal. Chem.*, 49(1), 49-57.

- Huber, S.A. and Frimmel, F.H. (1996). Size-exclusion chromatography with organic carbon detection (LC-OCD): a fast and reliable method for the characterization of hydrophilic organic matter in natural waters. *Vom Wasser*, 86, 277-290.
- Joret, J.C. and Levy, Y. (1986). Méthode rapide d'évaluation du carbone éliminable des eaux par voie biologique (Rapid method for evaluation of biological degradable organic carbon). *Trib. Cebedeau*, 39(510), 3-9.
- Lewis, W.K. and Whitman, W.G. (1924). Principles of gas absorption. *Ind. Eng. Chem.*, 16(12), 1215-1220.
- Matilainen, A., Vieno, N. and Tuhkanen, T. (2006). Efficiency of the activated carbon filtration in the natural organic matter removal. *Environ. Int.*, 32(3), 324-331.
- Newcombe, G., Morrison, J. and Hepplewhite, C. (2002). Simultaneous adsorption of MIB and NOM onto activated carbon. I. Characterisation of the system and NOM adsorption. *Carbon*, 40(12), 2135-2146.
- Orlandini, E., Kruithof, J.C., van der Hoek, J.P., Siebel, M.A. and Schippers, J.C. (1997). Impact of ozonation on disinfection and formation of biodegradable organic matter and bromate. *J. Water Supply Res. Technol. AQUA*, 46(1), 20-30.
- Park, H., Hwang, T., Kang, J., Choi, H. and Oh, H. (2001). Characterization of raw water for the ozone application measuring ozone consumption rate. *Water Res.*, 35(11), 2607-2614.
- Roustan, M., Duguet, J.P., Brette, B., Brodard, E. and Mallevalle, J. (1987). Mass balance analysis of ozone in conventional bubble contactors. *Ozone Sci. Eng.*, 9(3), 289-297.
- Roustan, M., Wang, R.Y. and Wolbert, D. (1996). Modeling hydrodynamics and mass transfer parameters in a continuous ozone bubble column. *Ozone Sci. Eng.*, 18(2), 99-115.
- Siddiqui, M.S., Amy, G.L. and Murphy, B.D. (1997). Ozone enhanced removal of natural organic matter from drinking water sources. *Water Res.*, 31(12), 3098-3106.
- Smeenk, J.G.M.M., van Rossum, W.J.M., Gademan, W.J.H. and Bruggink, C. (1994). Trace level determination of bromate and chlorite in drinking and surface water by ion chromatography with automated preconcentration. *Proceedings of the International Ion Chromatography Symposium*, Torino, Italy, 1994.

- Standard Methods (2005). *Standard Methods for the examination of water & wastewater 2005 21st edition*, American Public Health Association/American Water Works Association/Water Environment Federation, Baltimore, USA.
- van der Helm, A.W.C., Smeets, P.W.M.H., Baars, E.T., Rietveld, L.C. and van Dijk, J.C. (2007). Modeling of ozonation for dissolved ozone dosing. *Ozone Sci. Eng.*, Accepted for publication, February 2007.
- van der Kooij, D., Visser, A. and Hijnen, W.A.M. (1982). Determining the concentration of easily assimilable organic carbon in drinking water. *Am. Water Works Assoc. J.*, 74(10), 540-545.
- van der Kooij, D., Hijnen, W.A.M. and Kruithof, J.C. (1989). The effects of ozonation, biological filtration and distribution on the concentration of easily assimilable organic carbon (AOC) in drinking water. *Ozone Sci. Eng.*, 11, 297-311.
- von Gunten, U. (2003). Ozonation of drinking water: Part II. Disinfection and by-product formation in presence of bromide, iodide or chlorine. *Water Res.*, 37(7), 1469-1487.
- Westerhoff, P., Aiken, G., Amy, G. and Debroux, J. (1999). Relationships between the structure of natural organic matter and its reactivity towards molecular ozone and hydroxyl radicals. *Water Res.*, 33(10), 2265-2276.
- Zhou, H., Smith, D.W. and Stanley, S.J. (1994). Modeling of dissolved ozone concentration profiles in bubble columns. *J. Environ. Eng.*, 120(4), 821-840.

6. Integrated model for operational support and process control of ozonation

Pilot-scale experiments were performed with ozone bubble column installations at two drinking water treatment plants. The influent water quality of the two plants has distinct differences in dissolved organic carbon (DOC) concentration, UV absorbance at 254 nm (UVA_{254}) and bromide concentration. The experimental data were used to calibrate an integrated ozonation model that calculates ozone exposure (CT), *E. coli* disinfection, bromate formation and assimilable organic carbon (AOC) formation. For a number of model parameters, relationships were determined for the two different water types, based on water quality parameters. The model was used to evaluate the current control strategy of the full-scale ozone installation at Weesperkarspel and to assess other control strategies for operational support and for process control of ozonation.

Introduction

Water quality is the most important objective for the optimization of existing drinking water treatment plants (van der Helm et al., 2006). High quality drinking water with respect to microbiological safety, toxicity, chemical stability, and biological stability of the water should be guaranteed under all circumstances. With model-based operational support and process control, water quality can be improved and will become more stable. Since individual drinking water treatment steps influence subsequent treatment steps, the effects of changes in the operational conditions of individual drinking water treatment steps should be assessed for the entire treatment plant. Therefore, an integrated model has to incorporate all relevant integrated water quality parameters.

For the drinking water treatment plants of Waternet (the water cycle company for Amsterdam and surrounding areas), ozonation plays a key role in integrated optimization for microbiological safety, toxicity and biological stability of the water (van der Helm et al., 2006). An integrated model containing the water quality

parameters *Escherichia coli* (*E. coli*), bromate, assimilable organic carbon (AOC), dissolved organic carbon (DOC) and UV absorbance at 254 nm (UVA_{254}) has been developed for dissolved ozone dosing in a plug flow reactor (van der Helm et al., 2007a,b). Use of the integrated ozone model for the operational support and control of existing ozone bubble column installations requires that the model be extended to account for gas transfer for ozone transport from the gas phase to the liquid phase.

The objectives of this research are to incorporate gas transfer in bubble columns in the integrated ozone model, to determine relationships between model parameters of different treatment plants so the same model can be applied to different locations, and to use the model for the evaluation of control strategies for operational support and process control of ozonation.

Materials and methods

Installations

Experiments were performed in two different pilot-scale installations of Waternet. One pilot plant was at drinking water treatment plant Leiduin (LDN), and the other was at drinking water treatment plant Weesperkarspel (WPK). The characteristics for each of the installations are as follows:

1. Pilot-plant LDN: counter current ozone bubble column (5.30 m water height, diameter of 0.217 m with 12 sampling points) followed by a contact column (2.75 m water height, diameter of 0.217 m with 5 sampling points) and a subsequent pipe (63.5 m length, diameter ranging from 0.046 m to 0.153 m with 19 sampling points) with a flow of approximately 5 m³/h. The total residence time was 24.3 minutes.
2. Pilot-plant WPK: four counter current ozone bubble columns in series (5.30 m, 5.10 m, 4.90 m and 4.75 m water height, diameters of 0.404 m and all with 6 sampling points over the height) followed by a pipe (35.4 m length, diameter of 0.111 m with 5 sampling points) and 2 contact columns in series (2.60 m and 2.45 m water height, diameters of 1.025 m with sampling points in the effluent). The flow varied between 7.5 and 15 m³/h for the different experiments, resulting in a total residence time between 51.2 and 25.6 minutes.

At LDN and at WPK the Ozonia Ozat CFS-1A ozone generator was used. At LDN it was operated with pure oxygen and at WPK with air. At both plants the ozone in

gas concentration was measured with a BMT 964 Ozone Analyzer from BMT Messtechnik. At the WPK pilot plant the water flow was measured using a Yokogawa AE202MG flow meter and controlled using a Bürkert Control Valve type 2712, and the gas flow was measured and controlled using Bürkert MFC-8712 mass flow controllers. At the LDN pilot plant the ozone gas flow was controlled manually and measured using a Brooks 5860S gas flow meter and the water flows were controlled manually and measured using Endress & Hauser's 30D/33D and Yokogawa AE204MG flow meters.

Experiments

A number of experiments were performed at the LDN and WPK pilot plants. The conditions of the experiments and the influent water quality parameters are given in Tables 1 and 2. During the experiments described in Table 2, ozone was dosed in the first two bubble columns. The gas flows as given in Table 2 were equally divided over these two bubble columns. In the third and fourth bubble columns no ozone was used, so they functioned as contact columns.

Analysis methods

Ozone was analyzed according to the indigo method described by Bader and Hoigné (1982). Bromate samples were concentrated on two Ionpac AG9-SC columns and analyzed using a Dionex ICS3000 ion chromatograph with an anion micro membrane suppressor, UV detection (200 nm) and conductivity meter. Dionex Ionpac AG9-SC, and AS9-SC columns were used with a 0.7 mM NaHCO₃ eluent. The detection limit is 0.5 µg- BrO₃/l (Orlandini et al., 1997; Smeenk et al., 1994). Bromide samples were analyzed using a Dionex DX120 ion chromatograph with a chemical suppressor (12.5 mM H₂SO₄), UV detection (200 nm), and conductivity meter. A Dionex Ionpac AS9-SC column was used with a 0.2 mM NaHCO₃ / 1.4 mM Na₂CO₃ eluent (Orlandini et al., 1997). AOC was measured in duplicate, applying the simultaneous incubation of strains P17 and NOX (van der Kooij et al., 1982). DOC, pH, bicarbonate and UVA₂₅₄ expressed as the absorbance per meter of cell length were determined using standard procedures (Standard Methods, 2005). An *E. coli* WR1 strain was cultured on a low substrate as described in Smeets et al. (2006). Microbiological samples were taken in 1 liter sterile bottles containing sodium thiosulfate to immediately quench any remaining ozone. Samples were analyzed by direct filtration and inoculation of the filter or by dilution and direct inoculation of 0.1 ml on agar.

Table 1 Conditions and influent water quality parameters for the LDN pilot-plant experiments

Parameter	Unit	Experiment number					
		1	2	3	4	5	6
O ₃ dosage	mg-O ₃ /l	0.23	0.91	1.40	0.72	0.84	1.78
Water flow	m ³ /h	5.0	5.0	5.0	5.0	5.0	5.0
O ₃ gas flow	Nm ³ /h	0.268	0.289	0.509	0.024	0.039	0.084
O ₃ gas con.	g/Nm ³	4.4	15.7	13.7	151	108	106
<i>E. coli</i> ***	CFU/100 ml	12000	16000	14000	14700	10900	6800
pH	-	8.1	8.1	8.1	8.0	8.1	8.1
Bicarbonate	mg-HCO ₃ /l	196	195	196	194	190	194
UVA ₂₅₄	1/m	5.4	5.6	5.6	5.6	4.1	5.8
Bromide	µg/l	191*	191*	191*	184**	184**	184**
Bromate	µg-BrO ₃ /l	<0.5	<0.5	<0.5	<0.5	<0.5	<0.5
AOC-total	µg-C/l	39*	39*	39*	37**	37**	37**
DOC	mg-C/l	2.0	2.1	1.7	2.2	2.3	2.2
Temp.	°C	11.0	10.6	10.4	10.5	10.4	10.6

* measured at experiment 1 and assumed to be constant

** measured at experiment 4 and assumed to be constant

*** *E. coli* were dosed prior to ozonation

Table 2 Conditions and influent water quality parameters for the WPK pilot-plant experiments

Parameter	Unit	Experiment number						
		1	2	3	4	5	6	7
O ₃ dosage	mg-O ₃ /l	1.5	1.5	2.0	2.0	2.5	2.5	2.5
Water flow	m ³ /h	7.5	10.0	7.5	15.0	10.0	10.0	10.0
O ₃ gas flow	Nm ³ /h	1.00	0.50	1.00	1.00	0.50	0.75	1.00
O ₃ gas con.	g/Nm ³	11.3	30.0	15.0	30.0	50.0	33.3	25.0
pH	-	7.5	7.5	7.5	7.5	7.5	7.5	7.5
Bicarbonate	mg-HCO ₃ /l	203	198	197	201	195	203	202
UVA ₂₅₄	1/m	14.8	15.4	15.4	15.5	15.3	15.2	15.3
Bromide	µg/l	98	96	96	95	97	100	100
Bromate	µg-BrO ₃ /l	<0.5	-	<0.5	-	-	-	-
AOC-total	µg-C/l	7	-	7	-	-	-	-
DOC	mg-C/l	7.6	5.9	6.3	6.4	6.3	6.6	5.9
Temp.	°C	11.6	9.6	9.1	8.1	8.7	9.6	11.7

Parameter	Unit	Experiment number						
		8	9	10	11	12	13	14
O ₃ dosage	mg-O ₃ /l	2.5	3.0	3.5	3.5	3.5	4.0	4.0
Water flow	m ³ /h	15.0	12.5	7.5	7.5	7.5	7.5	7.5
O ₃ gas flow	Nm ³ /h	1.00	1.00	0.50	0.75	1.00	0.75	1.00
O ₃ gas con.	g/Nm ³	37.5	37.5	52.5	35.0	26.3	40.0	30.0
pH	-	7.5	7.5	7.5	7.4	7.5	7.4	7.5
Bicarbonate	mg-HCO ₃ /l	197	203	200	202	204	194	194
UVA ₂₅₄	1/m	15.8	15.2	15.3	15.1	15.2	15.7	15.5
Bromide	µg/l	99	99	99	98	98	97	99
Bromate	µg-BrO ₃ /l	<0.5	<0.5	-	<0.5	<0.5	-	<0.5
AOC-total	µg-C/l	9	8	-	10	35	-	7
DOC	mg-C/l	5.9	6.5	6.0	5.9	6.1	6.0	6.4
Temp.	°C	8.1	9.9	11.7	13.1	12.4	7.0	7.1

The CT value for ozonation was calculated using:

$$CT = \sum_{i=0}^{n_{SP}} c_{O_3,i} (t_i / 60 - t_{i-1} / 60) \quad [1]$$

where CT is the ozone exposure ((mg-O₃/l)*min), n_{SP} is the number of sampling points (-), c_{O_3} is the concentration of ozone in water (mg-O₃/l) and t is time (s).

Hydraulic properties of the pilot plants

From residence time distribution (RTD) curves, the number of CSTRs was determined by parameter estimation through numerical integration of advection as described by van der Helm et al. (2007b) for the bubble and contact columns at the WPK pilot plant. For the LDN pilot plant, the number of CSTRs was determined with Taylor approximation as described by Wols et al. (2006). The RTD curves were measured with Hannah Instruments EC215R conductivity meters during step-tracer experiments using a salt solution, and measuring intervals ranging from 3 to 7 seconds.

Modeling of ozonation bubble column installations

The model used by van der Helm et al. (2007a) to describe ozone decay in a plug flow reactor where dissolved ozone was dosed was extended with gas exchange according to the model of Rietveld (2005) for application in ozone bubble columns. In the model rapid ozone consumption was determined by the decrease in UVA₂₅₄:

$$\frac{\partial c_{O_3}}{\partial t} = -u \frac{\partial c_{O_3}}{\partial x} + k_L RQ \frac{u}{u_g d_b} \frac{6}{\alpha} (\alpha k_D c_{O_3g} - c_{O_3}) - k_{UVA} (UVA - UVA_o) Y - k_{O_3} c_{O_3} \quad [2]$$

where u is the water velocity (m/s), x is the length of the reactor (m), k_L is the gas transfer coefficient (m/s), RQ is the gas to water flow ratio (Q_g/Q) (Nm³/m³), Q and Q_g are the water flow (m³/h) and gas flow (Nm³/h), respectively, u_g is the gas velocity (m/s), d_b is the bubble diameter (m), α is the temperature and pressure correction factor $\alpha=(P_g/P_o)(T_o/T_g)$, P_o and P_g are the standard pressure (101325 Pa) and the gas pressure in the reactor (Pa), respectively, T_o and T_g are the standard temperature (273.15 K) and the gas temperature in the reactor (K), respectively, k_D is the distribution coefficient (-), c_{O_3g} is the ozone in gas concentration (g-O₃/Nm³), k_{UVA} is UVA₂₅₄ decay rate (1/s), UVA is UVA₂₅₄ in water

(1/m), UVA_o is the stable UVA_{254} after completion of the ozonation process (1/m), Y is the yield for ozone consumed per UVA_{254} decrease ((mg- O_3 /l)/(1/m)) and k_{O_3} is the slow ozone decay rate (1/s). The α is determined by the gas temperature and the water height in the bubble columns, and thus changes over the height of the bubble column. u_g was calculated using the equation for the rising velocity of a bubble in stagnant water derived by Wallis (1969):

$$u_b = 0.0135 \left(\frac{20000\sigma}{\rho_w d_b} \right)^{0.5} \quad [3]$$

where σ is the surface tension (N/m) and ρ_w is the water density (kg/m³). For co-current bubble columns, $u_g = u_b + u$, and for counter current bubble columns $u_g = u_b - u$. The ozone concentration in the gas phase was described by the following equation (Rietveld, 2005):

$$\frac{\partial c_{O_3g}}{\partial t} = -u_g \frac{\partial c_{O_3g}}{\partial x} + k_L \frac{6}{d_b} (\alpha k_D c_{O_3g} - c_{O_3}) \quad [4]$$

For the gas transfer coefficient, k_L , the expression by Hughmark (1967) was used:

$$k_L = \frac{D_{O_3}}{d_b} \left(2 + a \left(\left(\frac{u_b d_b}{\nu} \right)^{0.484} \left(\frac{\nu}{D_{O_3}} \right)^{0.339} \left(\frac{d_b g^{1/3}}{D_{O_3}^{2/3}} \right)^{0.072} \right)^b \right) \quad [5]$$

where D_{O_3} is the diffusion coefficient of ozone (m²/s), a and b are empirical constants (for single gas bubbles $a = 0.061$ and $b = 1.61$, and for swarms of gas bubbles $a = 0.0187$ and $b = 1.61$), u_b is the bubble rising velocity (m/s), ν is the kinematic viscosity (m²/s) and g is the specific gravity (m/s²).

The equations used for UVA_{254} decrease, bromate formation, *E. coli* inactivation with the Hom model, the CT and AOC formation were from van der Helm et al. (2007a):

$$\frac{\partial(UVA)}{\partial t} = -u \frac{\partial(UVA)}{\partial x} - k_{UVA}(UVA - UVA_o) \quad [6]$$

$$\frac{\partial c_{BrO_3}}{\partial t} = -u \frac{\partial c_{BrO_3}}{\partial x} + k_{BrO_3} c_{O_3} \quad c_{BrO_3,ini} = F_{BrO_3,ini} c_{O_3,DOS} + c_{BrO_3,in} \quad [7]$$

$$\frac{\partial N}{\partial t} = -u \frac{\partial N}{\partial x} - \frac{k}{60} m N c_{O_3}^n t^{m-1} \quad [8]$$

$$\frac{\partial (CT)}{\partial t} = -u \frac{\partial (CT)}{\partial x} + c_{O_3} \quad [9]$$

$$c_{AOC} = F_{AOC} c_{O_3,DOS} c_{DOC,in} + c_{AOC,in} \quad [10]$$

where c_{BrO_3} is the bromate concentration ($\mu\text{g-BrO}_3/\text{l}$), k_{BrO_3} is the bromate formation rate constant ($(\mu\text{g-BrO}_3/\text{l})/((\text{mg-O}_3/\text{l})\cdot\text{min})$), $c_{BrO_3,ini}$ is the initial bromate formation ($\mu\text{g-BrO}_3/\text{l}$), $F_{BrO_3,ini}$ is the constant for initial bromate formation ($(\mu\text{g-BrO}_3/\text{l})/((\text{mg-O}_3/\text{l}))$), $c_{O_3,DOS}$ is the ozone dosage ($\text{mg-O}_3/\text{l}$), $c_{BrO_3,in}$ is the influent bromate concentration ($\mu\text{g-BrO}_3/\text{l}$), N is the number concentration of organisms (CFU/100 ml), k is the inactivation rate coefficient ($1/(\text{mg-O}_3\cdot\text{min})$ for $n=1$ and $m=1$) and n and m are empirical constants (-), c_{AOC} is the AOC concentration ($\mu\text{g-C/l}$), F_{AOC} is the constant for AOC formation per DOC ($(\mu\text{g-C/l})/(\text{mg-O}_3/\text{l}\cdot\text{mg-C/l})$), $c_{DOC,in}$ is the influent dissolved organic carbon concentration (mg-C/l) and $c_{AOC,in}$ is the influent AOC concentration ($\mu\text{g-C/l}$).

The Equations [2], [4] and [6] to [9] were numerically solved in the Stimela environment that was programmed in Matlab[®]/Simulink[®] (van der Helm and Rietveld, 2002). In the Stimela model it is possible to simulate short-circuiting in the bubble column. As a result, part of the water flow through the bubble column has no contact with ozone and mixes at the bottom of the bubble column. This possibility is created, because, in earlier experiments in the LDN bubble column pilot plant, where UVA_{254} was measured over the height of the bubble column (ozone was quenched with Na_2SO_3), an increase in UVA_{254} at the bottom of the bubble column was observed (see Figure 1). An increase in UVA_{254} is only possible when water without ozone but with a high UVA_{254} mixes with ozonated water with a lower UVA_{254} . The short-circuit flow in the bubble column relative to the total flow is given by:

$$SC_{BC} = \frac{Q_{SC,BC}}{Q} \quad [11]$$

where SC_{BC} is the factor for short-circuiting in the bubble column (-) and $Q_{SC,BC}$ is the short-circuiting flow in the bubble column (m^3/h).

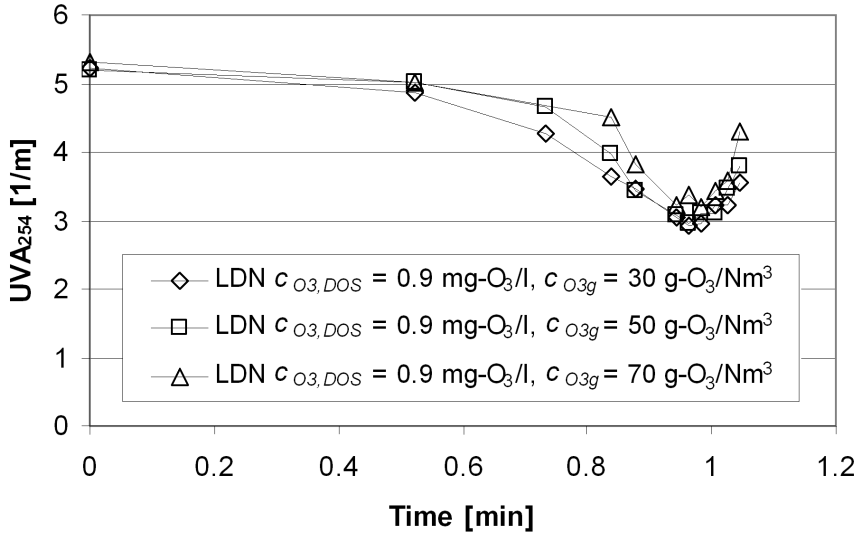


Figure 1 *UVA₂₅₄ decrease in the bubble column at the LDN pilot plant for three experiments with an ozone dosage of 0.9 mg-O₃/l realized with different ozone in gas concentrations*

Model parameters for LDN and WPK

Model parameters used in the calculations were the parameters determined in previous research by van der Helm et al. (2007a) with the pilot-scale dissolved ozone plug flow reactor (DOPFR), parameters determined from the literature, and parameters determined from model calibration with experimental data from this research on bubble column installations (see Table 3).

Table 3 Model parameters for ozone bubble column pilot plants at LDN and WPK

Parameter	Value	Unit	Remark	
k_{O_3}	LDN	$0.1454e^{-4.372C_{O_3,Dos}}$	1/s	van der Helm et al. (2007a)
	WPK	calibrate		experiments this research
k_{UVA}		$3.75e^{-3.443C_{O_3,Dos}}$	1/s	van der Helm et al. (2007a)
γ	LDN	0.137	$\frac{mg-O_3}{l}$	van der Helm et al. (2007a)
	WPK	calibrate	1/m	experiments this research
UVA_{0^*}	LDN	$UVA_{in} - (1.261c_{O_3,Dos} + 1.0237)$	1/m	van der Helm et al. (2007a)
	WPK	calibrate		experiments this research
k_D^{**}		$e^{-0.45-0.043T}$	-	Langlais et al. (1991) for: $0^\circ C < T < 35^\circ C$
d_b		0.003	m	Analogous to Rietveld (2005)
$D_{O_3}^{***}$		$5.97 \cdot 10^{-15} \frac{T + T_o}{\nu \rho}$	m^2/s	Nernst-Einstein equation****
σ^{**}		$-1.47 \cdot 10^{-4} T + 7.56 \cdot 10^{-2}$	N/m	Approximation based on data Degrémont (1991) for: $0^\circ C < T < 30^\circ C$.
A	LDN	calibrate	-	Single gas bubbles $a=0.061$
	WPK	calibrate	-	and swarms of gas bubbles $a=0.0187$ (Hughmark, 1967)
B		1.61	-	Hughmark (1967)
ν^{**}		$\frac{497 \cdot 10^{-6}}{(42.5 + T)^{1.5}}$	m^2/s	Approximation based on data from Degrémont (1991) for: $0^\circ C < T < 35^\circ C$.
ρ_w		1000	kg/m^3	
G		9.81	m/s^2	
SC_{BC}	LDN	calibrate	-	experiments this research
	WPK	calibrate		
$F_{BrO_3,ini}^{***}$	LDN	2.17	$\frac{\mu g-BrO_3}{l}$	van der Helm et al. (2007a)
	WPK	0	$mg-O_3/l$	experiments this research
k_{BrO_3}	LDN	1.66	$\frac{\mu g-BrO_3}{l}$	van der Helm et al. (2007a)
	WPK	calibrate	$(mg-O_3/l) \cdot min$	experiments this research
K		$4.49e^{-3.305C_{O_3,Dos}}$	$\frac{l}{mg-O_3 \cdot min} \frac{1}{s}$	van der Helm et al. (2007a)
N		1	-	van der Helm et al. (2007a)
M		2	-	van der Helm et al. (2007a)
F_{AOC}	LDN	45	$\frac{\mu g-C}{l}$	van der Helm et al. (2007a)
	WPK	calibrate	$mg-O_3/l \cdot mg-C/l$	experiments this research

* where UVA_{in} is the influent UVA_{254} (1/m)

** where T is the temperature of the water ($^\circ C$)

*** $F_{BrO_3,ini}$ cannot be determined from bubble column experiments. Therefore, it is assumed for WPK that the bromate concentration increases linearly with the CT value, without an initial fast increase

**** determined from $D_{O_3} = 1.74 \cdot 10^{-9} m^2/s$ at $20^\circ C$ (Langlais et al., 1991)

First, the unknown model parameters for describing the ozone concentration and UVA_{254} decrease were calibrated. This means that for the LDN model the a and SC_{BC} were calibrated, and for the WPK model k_{O_3} , Y , UVA_0 , a and SC_{BC} were calibrated. Subsequently, the unknown model parameters for describing bromate and AOC formation were calibrated. This means that k_{BrO_3} and F_{AOC} were calibrated for the WPK model; for the LDN model these parameters were already determined (see Table 3). The last step, for k_{O_3} , Y , UVA_0 , k_{BrO_3} and F_{AOC} , the possibilities were studied to combine the expressions for LDN and WPK into a more general expression based on the differences in water quality. For k_{O_3} and Y the difference was characterized by the influent DOC concentration, for UVA_0 by the influent UVA_{254} concentration and for k_{BrO_3} by the influent pH and the influent bromide concentrations.

k_{UVA} could not be determined from bubble column experiments, therefore, the expression derived from the DOPFR experiments for LDN were also used for WPK. Since the gas transfer rate for ozone in a bubble column is one or more orders slower compared to k_{UVA} (van der Helm et al., 2007c) and the main part of UVA_{254} decrease and thus rapid ozone consumption will take place in the bubble column, the ozone profile in the installation is not influenced by k_{UVA} .

Control strategies

Based on model calculations, the effects on CT, bromate and AOC formation were evaluated for different control strategies of the WPK ozonation pilot plant. For the ozonation water quality influent parameters, monthly or yearly average values were used from the year 2004. For every month during one year, a new setting for the ozone dosage was determined based on the following different control strategies:

1. The current control strategy at WPK that is applied in the full-scale ozone installation at WPK, where the ozone dosage is 1.7 mg- O_3 /l when the water temperature is above 12°C and 2.2 mg- O_3 /l when the water temperature is below 12°C. The lower ozone dosage at higher temperatures is to limit AOC formation in order to prevent rapid clogging of the BAC filters.
2. The maximal CT control strategy, where the ozone dosage is calculated for the situation that a maximum allowed effluent bromate concentration is reached and for the situation that a maximum allowed AOC concentration is reached. Set point for the ozone dosage is the higher of the two calculated dosages.
3. The log inactivation control strategy, where the ozone dosage is determined by a set point for the log inactivation of *Giardia*.

Because the WPK experiments were performed within a small temperature range of 7.0°C to 13.1°C, the temperature dependency for reaction rate constants were used from the literature. The influence of temperature was modeled using Arrhenius' equation, given by:

$$k = Ae^{(-E_a/RT_a)} \quad [12]$$

where A is the frequency factor (unit depending on the unit of k), E_a is the activation energy (J/mol), $R = 8.314 \text{ J}/(\text{mol}\cdot\text{K})$ is the ideal gas constant and T_a is the absolute temperature of the water (K).

Results and discussion

Hydraulic properties of the pilot plants

The resulting numbers of CSTRs for the bubble and contact columns at the LDN and WPK pilot plants determined from measured RTD curves are shown in Table 4. From Table 4 it can be seen that the LDN pilot-plant bubble and contact columns have a better plug flow compared to the WPK pilot-plant bubble and contact columns. In addition, it can be observed that the hydraulic characteristics of a bubble column in which ozone is dosed has fewer CSTRs than the same column where no ozone is dosed. The same number of CSTRs is used in the models describing ozonation at the LDN and WPK pilot plants. The short-circuit flow through the bubble columns could not be determined from the step-tracer experiments. This indicates that the main flow and the short-circuit flow have about the same RTD.

Table 4 Results for step-tracer experiments at the LDN and WPK pilot plants

Installation		Water flow [m ³ /h]	Gas flow [Nm ³ /h]	Diameter [m]	CSTRs [-]
Pilot plant at LDN	Bubble column	10.5	0.180	0.217	30
	Contact column	10.5	-	0.217	50
	Pipe	2.5	-	0.046-0.153	>200
Pilot plant at WPK	Bubble column 1	10.0	0.400	0.404	6
	Bubble column 2	10.0	0.400	0.404	6
	Bubble column 3	10.0	0.000	0.404	12
	Bubble column 4	10.0	0.000	0.404	12
	Pipe	10.0	-	0.111	14
	Contact column 1	10.0	-	1.025	1
	Contact column 2	10.0	-	1.025	1

Calibration of the model parameters for describing the ozone concentration and UVA_{254} decrease

For the LDN bubble column pilot plant, known model parameters were used from Table 3, and a and SC_{BC} were calibrated on the basis of the results of the LDN experiments described in Table 1. The calibration results are given in Table 5. For the LDN experiments 1 and 2, with approximately the same gas flow as each other, the calibrated values for a and SC_{BC} are the same. LDN experiment 3, with a gas flow twice as high as experiments 1 and 2, had a lower a , thus the gas flow is more similar to swarms of bubbles, and a lower SC_{BC} , thus the short-circuit flow decreased due to the higher gas flow. This indicates that for an increasing RQ , the bubble flow shifts towards swarms of bubbles and the short-circuit flow decreases.

Table 5 Calibration results for LDN experiments 1, 2 and 3

Parameter	Unit	Experiment number		
		1	2	3
a	-	0.04	0.04	0.0187
SC_{BC}	-	0.50	0.50	0.40

In Figure 2 the measured and calculated ozone concentrations are shown for LDN experiments 1, 2 and 3 with an ozone dosage of 0.23, 0.91 and 1.4 mg-O₃/l, respectively. First, the ozone concentration increased in the counter current bubble column. Then, there was a sharp decrease in the ozone concentration at the bottom of the bubble column. The sharp decrease occurred when the water containing ozone mixed with the short-circuit flow without ozone. The decrease was due to dilution of the ozone concentration and to the rapid ozone consumption in the short-circuit flow. In addition, it was found from the model calculations that the sharp decrease in the ozone concentration could not be achieved by rapid ozone consumption alone. After the sharp decrease, the ozone concentration decreased further to 0 mg-O₃/l in the contact column and in the subsequent pipe. The model parameters used were based on experiments with ozone dosages ranging from approximately 0.3 mg-O₃/l to 1.0 mg-O₃/l (van der Helm et al., 2007a). From Figure 2 it can be observed that the equation for the slow ozone decay rate given in Table 3 appeared not to be valid for experiment 3 with an ozone dosage of 1.4 mg-O₃/l, where k_{O_3} is too low. This will be addressed further when discussing the combined expression for k_{O_3} valid for LDN and WPK.

For the WPK bubble column pilot plant, known model parameters were used from Table 3, and k_{O_3} , Y , UVA_0 , a and SC_{BC} were calibrated on the basis of the results

of the WPK experiments described in Table 2. The results for experiments 1, 7 and 13 with an ozone dosage of 1.5, 2.5 and 4.0 mg-O₃/l, respectively, are given in Table 6. Analogous to the results for the LDN experiments, *a* and SC_{BC} decreased with increasing RQ.

Table 6 Calibration results for WPK experiments 1, 7 and 13

Parameter	Unit	Experiment number		
		1	7	13
<i>k</i> _{O₃}	1/s	$0.0663e^{-0.7693C_{O_3,DOS}}$		
<i>Y</i>	(mg-O ₃ /l)/(1/m)	0.030		
<i>UVA</i> ₀	1/m	$UVA_{in} - (1.392C_{O_3,DOS} + 1.872)$		
<i>a</i>	-	0.05	0.061	0.061
SC _{BC}	-	0.25	0.30	0.30

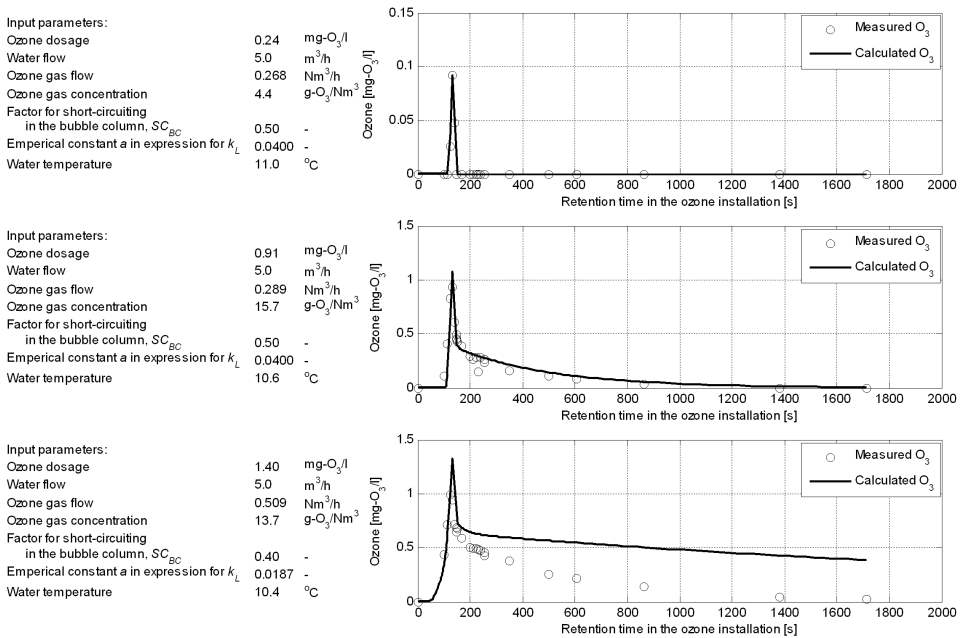


Figure 2 Ozone decay for LDN experiments 1 (top), 2 (middle) and 3 (bottom)

In Figure 3 the measured and calculated ozone concentrations in the WPK pilot plant are shown for WPK experiments 1, 7 and 13. The first increase in the ozone concentration was due to the first counter current bubble column, then a short retention time in the piping followed; the second increase was due to the second

ozone counter current bubble column. After both ozone bubble columns, a sharp decrease in the ozone concentration can be observed as a result of the mixing of ozonated water with the short-circuit flow. Subsequently, the ozone concentration decreased when the water flowed through the two ozone bubble columns where no ozone was dosed and through the two large ozone contact columns. Since the flow through the installation was $7.5 \text{ m}^3/\text{h}$ in experiments 1 and 13 and $10 \text{ m}^3/\text{h}$ in experiment 7, the peaks in ozone concentration, due to gas exchange in the bubble columns, appeared after shorter residence times for experiment 7.

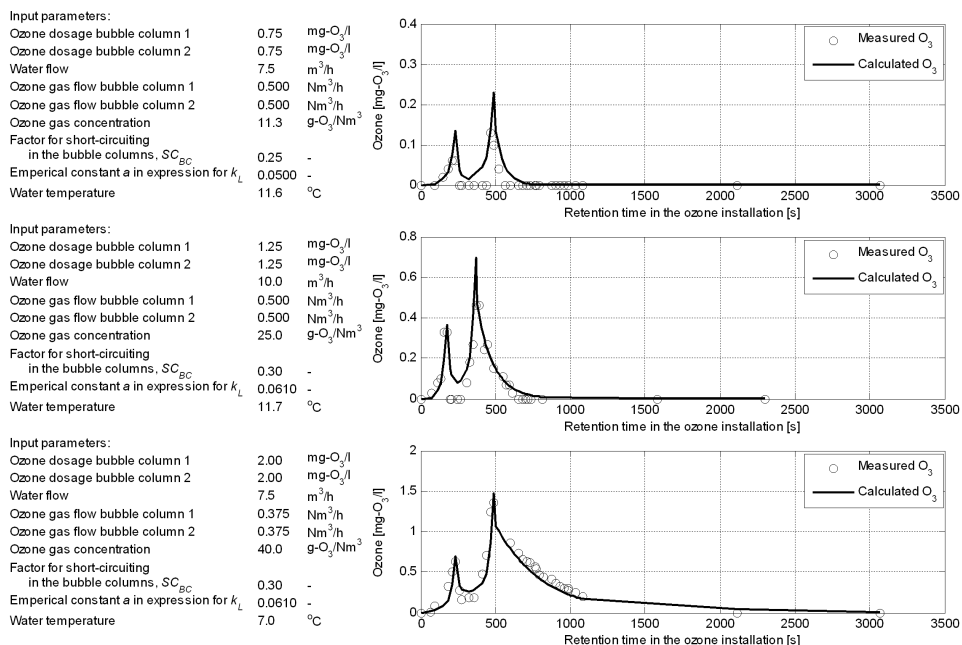


Figure 3 Ozone decay for experiments WPK 1 (top), 7 (middle) and 13 (bottom)

The resulting UVA_{254} decrease for LDN experiments 1, 2 and 3 and WPK experiments 1, 7 and 13 are given in Figure 4 and Figure 5, respectively. UVA_{254} decreased in the bubble columns due to rapid ozone consumption. The rate, however, was not determined by UVA_{254} decay rate (rapid ozone consumption rate) but by the gas exchange rate of ozone from the gas bubbles into the water. At the bottom of the bubble columns, UVA_{254} increased due to the mixing of the ozonated water flow with the short-circuit flow. After that UVA_{254} decreased further until stable UVA after ozonation (UVA_0) was reached.

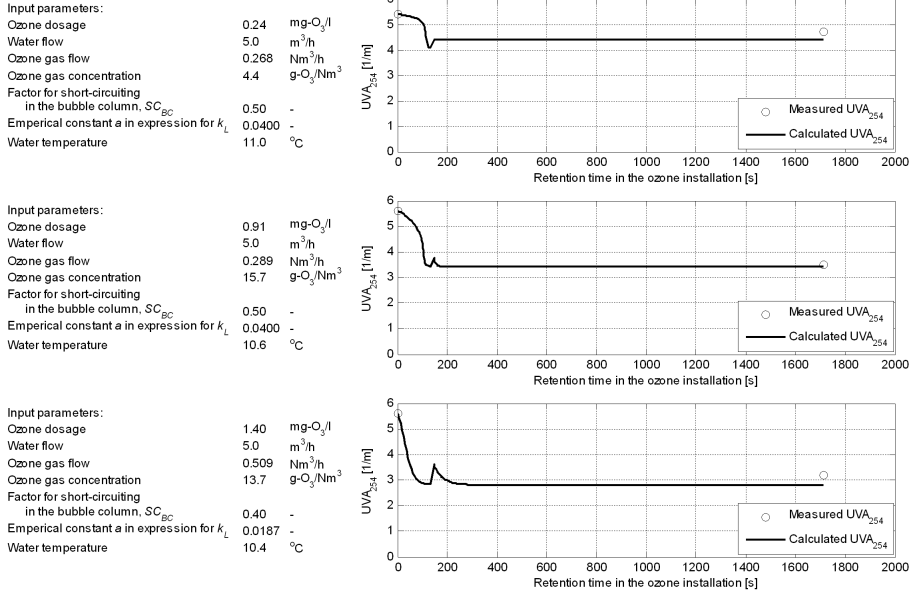


Figure 4 UVA₂₅₄ decrease for LDN experiments 1 (top), 2 (middle) and 3 (bottom)

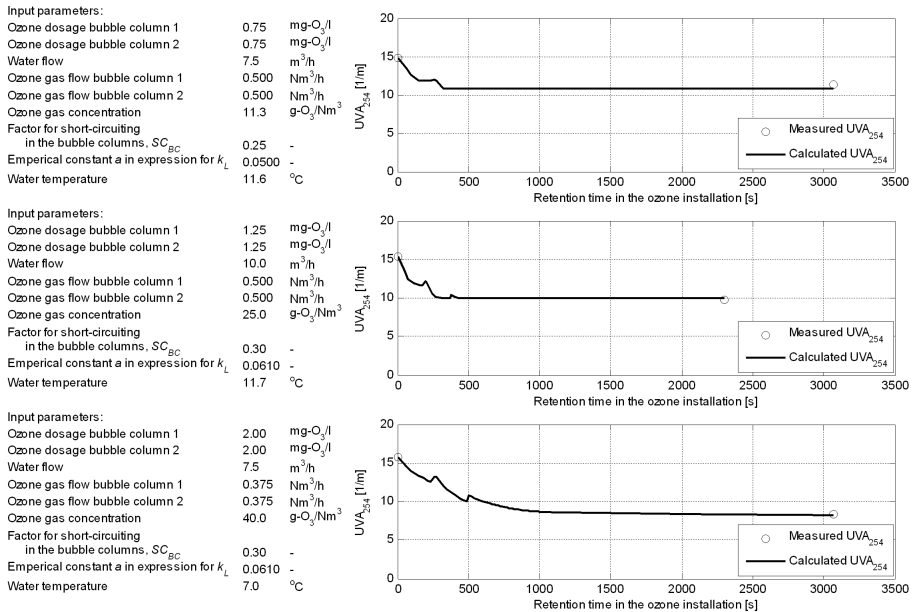


Figure 5 UVA₂₅₄ decrease for WPK experiments 1 (top), 7 (middle) and 13 (bottom)

Calibration of the model parameters for describing the bromate and AOC formation

For the LDN bubble column pilot plant, the model parameters for bromate and AOC formation were used from the DOPFR experiments (see Table 3). For the WPK bubble column pilot plant, k_{BrO_3} , and F_{AOC} were calibrated from the measured data shown in Figure 6:

$$k_{BrO_3} = 0.69 \quad (\mu\text{g-BrO}_3/\text{l})/((\text{mg-O}_3/\text{l})\cdot\text{min})$$

$$F_{AOC} = 5.0 \quad (\mu\text{g-C/l})/(\text{mg-O}_3/\text{l}\cdot\text{mg-C/l})$$

Although the correlation for F_{AOC} is very low (see Figure 6, right) it will be used in further model calculations. In addition to the method of van der Kooij et al. (1982), AOC formation was measured on-line with a spectro:lyser™, which is a submersible spectrophotometer from scan Messtechnik. This instrument measures absorbance of ultraviolet and visible light from 200 to 750 nm (Langergraber et al., 2003). From AOC measurements and on-line UV absorbance spectrum measurements before and after ozonation, before and after pellet softening and before and after biological activated (BAC) filtration at the WPK pilot plant, van den Broeke et al. (2007) found a correlation between the AOC formation and AOC removal and the differential UV spectra. The measurements carried out before and after ozonation were performed simultaneously with WPK experiments 1, 8, 9, 11, 12 and 14, and gave promising results for the on-line measurement of AOC (van den Broeke et al., 2007).

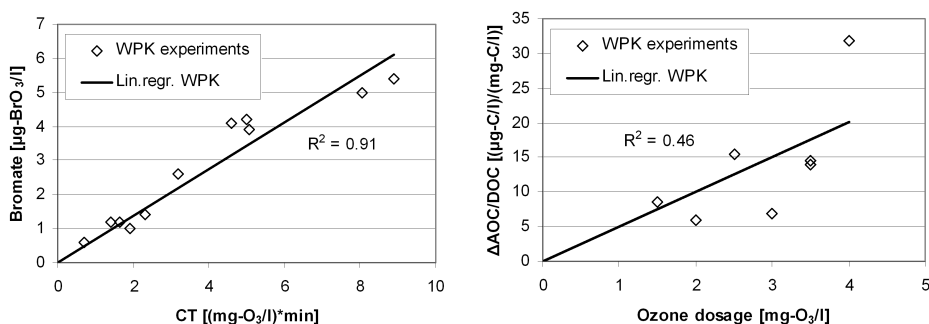


Figure 6 Bromate concentration after ozonation versus the total CT (left) and AOC formation per DOC as a function of the ozone dosage (right)

Combined expressions for ozonation model parameters for LDN and WPK

For k_{O_3} , UVA_0 , Y , F_{AOC} and k_{BrO_3} , the possibilities were studied for combining the expressions derived for LDN and WPK. Data from the bubble column experiments described in this research and data from pilot-plant DOPFR experiments (van der Helm et al., 2007a) were used. In Figure 7 the results are shown for k_{O_3} and UVA_0 .

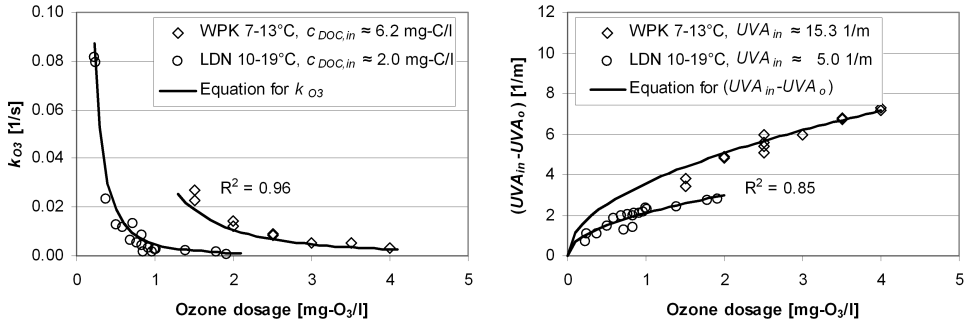


Figure 7 Slow ozone decay rate (left) and UVA_{254} decrease (right) versus the ozone dosage for WPK and LDN experiments

The equations describing k_{O_3} and UVA_0 for the data sets from LDN and WPK as shown in Figure 7 are:

$$k_{O_3} = 0.0011 \frac{c_{DOC,in}^2}{c_{O_3,DOS}^2} \quad [13]$$

$$UVA_0 = UVA_{in} - 0.914 c_{O_3,DOS}^{1/2} UVA_{in}^{1/2} \quad [14]$$

Y has the properties of a stoichiometric coefficient, that is independent of the ozone dosage (van der Helm et al., 2007b), meaning that there is one calibrated value for the LDN data, which was 0.137 (mg- O_3 /l)/(1/m), and one value for the WPK data, which was 0.010 (mg- O_3 /l)/(1/m). Based on only two data points it is not possible to determine a relationship between the Y and differences in water quality parameters at LDN and WPK.

The same applies to F_{AOC} and k_{BrO_3} . For bromate formation, however, empirical relationships can be found in the literature based on water quality parameters, such as the multiple linear regression model described by Sohn et al. (2004):

$$c_{BrO_3} = 1.55 \cdot 10^{-6} (c_{DOC,in})^{-1.26} (pH_{in})^{5.82} (c_{O_3,DOS})^{1.57} (c_{Br,in})^{0.73} \left(\frac{t}{60}\right)^{0.28} (1.035)^{T-20} \quad [15]$$

where $1.1 \leq c_{DOC,in} \leq 8.4$, $6.5 \leq pH_{in} \leq 8.5$, $1.1 \leq c_{O_3,DOS} \leq 10.0$, $c_{Br,in}$ is the influent bromide concentration ($\mu\text{g-Br/l}$), $70 \leq c_{Br,in} \leq 440$, $1 \leq t/60 \leq 120$ and $2 \leq T \leq 24$.

When describing bromate formation as a linear function of CT, as in Equation [7], bromate formation in different water types is only dependent on pH, bromide concentration and temperature. The water temperature for the LDN and WPK bubble column experiments were approximately the same, so there are no differences in bromate formation due to temperature differences. This means that the ratio between the bromate formation rate constants determined for LDN and WPK water should be equal to the ratio determined by the differences in pH and bromide concentration given by Equation [15]. For the average pH and bromide concentrations of the bubble column experiments the ratios are:

$$\frac{k_{BrO_3,LDN}}{k_{BrO_3,WPK}} = \frac{1.66}{0.69} = 2.41$$

$$\frac{(pH_{in,LDN})^{5.82} (c_{Br,in,LDN})^{0.73}}{(pH_{in,WPK})^{5.82} (c_{Br,in,WPK})^{0.73}} = \frac{(8.07)^{5.82} (187.5)^{0.73}}{(7.5)^{5.82} (97.9)^{0.73}} = 2.46$$

Since the ratios are approximately equal, k_{BrO_3} can be expressed as a function of pH and bromide, and the equation for bromate formation as a function of CT is:

$$c_{BrO_3} = k_{BrO_3} CT = 1.94 \cdot 10^{-7} CT (pH_{in})^{5.82} (c_{Br,in})^{0.73} \quad [16]$$

In Figure 8 the bromate formation during ozonation is plotted against CT for the LDN experiments 2 to 6 and the WPK experiments 3 and 5 to 14, together with the bromate formation determined from Equation [16]. For LDN experiment 1 and WPK

experiments 1, 2 and 4, the bromate formation was below the detection limit of 0.5 $\mu\text{g-BrO}_3/\text{l}$.

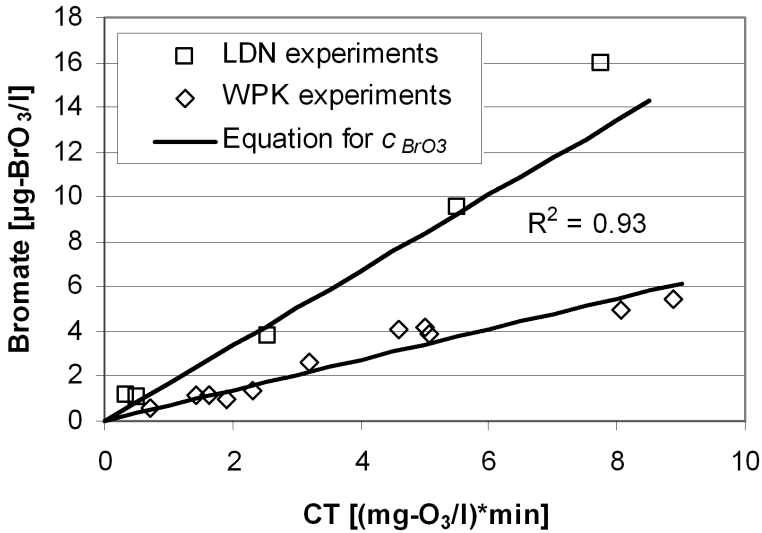


Figure 8 Bromate formation for LDN experiments 2 to 6 and WPK experiments 3 and 5 to 14 and the results from Equation [16]

When temperature as described in Equation [15] is also included, the equation for k_{BrO_3} in Equation [16] becomes:

$$k_{BrO_3} = 2.74 \cdot 10^{-7} (pH_{in})^{5.82} (c_{Br,in})^{0.73} (1.035)^{T-20} \quad [17]$$

The temperature dependency of Equation [17] is in agreement with the temperature dependency determined in LDN pilot-plant DOPFR experiments (van der Helm et al., 2007a).

In Table 7 all unknown parameters from Table 3 and the parameters for which combined relationships for LDN and WPK are determined are given.

Table 7 Calibrated parameters of ozonation models for bubble column pilot plants at LDN and WPK

Parameter	Value	Unit	Remark
k_{O_3}	LDN and WPK $0.0011 \frac{c_{DOC,in}^2}{c_{O_3,DOS}^2}$	1/s	van der Helm et al. (2007a) & experiments this research
γ	LDN 0.137 WPK 0.030	$\frac{mg-O_3/l}{1/m}$	van der Helm et al. (2007a) experiments this research
UVA_0	LDN and WPK $UVA_m - 0.914c_{O_3,DOS}^{1/2}UVA_m^{1/2}$	1/m	van der Helm et al. (2007a) & experiments this research
a	LDN 0.0187 – 0.04 WPK 0.05 – 0.061	-	For single gas bubbles $a=0.061$ and for swarms of gas bubbles $a=0.0187$ (Hughmark, 1967)
SC_{BC}	LDN 0.40 – 0.50 WPK 0.25 – 0.30	-	experiments this research
$F_{BrO_3,ini}$	0	$\frac{\mu g-BrO_3/l}{mg-O_3/l}$	experiments this research
k_{BrO_3}	LDN and WPK $2.74 \cdot 10^{-7} (pH_{in})^{5.82} (c_{Br,in})^{0.73} (1.035)^{T-20}$	$\frac{\mu g-BrO_3/l}{(mg-O_3/l)*min}$	van der Helm et al. (2007a) & experiments this research
F_{AOC}	LDN 45 WPK 5.0	$\frac{\mu g-C/l}{mg-O_3/l*mg-C/l}$	van der Helm et al. (2007a) experiments this research

In Figure 9 ozone decay, bromate formation, UVA_{254} decrease and disinfection are shown for LDN experiment 3 based on Table 3 and Table 7 including the combined expressions for ozonation model parameters for WPK and LDN. From Figure 9 it can be observed that the calculated *E. coli* disinfection underestimates the actual disinfection measured in the bubble column. The ozone concentrations calculated by the model are fairly good, in contrast to the calculated concentrations shown in Figure 2. The DOC concentration used to determine k_{O_3} is 2.1 mg-C/l instead of 1.7 mg-C/l, because the latter value is likely to be an analysis error when all values in Table 1 are considered. When the calculations were performed with a DOC concentration of 2.1 mg-C/l, the calculated ozone concentrations were in agreement with the measured ozone concentrations. Thus, the model calculations can also be used to validate laboratory measurements. In Figure 10 the results are shown for WPK experiment 13 based on the combined expressions for ozonation model parameters for WPK and LDN. Due to the high ozone concentrations, the *E. coli* disinfection predicted by the model is more than 4 log units in the first 70 seconds of contact time.

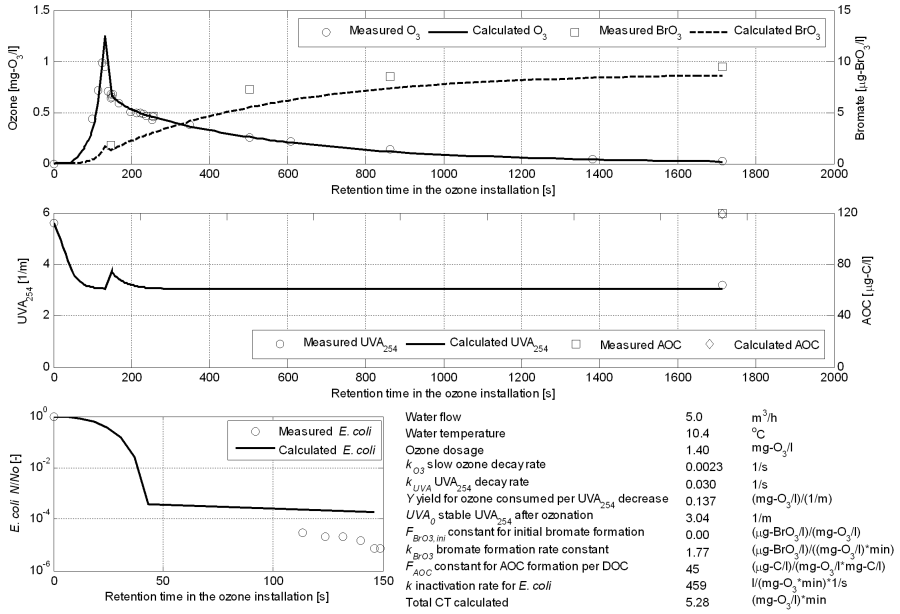


Figure 9 Results for LDN experiment 3

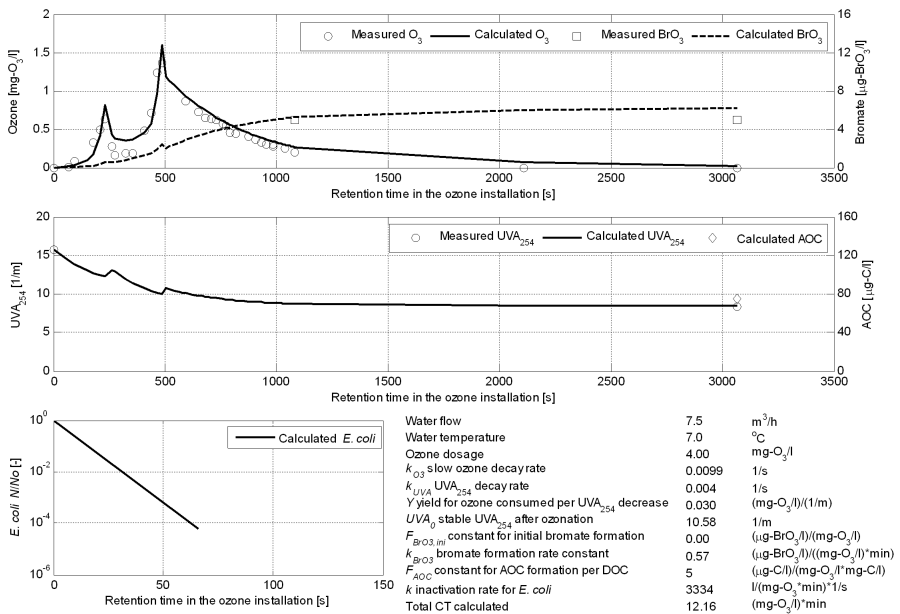


Figure 10 Results for WPK experiment 13

Control strategies

The control strategies were evaluated for the year 2004. In Figure 11, the temperature of the ozonation influent throughout the year is shown together with the monthly average temperatures. The temperature ranges from approximately 1°C to 23°C. The model parameters for WPK were determined based on a temperature range of 7.0 °C to 13.1°C. This range is too small to determine temperature dependencies of the model parameters in order to perform model calculations for a whole year. Therefore, temperature dependencies were used from the literature. The values are arbitrary and the calculations for the control strategies have to be regarded as examples. The activation energy used for the slow ozone decay rate was 70 kJ/mol, as determined by Elovitz et al. (2000) for Lake Zürich water. The frequency factor was determined for different ozone dosages by calculating k_{O_3} value with Equation [13] for the average temperature of the WPK experiments (10°C). k_{UVA} is, for the main part, limited by gas transfer and will therefore not be corrected for temperature. Y and UVA_o were assumed to be temperature independent. For F_{AOC} the activation energy was used that was determined from LDN pilot-plant DOPFR experiments (van der Helm et al., 2007a), where E_a was 80.5 kJ/mol. The frequency factor A was determined from the F_{AOC} for WPK for the average temperature of 10°C from Table 7 and is $3.55 \cdot 10^{15}$ ($\mu\text{g-C/l}/(\text{mg-O}_3/\text{l} \cdot \text{mg-C/l})$).

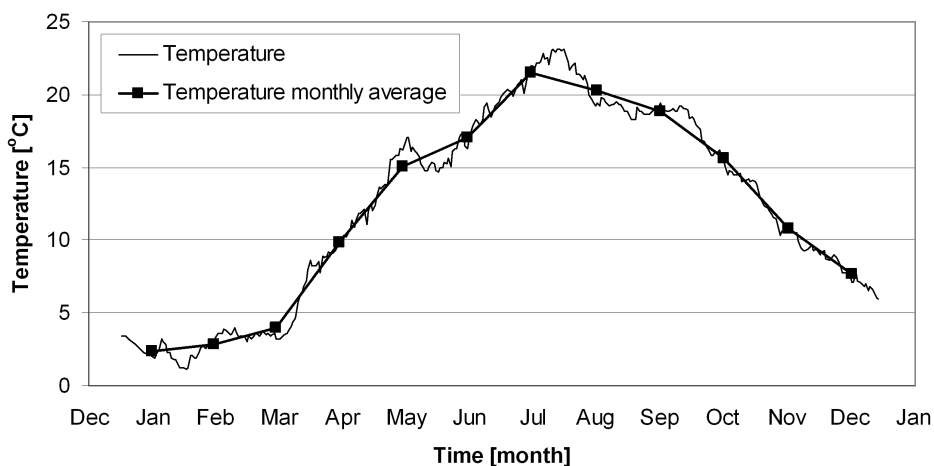


Figure 11 Temperature of ozonation influent throughout the year and the monthly averages

The results for the current control strategy at WPK where the ozone dosage is 1.7 mg-O₃/l when the water temperature is above 12°C and 2.2 mg-O₃/l when the water temperature is below 12°C are shown in Figure 12. It can be observed that by choosing a fixed set point for the ozone dosage, neither CT, nor bromate nor AOC is actively controlled; the water temperature mainly determines the values. The results for the maximal CT control strategy are shown in Figure 13. The ozone dosage is calculated for the situation that a maximum allowed effluent bromate concentration is reached and for the situation that a maximum allowed AOC concentration is reached. Set point for the ozone dosage is the higher of the two calculated dosages. In this example the maximal allowed bromate concentration was 3.0 µg-BrO₃/l and the maximal allowed AOC concentration was 110 µg-C/l, which is the average effluent concentration of the current control strategy shown in Figure 12. From Figure 13 it can be observed that the CT value is high from December to April and almost 0 (mg-O₃/l)*min in July, August and September. By limiting AOC formation to 110 µg-C/l, the ozonation has no disinfection capacity when the water temperature is high. The results for the log inactivation control strategy, where the ozone dosage is determined by a set point for the log inactivation of *Giardia*, are shown in Figure 14. The set point used was a 2.0 log inactivation for *Giardia* throughout the year. The CT for *Giardia* inactivation for different temperatures was determined from Table 8 (USEPA, 1989).

Table 8 CT values for inactivation of *Giardia* by ozone (USEPA, 1989)

<i>Giardia</i> log inactivation	Temperature [°C]					
	0.5	5	10	15	20	25
0.5	0.48	0.32	0.23	0.16	0.12	0.08
1.0	0.97	0.63	0.48	0.32	0.24	0.16
1.5	1.5	0.95	0.72	0.48	0.36	0.24
2.0	1.9	1.3	0.95	0.63	0.48	0.32
2.5	2.4	1.6	1.2	0.79	0.60	0.40
3.0	2.9	1.9	1.4	0.95	0.72	0.48

In Figure 14 it can be observed that the ozone dosage has to increase in the warm water months, rather than decrease according to the current strategy, in order to maintain the *Giardia* inactivation at 2 log units. This gives higher AOC values than for the current strategy. The bromate concentration does not exceed 1.0 µg-BrO₃/l. By taking the disinfection capacity of the other processes into consideration, a decision can be made about the possibility of controlling AOC formation at the expense of the disinfection capacity. When the disinfection capacity of the ozone installation is needed from May to October, a higher AOC concentration has to be

accepted during these months depending on the desired disinfection capacity. When this is unacceptable, scenario calculations can be performed with the model, for instance DOC removal prior to ozonation.

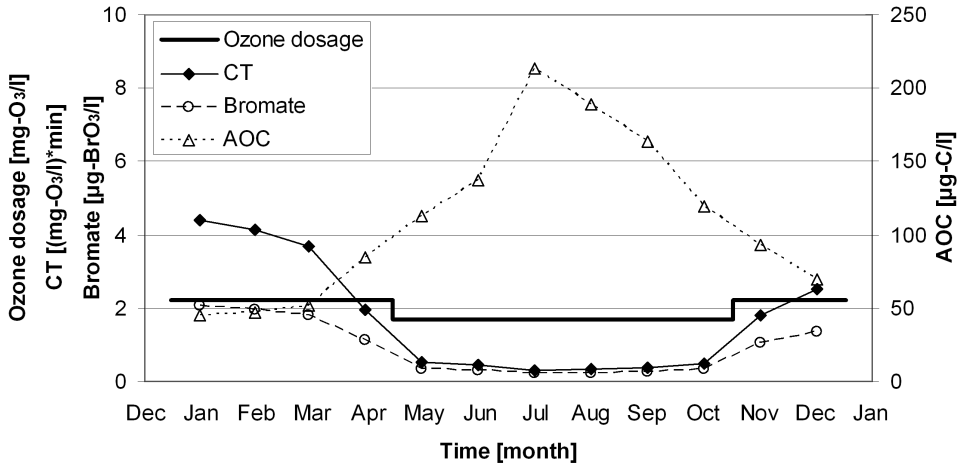


Figure 12 Current ozonation control strategy at WPK

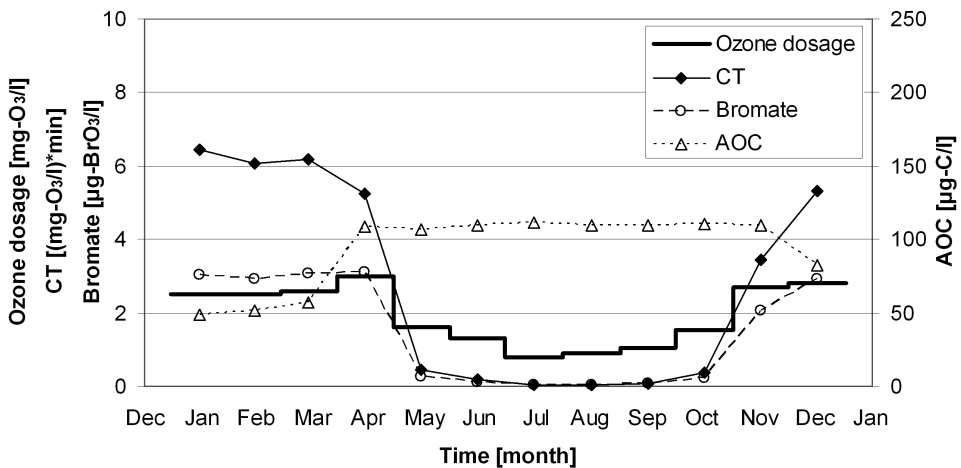


Figure 13 Control strategy for maximal CT limited by a maximal allowed bromate concentration of 3.0 µg-BrO₃/l and a maximal allowed AOC concentration of 110 µg-C/l.

The discussed control strategies were applied to historical data and set points were calculated once every month. With the model it is also possible to continuously predict the CT, bromate and AOC formation based on laboratory data and on-line measurements. For an accurate prediction it is important to use a moving average for the measurements to exclude outliers. For on-line measurements this is not a problem because they have high data densities, but for laboratory measurements densities can be very low: down to 12 measurements a year for AOC. Especially for DOC, it is important to use a moving average since the determination of slow ozone decay is important for the calculated CT and the slow ozone decay is very sensitive to the DOC concentration. The standard deviation of a DOC measurement of 5.0 mg-C/l in natural water is 0.36 mg-C/l when measured by an accredited laboratory. This means that substantial deviations between calculated and actual ozone concentrations in the installation can occur when model calculations are based on single DOC values. By using on-line UV/vis spectrometry, DOC can be measured continuously (Rieger et al., 2004). This can be used to increase data density for DOC. For AOC both the standard deviation and the data density should be increased for a more accurate control of ozonation with regard to AOC formation. Van den Broeke et al. (2007) and Ross et al. (2007) started research on on-line measurement of AOC formation during ozonation with on-line UV/VIS spectrometry. This measurement has the potential to further improve the control of ozone installations.

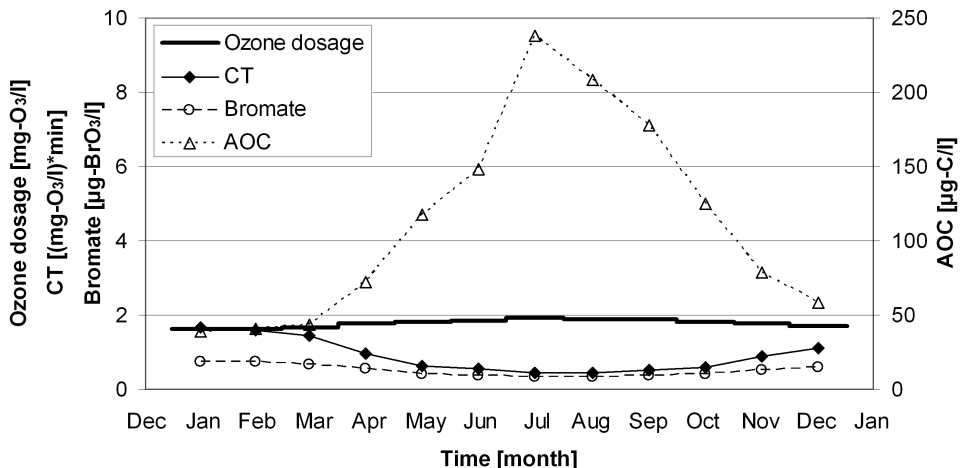


Figure 14 Control strategy for 2 log inactivation for Giardia

Conclusions

The integrated ozonation model is a valuable tool for controlling the balance between disinfection, bromate formation and AOC formation and can be used for evaluation of control strategies for operational support and for process control. It is a tool that directly shows the consequences of changes in operation of the ozone installation. It enables water supply companies to make more objective choices for operational settings. The model can be applied to different ozonation plants, and by using parameters that can be measured on-line, such as ozone and UVA_{254} , the model has the potential to be calibrated and validated on-line. For the case of Waternet with relatively low ozone dosages compared to the DOC concentrations, ozone concentrations in the bubble columns can also be determined for a more accurate prediction of disinfection capacity and bromate formation. In pilot-plant bubble columns, with relatively good hydraulic characteristics compared to full-scale installations, already large short-circuit flows occur: up to half the total flow through a bubble column. In order to obtain good results from dynamic models using order differential equations, the modeled hydraulic characteristics, in this case the number of CSTRs and the short-circuit flow, have a distinct influence on the results. This is important when applying the model to other ozonation pilot plants and full-scale installations.

Acknowledgement

This research was carried out as part of the project 'Promicit', a cooperation of Waternet, Delft University of Technology, DHV B.V. and ABB B.V. and was subsidized by SenterNovem, agency of the Dutch Ministry of Economic Affairs. The aim of the project was to achieve a breakthrough in drinking water quality control by developing an integrated model of the total water treatment and using this model as a basis for operation.

Nomenclature

AOC	assimilable organic carbon
CSTR	completely stirred tank reactor
DOC	dissolved organic carbon
DOPFR	dissolved ozone plug flow reactor
<i>E. coli</i>	<i>Escherichia coli</i>

LDN	drinking water treatment plant Leiduin of Waternet
RTD	residence time distribution
UVA ₂₅₄	UV absorbance at 254 nm
Waternet	water cycle company for Amsterdam and surrounding areas
WPK	drinking water treatment plant Weesperkarspel of Waternet
α	temperature and pressure correction factor $\alpha=(P_g/P_o)(T_o/T_g)$
A	frequency factor (unit depending on the unit of k)
a, b	empirical constants (for single gas bubbles $a=0.061$ and $b=1.61$ and for swarms of gas bubbles $a= 0.0187$ and $b=1.61$)
a_{BrO_3}	multiple linear regression constant for bromate formation
C_{AOC}	AOC concentration ($\mu\text{g-C/l}$)
$C_{AOC,in}$	influent AOC concentration ($\mu\text{g-C/l}$)
$C_{Br,in}$	influent bromide concentration ($\mu\text{g-Br/l}$)
C_{BrO_3}	bromate concentration ($\mu\text{g-BrO}_3/\text{l}$)
$C_{BrO_3,in}$	influent bromate concentration ($\mu\text{g-BrO}_3/\text{l}$)
$C_{BrO_3,ini}$	initial bromate formation ($\mu\text{g-BrO}_3/\text{l}$)
$C_{DOC,in}$	influent dissolved organic carbon concentration (mg-C/l)
C_{O_3}	concentration of ozone in water ($\text{mg-O}_3/\text{l}$)
$C_{O_3,DOS}$	ozone dosage ($\text{mg-O}_3/\text{l}$)
C_{O_3g}	ozone in gas concentration ($\text{g-O}_3/\text{Nm}^3$)
CT	ozone exposure ($(\text{mg-O}_3/\text{l})\cdot\text{min}$)
d_b	bubble diameter (m)
D_{O_3}	diffusion coefficient of ozone (m^2/s)
E_a	activation energy (J/mol)
F_{AOC}	constant for AOC formation per DOC ($(\mu\text{g-C/l})/(\text{mg-O}_3/\text{l}\cdot\text{mg-C/l})$)
$F_{BrO_3,ini}$	constant for initial bromate formation ($(\mu\text{g-BrO}_3/\text{l})/(\text{mg-O}_3/\text{l})$)
g	specific gravity (m/s^2)
k	inactivation rate coefficient ($1/(\text{mg-O}_3\cdot\text{min})$ for $n=1$ and $m=1$)
k_{BrO_3}	bromate formation rate constant ($(\mu\text{g-BrO}_3/\text{l})/((\text{mg-O}_3/\text{l})\cdot\text{min})$)
k_D	distribution coefficient (-)
k_L	gas transfer coefficient (m/s)
k_{O_3}	slow ozone decay rate (1/s)
k_{UVA}	UVA ₂₅₄ decay rate (1/s)
ν	kinematic viscosity (m^2/s)
N	number concentration of organisms (CFU/100 ml)
n_{SP}	number of sampling points (-)
n, m	empirical constants (-)

P_o	standard pressure (101325 Pa),
P_g	gas pressure in the reactor (Pa)
pH_{in}	influent pH
Q	water flow (m^3/h)
Q_g	gas flow (Nm^3/h)
$Q_{SC,BC}$	short-circuiting flow in the bubble column (m^3/h)
ρ_w	water density (kg/m^3).
R	ideal gas constant (8.314 J/(mol*K))
RQ	gas to water flow ratio (Q_g/Q) (Nm^3/m^3)
σ	surface tension (N/m)
SC_{BC}	factor for short-circuiting in the bubble column (-)
t	time (s)
T	temperature of the water ($^{\circ}C$)
T_a	absolute temperature of the water (K)
T_g	gas temperature in the reactor (K)
T_o	standard temperature (273.15 K)
u	water velocity (m/s)
u_b	bubble rising velocity (m/s)
u_g	gas velocity (m/s)
UVA	UVA_{254} in water (1/m)
UVA_o	stable UVA_{254} after completion of the ozonation process (1/m)
UVA_{in}	influent UVA_{254} (1/m)
x	length of the reactor (m)
Y	yield for ozone consumed per UVA_{254} decrease ($(mg-O_3/l)/(1/m)$)

References

- Bader, H. and Hoigné, J. (1982). Determination of ozone in water by the indigo method; a submitted standard method. *Ozone Sci. Eng.*, 4(4), 169-176.
- Degrémont (1991). *Water treatment handbook – Volume 1*. Lavoisier Publishing, Paris, France.
- Elovitz, M.S., von Gunten, U. and Kaiser, H.P. (2000). Hydroxyl radical/ozone ratios during ozonation processes. II. The effect of temperature, pH, alkalinity, and DOM properties. *Ozone Sci. Eng.*, 22(2), 123-150.
- Hughmark, G.A. (1967). Holdup and mass transfer in bubble columns. *Ind. Eng. Chem. Process Des. Dev.*, 6(2), 218-220.

- Langergraber, G., Fleischmann, N. and Hofstädter, F. (2003). A multivariate calibration procedure for UV/VIS spectrometric quantification of organic matter and nitrate in wastewater. *Wat. Sci. Technol.*, 47(2), 63-71.
- Langlais, B., Reckhow, D.A. and Brink, D.R. (1991). *Ozone in water treatment: Application and Engineering*. Lewis Publishers, Chelsea, USA.
- Orlandini, E., Kruithof, J.C., van der Hoek, J.P., Siebel, M.A. and Schippers, J.C. (1997). Impact of ozonation on disinfection and formation of biodegradable organic matter and bromate. *J. Water Supply Res. Technol. AQUA*, 46(1), 20-30.
- Rieger, L., Langergraber, G., Thomann, M., Fleischmann, N. and Siegrist, H. (2004). Spectral in-situ analysis of NO₂, NO₃, COD, DOC and TSS in the effluent of a WWTP. *Wat. Sci. Technol.*, 50(11), 143-152.
- Rietveld, L.C. (2005). *Improving operation of drinking water treatment through modelling*. PhD Thesis, Faculty of Civil Engineering and Geosciences, Delft University of Technology.
- Ross, P.S., van der Helm, A.W.C., van den Broeke, J., van der Aa, L.T.J., Rietveld, L.C. and van Dijk, J.C. (2007). Characterization of NOM by UV-spectrography in drinking water treatment processes to assess biological stability. *Proceedings of the 4th IWA Leading-Edge Conference and Exhibition on Water and Wastewater Technologies*, Singapore, Republic of Singapore, 2007.
- Smeenk, J.G.M.M., van Rossum, W.J.M., Gademan, W.J.H. and Bruggink, C. (1994). Trace level determination of bromate and chlorite in drinking and surface water by ion chromatography with automated preconcentration. *Proceedings of the International Ion Chromatography Symposium*, Torino, Italy, 1994.
- Smeets, P.W.M.H., van der Helm, A.W.C., Dullemont, Y.J., Rietveld, L.C., van Dijk, J.C. and Medema, G.J. (2006). Inactivation of *Escherichia coli* by ozone under bench-scale plug flow and full-scale hydraulic conditions. *Water Res.*, 40(17), 3239-3248.
- Sohn, J., Amy, G., Cho, J., Lee, Y. and Yoon, Y. (2004). Disinfectant decay and disinfection by-products formation model development: chlorination and ozonation by-products. *Water Res.*, 38(10), 2461-2478.
- Standard Methods (2005). *Standard Methods for the examination of water & wastewater 2005 21st edition*, American Public Health Association/American Water Works Association/Water Environment Federation, Baltimore, USA.

- USEPA (1989). *Guidance manual for compliance with the filtration and disinfection requirements for public water systems using surface water supplies*. USEPA, Washington, D.C.
- van den Broeke, J., Ross, P.S., van der Helm, A.W.C., Baars, E.T. and Rietveld, L.C. (2007). Use of on-line UV/Vis-spectrometry in the measurement of dissolved ozone and AOC concentrations in drinking water treatment. *Proceedings of the IWA AutMoNet 2007*, Gent, Belgium, 2007.
- van der Helm, A.W.C. and Rietveld, L.C. (2002). Modelling of drinking water treatment processes within the Stimela environment. *Water Sci. Technol.: Water Supply*, 2(1), 87-93.
- van der Helm, A.W.C., Rietveld, L.C., van der Aa, L.T.J. and van Dijk, J.C. (2006). Integral optimisation of drinking water treatment plants. *Proceedings of the AWWA Water Quality Technology Conference & Exposition*, Denver, USA, 2006.
- van der Helm, A.W.C., Rietveld, L.C., Baars, E.T. and van Dijk, J.C. (2007a). Disinfection and by-product formation during ozonation in a pilot-scale plug flow reactor and CSTR. *J. Water Supply Res. Technol. AQUA*, submitted for publication, September 2007.
- van der Helm, A.W.C., Smeets, P.W.M.H., Baars, E.T., Rietveld, L.C. and van Dijk, J.C. (2007b). Modelling of Ozonation for Dissolved Ozone Dosing. *Ozone Sci. Eng.*, accepted for publication, February 2007.
- van der Helm, A.W.C., Grefte, A., Baars, E.T., Rietveld, L.C., van Dijk, J.C. and Amy, G.L. (2007c). Effects of natural organic matter (NOM) character and removal on efficiency of ozonation. *J. Water Supply Res. Technol. AQUA*, submitted for publication, April 2007.
- van der Kooij, D., Visser, A. and Hijnen, W.A.M. (1982). Determining the concentration of easily assimilable organic carbon in drinking water. *Am. Water Works Assoc. J.*, 74(10), 540-545.
- Wallis, G.B. (1969). *One-dimensional two-phase flow*, McGraw-Hill, New York, USA.
- Wols, B.A., Hofman, J.A.H.M., Uijttewaal, W.S.J. and van Dijk, J.C. (2006). The effect of turbulent diffusion on the performance of ozone systems. *Proceedings of the Workshop Developments in Drinking Water Treatment Modelling*, Delft University of Technology, Delft, the Netherlands, 2006.

7. Conclusions

Objectives for optimization

In the present thesis integrated modeling of ozonation for optimization of drinking water treatment was investigated. Part of the study was to determine what the objectives for optimization of the operation of drinking water treatment plants should be. Three possible objectives were assessed: environmental impact, costs and water quality. The assessments were carried out for the case of the drinking water treatment plant Weesperkarspel (WPK) and its pre-treatment plant Loenderveen (LNV) of Waternet (the water cycle company for Amsterdam and surrounding areas). The pre-treatment plant LNV consists of coagulation, sedimentation, storage in a lake-water reservoir and rapid sand filtration. Subsequently, water is transported to WPK that consists of ozonation, pellet softening, biological activated carbon (BAC) filtration and slow sand filtration.

It can be concluded that the environmental impact of the operation of drinking water production is relatively low compared to other activities, such as driving a car. A decrease of 10% in environmental impact by changes in operation of LNV and WPK is equivalent to a decrease in car mileage of approximately 3 km per drinking water consumer in Amsterdam per year. The operational costs of drinking water production are less than 10% of the total costs of drinking water that include also water distribution, investment costs, taxes, salaries of office personnel etc. Therefore, the possible reduction of the total costs by changes in the operation of drinking water production is small. Based on social, environmental and economical considerations, it can be concluded that governments and drinking water supply companies should aim for an impeccable tap water quality and a reliable, healthy, and environmentally sound image of tap water in order to at least stop the increase in bottled water use. Based on these considerations, it was concluded in Chapter 2 that the objective for integrated optimization of the operation of drinking water treatment plants should be the improvement of water quality and not an a priori reduction of environmental impact or costs, although the environmental impact and costs will benefit from water quality optimization, since water quality optimization also involves optimal usage of chemical dosages.

From the water quality assessment it can be concluded that chemical stability, biological stability and disinfection are the most important water quality objectives for integrated optimization of LNV and WPK. Toxicity (e.g. caused by bromate) is not a problem in the current operation but should be a point of constant attention. For chemical stability, the saturation index (SI) should be used as a parameter for optimization; for biological stability, the parameters should be assimilable organic carbon (AOC) and dissolved organic carbon (DOC), and for disinfection, the parameters should include selected indicators for pathogens. Because the SI, AOC, DOC and pathogen concentrations are influenced by multiple processes and influence multiple processes, an integrated approach to these parameters is necessary. Because of the complexity of the relationships and the effects on these parameters by changes in the operational settings, the settings can best be evaluated by an integrated model. The integrated pH model for SI control including all chemical dosages influencing SI is part of separate research at Waternet. For AOC, DOC and pathogens, ozonation plays a key role in integrated optimization. Ozonation is influenced by the pre-treatment and influences softening and the BAC filtration. In addition, ozonation is the only process in which disinfection can be actively influenced. Therefore, the focus in this research has been on the integrated modeling of ozonation.

When some water quality objectives cannot be achieved by operational optimization, changes in the reactor design of the current treatment steps should be considered. When changes in the design are not sufficient, changes in the treatment concept should be considered, such as replacing and/or adding treatment steps. In the following section, the three steps from operational optimization to changes in design and the treatment concept are discussed for the case of WPK.

Operational optimization

The consequence of the conclusion that the improvement of water quality should be the objective for operational optimization will have an impact on the current operation of the drinking water treatment plant WPK. The current regeneration time of the BAC filters at WPK is 18 months, and the current ozone dosage is 2.5 mg- O_3 /l. When it is assumed that the AOC concentration for the produced drinking water should be set at a maximum of 10 $\mu\text{g-C/l}$, as proposed by van der Kooij (1992) in order to prevent regrowth in the distribution system, then the effluent

concentration of the BAC filters should be a maximum of 15 $\mu\text{g-C/l}$. In the subsequent slow sand filters the AOC removal is 5 $\mu\text{g-C/l}$ on average, see Chapter 2. From data presented by van der Aa et al. (2003), the cumulative time-weighted average AOC concentration after BAC filtration at WPK is determined, representing the average effluent AOC concentration of multiple BAC filters, as a function of the regeneration time. In Figure 1 these are shown for ozone dosages of 2.5 $\text{mg-O}_3/\text{l}$, 1.5 $\text{mg-O}_3/\text{l}$, 0.5 $\text{mg-O}_3/\text{l}$ and 0.0 $\text{mg-O}_3/\text{l}$. According to these data, in the current situation, the effluent concentration of the BAC filters is around 30 $\mu\text{g-C/l}$. A maximum AOC concentration of 15 $\mu\text{g-C/l}$ after BAC filtration through changes in operation can be achieved by a decrease in regeneration time or by a decrease in ozone dosage. Decreasing the regeneration time in order to reach 15 $\mu\text{g-C/l}$ would result in a regeneration time of 5 months, see Figure 1. Decreasing the ozone dosage to 0.0 $\text{mg-O}_3/\text{l}$ will also lead to an effluent AOC concentration below 15 $\mu\text{g-C/l}$ after BAC filtration, see Figure 1. Next to these extremes, also combinations of changes in regeneration time and ozone dosage can be applied to ensure an effluent AOC concentration in the produced drinking water of 10 $\mu\text{g-C/l}$, see Table 1. In Table 1 also the resulting DOC concentrations of the produced drinking water are shown for the different measures. When the current company standard of 2.5 mg-C/l for DOC is applied, this leads to an ozone dosage 0.95 $\text{mg-O}_3/\text{l}$ and a regeneration time of 8 months.

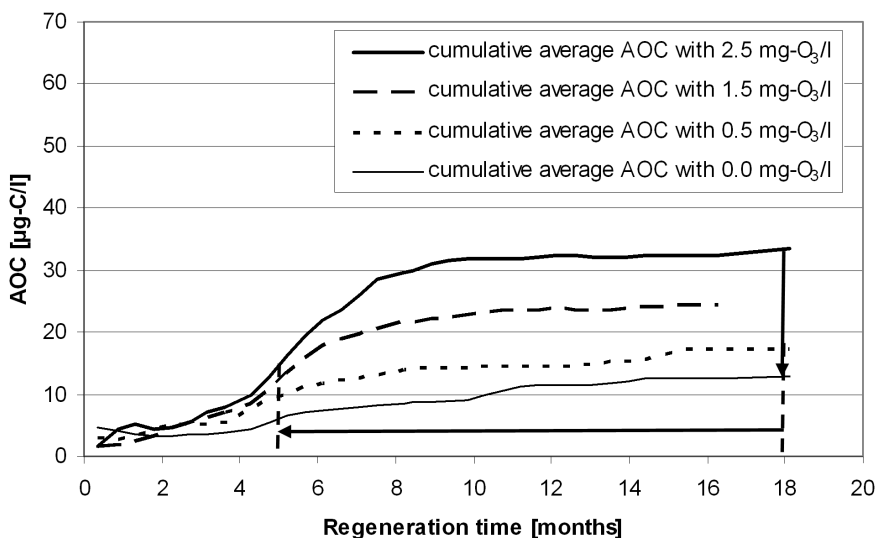


Figure 1 AOC concentration after BAC filtration at WPK for an ozone dosage of 2.5 $\text{mg-O}_3/\text{l}$, 1.5 $\text{mg-O}_3/\text{l}$, 0.5 $\text{mg-O}_3/\text{l}$ and 0.0 $\text{mg-O}_3/\text{l}$

From the performed life cycle assessment and the life cycle costing analysis of the operation of WPK, as described in Chapter 2, the effects on the environmental and financial impact can be determined for the changes in the regeneration time and the ozone dosage. For the situation of an ozone dosage of 0.95 mg-O₃/l and a regeneration time of 8 months, the increase in the total costs of drinking water for the consumer would be 2.1%, which is 0.03 €/m³. The increase in environmental impact is 17.6%, which is equivalent to an increase in car mileage of approximately 6 km per drinking water consumer in Amsterdam per year, see Table 1.

Table 1 Effects of change in ozone dosage and regeneration time for WPK on produced drinking water

Ozone dosage	Regeneration time	AOC drinking water	DOC drinking water	Change in environmental impact		Change in financial impact	
[mg-O ₃ /l]	[months]	[µg-C/l]	[mg-C/l]	[%]	[km car mileage]	[%]	[€/m ³]
2.50	18.0	28	3.0	0.0	0.0	0.0	0.00
2.50	5.0	10	1.2	36.2	11.8	4.6	0.07
1.50	5.5	10	1.8	31.6	10.4	4.0	0.06
0.95	7.9	10	2.5	17.6	5.8	2.1	0.03
0.50	13.2	10	3.2	4.9	1.6	0.3	0.01
0.00	18.0	8	3.8	-0.2	-0.1	-0.7	-0.01

Process design

When the ozone dosage at WPK is lowered to 0.95 mg-O₃/l, disinfection will probably not be sufficient. Since ozonation is the only process at WPK in which disinfection can be actively influenced, the boundaries for operational optimization are likely to be reached. This can be solved by adaptation of the current design of the ozonation system consisting of bubble diffusion chambers with consecutive contact chambers.

Research performed by van der Veer et al. (2005) illustrates the poor mixing of ozone over the cross-section after a conventional bubble diffusion chamber. Van der Veer measured dissolved ozone in a grid under the baffle after a counter current bubble diffusion chamber. The data showed areas with water containing almost no ozone and areas with water containing relatively high ozone concentrations. Wols and Hofman (2007a) performed research on computational fluid dynamics (CFD) modeling of the full-scale ozonation installation at drinking water treatment plant Leiduin (LDN) of Waternet. They found that the ozone contactor hydraulics are described by fewer completely stirred tank reactors

(CSTRs) than the number of ozone contact chambers. From these studies it can be concluded that the ozone concentration in a bubble chamber is far from perfectly mixed and the hydraulic properties of contact chambers are far from plug flow. This means that an ozonation system consisting of bubble chambers and contact chambers is inefficient for disinfection, but disinfection by-products are formed.

From pilot-plant experiments at LDN it was found that the disinfection capacity for the ozone-sensitive organism *E. coli* is 3 to 5 times higher when ozone contactor hydraulics approach a plug flow reactor (PFR) compared to a CSTR, see Chapter 4. For an efficient disinfection it is important that the dosed ozone be completely mixed as quickly as possible, to avoid having water parts with ozone concentrations lower than the average concentration. This specifically holds true at relatively low ozone dosages, as is 0.95 mg-O₃/l in combination with a DOC concentration of approximately 6 mg-C/l. The dissolved ozone plug flow reactor (DOPFR) design addresses both issues. In the DOPFR, ozone is dissolved in a pre-treated side stream and dosed just before a static mixer. By dosing dissolved ozone, the gas transfer of ozone into water is eliminated from the mixing process. Two liquid flows mix much better and more quickly than a gas and a liquid flow. In this way, with a static mixer, the dosed ozone can be almost instantly mixed over the total water flow. Subsequently, contact time in the DOPFR is created in a pipe with plug flow characteristics, see Chapter 3 and Chapter 4. When applied to the WPK situation, see Chapter 6 for the relationship between the ozonation processes at WPK and LDN, the plug flow reactor can be relatively short because ozone will be depleted quickly for an ozone dosage of 0.95 mg-O₃/l. From research with pilot-plant ozone bubble columns, with relatively good hydraulic characteristics compared to full-scale installations, it was found that large short-circuit flows occur, up to half of the total flow through a bubble column, see Chapter 6. Realizing the importance of hydraulics it can be concluded that the design of conventional ozone installations needs to be reconsidered.

For the current design at WPK, Dullemont (2006a) found that *Campylobacter* removal is 4 log units for an ozone dosage of 1.5 mg-O₃/l for water temperatures above 12°C and that *E. coli* removal underestimates the *Campylobacter* removal. Based on this information and the high removal of *E. coli* at low ozone exposure (CT) values measured in the PFR in LDN, it is expected that with the DOPFR design applied to WPK the same removal should be possible for an ozone dosage of 0.95 mg-O₃/l. *Enterovirus* concentrations were very low in ozonation influent,

and bacteriophages had a 3.4 log removal (Dullemont, 2006b). So, for viruses it is also expected that an ozone dosage of 0.95 mg-O₃/l will be sufficient in the DOPFR design. *Cryptosporidium* and *Giardia* removal was assessed with spores of sulfite-reducing clostridia that had a log 0.3 removal (Dullemont, 2006c). Since hydraulics have little effect on the inactivation of ozone resistant organisms, such as *Cryptosporidium* (Smeets et al., 2006), the removal will probably decrease in the DOPFR design for an ozone dosage of 0.95 mg-O₃/l. Since at WPK filtration steps, such as slow sand filtration, are the main barriers for protozoa and not ozonation, this will not be a problem (Hijnen et al., 2007). Apart from changes in the process design of ozonation, other design changes, such as changing the filter media or changing the filtration rate of the slow sand filters can also be considered for improvement of disinfection. Research for changes in the design of slow sand filtration is in preparation.

Changes in the design of the ozonation process will not lead to big changes in the environmental and financial impact of the operation of WPK, as shown in Table 1. However, changing the current design will lead to investments and to activities that will have an environmental impact. These are not quantified within this research.

Drinking water treatment concept

Instead of changes in the process design also a change in the drinking water treatment concept of WPK was investigated. In order to comply with the AOC standard of 10 µg-C/l, part of the NOM can be removed before ozonation, especially the part of the NOM leading to AOC formation during ozonation. For an ozone dosage of 0.95 mg-O₃/l, this will lead to higher disinfection with lower AOC formation and with lower total DOC concentrations of the produced drinking water. From experiments discussed in Chapter 5, where part of the NOM was removed by either ion exchange (IEX) or granular activated carbon (GAC) filtration, it was concluded that for the same ozone dosages the CT is higher when NOM is removed by IEX or GAC compared to the situation without NOM removal. In addition it was concluded that the humic substances fraction (molecular weight ~ 1000 g/mol) and the building blocks fraction (molecular weight 300-500 g/mol) of NOM, as determined by size exclusion chromatography with DOC detection, are the ozone reactive fractions. Ozonation efficiency improved more with the removal of the humic substances fraction as compared to the removal of the building blocks fraction because it led to less bromate formation and less AOC formation. It was

concluded that for NOM removal before ozonation, IEX is preferred, because the IEX resin that was tested removed more humic substances than the GAC tested. By removing half of the NOM with the IEX tested, lowering DOC concentrations from 6 mg-C/l to 3 mg-C/l, and subsequently dosing of 0.95 mg-O₃/l, the disinfection during ozonation will improve significantly and the AOC and DOC concentrations in the produced drinking water will be lower than 10 µg-C/l and 2.5 mg-C/l, respectively.

An additional treatment step will lead to an added environmental impact and significant investment costs. It will also lead to changes in the environmental and financial impact of the operation of the WPK drinking water treatment plant. These changes have not been quantified within this research but should be further investigated when considering additional processes.

Integrated modeling

Integrated modeling has proven to be the driving force for operational optimization, based on explicit objectives, for new developments in design and for exploring changes in the concept of a drinking water treatment plant, as shown schematically in Figure 2. The most important property of an integrated model is its ability to predict the water quality parameters that are influenced by preceding processes, or influence subsequent processes. The integrated model for ozonation is able to predict ozone decay, CT value, *E. coli* disinfection, the decrease in UV absorbance at 254 nm (UVA₂₅₄), the increase in AOC concentration and bromate formation on the basis of influent water quality parameters and the applied ozone dosage, see Chapters 3, 4 and 6.

In the tested bench-scale DOPFR and pilot-scale DOPFR it was possible to measure ozone concentrations starting from 1 to 2 seconds, in contrast to other research where the first samples are usually taken after 30 seconds or one minute. This gave the possibility to measure rapid ozone consumption that occurs due to the reaction between ozone and NOM upon the first contact of ozone with natural water. From modeling the measured rapid ozone consumption it was found that the rate of rapid ozone consumption in the first 20 seconds of contact time follows diffusion-limited kinetics.

From the experimental work, model calibration runs and validation runs, it can be concluded that the UVA_{254} is an effective parameter for the estimation of rapid ozone consumption. The majority of the ozone-sensitive organism *E. coli* is inactivated during the rapid ozone consumption phase. The disinfection capacity for *E. coli* is 3 to 5 times higher in a PFR compared to a CSTR for the same amount of ozone dosed. CT values in ozone bubble column reactors are not determined by the rapid ozone consumption rate but by the amount of ozone consumed during rapid ozone consumption in combination with the slow ozone decay rate. The integrated ozonation model is a valuable tool for controlling the balance between disinfection, bromate formation and AOC formation and can be used for evaluation of control strategies for operational support and for process control. It is a tool that directly shows the consequences of changes in operation of the ozone installation. It enables water supply companies to make more objective choices for operational settings, see Chapter 6.

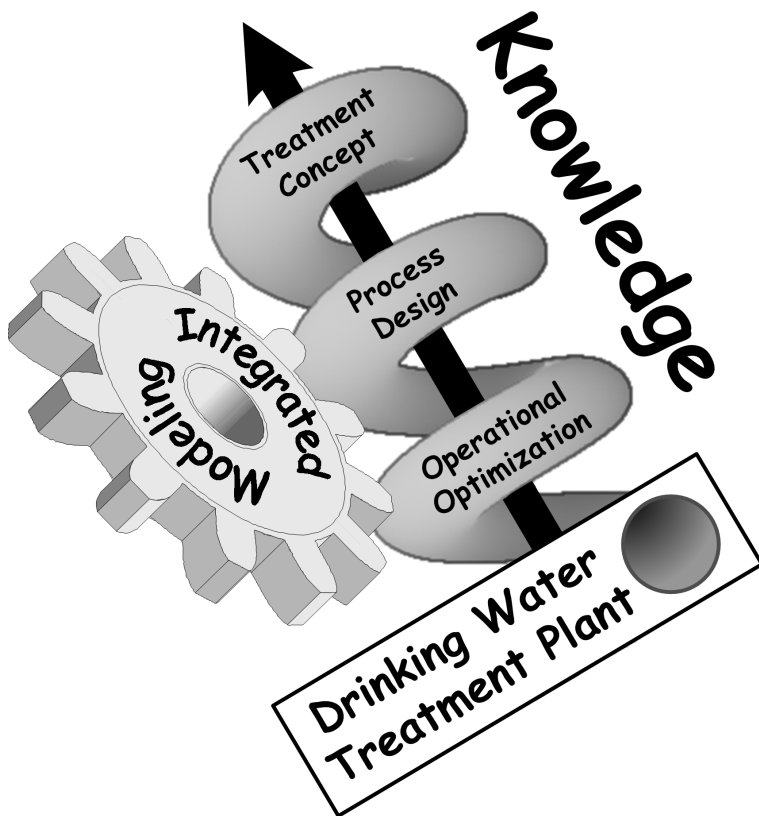


Figure 2 Integrated modeling as the driving force for increasing knowledge

When the Promicit project started in January 2003 (of which this research is a part, see Chapter 1), the ideas for integrated modeling and model-based control of drinking water treatment plants were just starting to develop. In the Netherlands only a select group was involved in the modeling of drinking water treatment processes and the benefits and results of the research were difficult to predict. The project is not finished yet, so not all of its results can be presented, but a number can be mentioned here. From this research, insight has been gained regarding the processes that take place during ozonation, NOM characterization, disinfection, costs of operation, environmental impact of operation, interactions between treatment processes, model calibration and validation, model development, on-line measuring methods, laboratory analyses and new data logging methods. Besides the modeling efforts described in this research, other modeling activities are also being carried out within the Promicit project, such as:

- modeling pellet softening (van Schagen et al., 2005 and 2006);
- modeling integrated pH control;
- modeling the behavior of organic micro-pollutants in drinking water treatment processes using quantitative structure-activity relationships (van der Horst et al., 2006);
- modeling clogging of BAC filters (Ross et al., 2007a);
- modeling slow sand filtration (Schijven et al. 2007);
- modeling nitrification in rapid sand filters.

In general it can be stated that in order to be able to model a process, the process has to be understood. Thus, modeling efforts lead to the increase in knowledge, application of knowledge and recordation of knowledge.

Related ongoing research

The integrated ozone model will be used in further research for control of the ozone bubble column pilot-plant at the WPK drinking water treatment plant. That research focuses on the application of water quality models for on-line model-based control of water treatment plants and is being carried out within the Promicit project, in which the present work was also conducted (van Schagen et al., 2005 and 2006).

As a continuation of the present work, the integrated ozone model will be validated on several other drinking water production plants in Europe. The research is being

carried out by the Delft University of Technology and is part of the European Union's 6th framework project TECHNEAU, that started in January 2006. The UVA_{254} has been used for prediction of AOC formation during ozonation, but the use of differential UV absorbance spectra determined on-line before and after ozonation seems to give better results and will be further investigated within the TECHNEAU project (van den Broeke et al., 2007; Ross et al., 2007b).

The step-tracer experiments for determining the hydraulic properties of the bench-scale and pilot-scale dissolved ozone plug flow reactors were used in research focusing on the use of CFD in drinking water treatment (Wols and Hofman, 2007a; Wols et al., 2007b). The research started in January 2006 and is being carried out at Delft University of Technology in cooperation with Waternet and Kiwa Water Research. The full-scale ozonation plant LDN of Waternet will be modeled using particle tracking, and the CFD model will be extended with the integrated ozone model developed in the present thesis.

The integrated ozone model will also be used within the Waterspot simulator for off-line and on-line optimization, training and education (Worm et al., 2007). The model will be applied to full-scale drinking water treatment plants and control strategies can be further developed. The Waterspot simulator is the subject of research carried out by the water supply companies Duinwaterbedrijf Zuid-Holland, Waternet, PWN Water Supply Company North-Holland, Vitens and by Ureason, DHV B.V., ABB B.V., Delft University of Technology and Kiwa Water Research. The project started in November 2006.

The removal of specific NOM fractions by different types of IEX resins and sorbent resins and their effect on treatment efficiency is being studied within the IS NOM project (Cornelissen et al., 2007; Grefte et al., 2007). Within the IS NOM project different aspects of NOM and biological stability during drinking water treatment and distribution are being investigated. The model can be used for predicting the effect of NOM removal on ozonation. The IS NOM project, that started January 2006, is a joint research project of Kiwa Water Research, UNESCO-IHE, Delft University of Technology, the water supply companies Vitens and Waternet.

Nomenclature

AOC	assimilable organic carbon
BAC	biological activated carbon
CFD	computational fluid dynamics
CSTR	completely stirred tank reactor
CT	ozone exposure ((mg-O ₃ /l)*min
DOC	dissolved organic carbon
DOPFR	dissolved ozone plug flow reactor
GAC	granular activated carbon
IEX	ion exchange
LDN	drinking water treatment plant Leiduin of Waternet
LNV	pre-treatment plant Loenderveen of Waternet
PFR	plug flow reactor
SI	saturation index
UVA ₂₅₄	UV absorbance at 254 nm
Waternet	water cycle company for Amsterdam and surrounding areas
WPK	drinking water treatment plant Weesperkarspel of Waternet

References

- Cornelissen, E.R., Moreau, N., Siegers, W.G., Abrahamse, A.J., Rietveld, L.C., Grefte, A., Dignum, M., Amy, G.L. and Wessels, L.P. (2007). Selection of anionic exchange resins for removal of natural organic matter (NOM) fractions. *Water Res.*, accepted for publication, July 2007.
- Dullemont, Y.J. (2006a). *QMRA Campylobacter locatie Weesperkarspel over de jaren 2003 en 2004 (QMRA Campylobacter location Weesperkarspel for the years 2003 and 2004)*. Report Waternet, Amsterdam, the Netherlands.
- Dullemont, Y.J. (2006b). *QMRA Enterovirussen locatie Weesperkarspel over de jaren 2003 en 2004 (QMRA Enteroviruses location Weesperkarspel for the years 2003 and 2004)*. Report Waternet, Amsterdam, the Netherlands.
- Dullemont, Y.J. (2006c). *QMRA Cryptosporidium en Giardia locatie Weesperkarspel over de jaren 2003 en 2004 (QMRA Cryptosporidium and Giardia location Weesperkarspel for the years 2003 and 2004)*. Report Waternet, Amsterdam, the Netherlands.

- Grefte, A., Dignum, M., van der Helm, A.W.C., Rietveld, L.C., Cornelissen, E.R., Amy, G.L. and van Dijk, J.C. (2007). Removal of NOM fractions by different anion exchange and sorbent resins. *Proceedings of the 4th IWA Leading-Edge Conference and Exhibition on Water and Wastewater Technologies*, Singapore, Republic of Singapore, 2007.
- Hijnen, W.A.M., Dullemont, Y.J., Schijven, J.F., Hanzens-Brouwer, A.J., Rosielle, M. and Medema, G.J. (2007). Removal and fate of *Cryptosporidium parvum*, *Clostridium perfringens* and small-sized centric diatoms (*Stephanodiscus hantzschii*) in slow sand filters. *Water Res.*, 41(10), 2151-2162.
- Ross, P.S., Rietveld, L.C., van der Aa, L.T.J. and van Dijk, J.C. (2007a). Modelling of clogging of biological activated carbon filters. *Proceedings of the AWWA Water Quality Technology Conference & Exposition*, Charlotte, USA, 2007.
- Ross, P.S., van der Helm, A.W.C., van den Broeke, J., van der Aa, L.T.J., Rietveld, L.C. and van Dijk, J.C. (2007b). Characterization of NOM by UV-spectrography in drinking water treatment processes to assess biological stability. *Proceedings of the 4th IWA Leading-Edge Conference and Exhibition on Water and Wastewater Technologies*, Singapore, Republic of Singapore, 2007.
- Schijven, J.F., Colin, M., Dullemont, Y.J., Hijnen, W.A.M., Magic-Knezev, A. and Oorthuizen, W.A. (2007). *Verwijdering van micro-organismen door langzame zandfiltratie (Removal of micro-organisms by slow sand filtration)*. Report RIVM 703719019/2007, Bilthoven, the Netherlands.
- Smeets, P.W.M.H., van der Helm, A.W.C., Dullemont, Y.J., Rietveld, L.C., van Dijk, J.C. and Medema, G.J. (2006). Inactivation of *Escherichia coli* by ozone under bench-scale plug flow and full-scale hydraulic conditions. *Water Res.*, 40(17), 3239-3248.
- van den Broeke, J., Ross, P.S., van der Helm, A.W.C., Baars, E.T. and Rietveld, L.C. (2007). Use of on-line UV/Vis-spectrometry in the measurement of dissolved ozone and AOC concentrations in drinking water treatment. *Proceedings of the IWA AutMoNet 2007*, Gent, Belgium, 2007.
- van der Aa, L.T.J., Kolpa, R.J., Magic-Knezev, A., Rietveld, L.C. and van Dijk, J.C. (2003). Biological activated carbon filtration: pilot experiments in the Netherlands. *Proceedings of the AWWA Water Quality Technology Conference and Exposition*, Philadelphia, USA, 2003.
- van der Horst, W., Ijpelaar, G.F., Scholte-Veenendaal, P., Rietveld, L.C. and van Dijk, J.C. (2006). Occurrence and removal of pharmaceuticals and endocrine disrupting compounds (EDCs) from drinking water. *Proceedings of the AWWA Water Quality Technology Conference & Exposition*, Denver, USA, 2006.

- van der Kooij, D. (1992). Assimilable organic carbon as an indicator of bacterial regrowth. *Am. Water Works Assoc. J.*, 84(2), 57-65.
- van der Veer, A.J., Schotsman, R.M., Martijn, B., Schurer, R. and van Dijk, J.C. (2005). Comparative small technical scale study on ozone disc diffusers and ejector system. *Proceedings of the IOA-EA3G 17th world congress and exhibition*, Strasbourg, France, 2005.
- van Schagen, K.M., Babuška, R., Rietveld, L.C., Wuister, J. and Veersma, A.M.J. (2005). Modeling and predictive control of pellet reactors for water softening. *Proceedings of 16th IFAC World Congress*, Prague, Czech Republic, 2005.
- van Schagen, K.M., Babuška, R., Rietveld, L.C. and Baars, E.T. (2006). Optimal flow distribution over multiple parallel pellet reactors: a model-based approach. *Water Sci. Technol.*, 53(4-5), 493-501.
- Wols, B.A. and Hofman, J.A.M.H. (2007a). *Verblijftijdspreiding ozon Leiduin (Residence time distribution ozonation Leiduin)*. Report Waternet, Amsterdam, the Netherlands.
- Wols, B.A., Hofman, J.A.M.H., Uijtewaal, W.S.J., Rietveld, L.C., Stelling, G.S. and van Dijk, J.C. (2007b). Residence time distributions in ozone contactors. *Proceedings of the IOA-IUVA world congress 2007*, Los Angeles, USA, 2007.
- Worm, G.I.M., Oudmans, J., van Schagen, K.M. and Rietveld, L.C. (2007). A company specific simulator of a drinking water treatment plant. *Proceedings of the 6th EUROSIM congress on modelling and simulation*, Ljubljana, Slovenia, 2007.

List of publications

International refereed publications

- van der Helm, A.W.C. and Rietveld, L.C. (2002). Modelling of drinking water treatment processes within the Stimela environment. *Water Sci. Technol.: Water Supply*, 2(1), 87-93.
- van der Helm, A.W.C., Smeets, P.W.M.H., Baars, E.T., Rietveld, L.C. and van Dijk, J.C. (2005). Dosing ratios for reduced bromate formation by dissolved ozone dosing. *Water Sci. Technol.: Water Supply*, 5(5), 35-40.
- Smeets, P.W.M.H., van der Helm, A.W.C., Dullemont, Y.J., Rietveld, L.C., van Dijk, J.C. and Medema, G.J. (2006). Inactivation of *Escherichia coli* by ozone under bench-scale plug flow and full-scale hydraulic conditions. *Water Res.*, 40(17), 3239-3248.
- Barrios, R., Siebel, M.A., van der Helm, A.W.C., Bosklopper, Th.G.J. and Gijzen, H.J. (2006). Environmental and financial life cycle impact assessment of drinking water production at Waternet. *J. Clean. Prod.*, doi:10.1016/j.jclepro.2006.07.052.
- Tapia, M., Siebel, M.A., van der Helm, A.W.C., Baars, E.T. and Gijzen, H.J. (2006). Environmental, financial and quality assessment of drinking water processes at Waternet. *J. Clean. Prod.*, doi:10.1016/j.jclepro.2006.07.053.
- van der Helm, A.W.C., Smeets, P.W.M.H., Baars, E.T., Rietveld, L.C. and van Dijk, J.C. (2007). Modeling of ozonation for dissolved ozone dosing. *Ozone Sci. Eng.*, accepted for publication, February 2007.
- van der Helm, A.W.C., Grefte, A., Baars, E.T., Rietveld, L.C., van Dijk, J.C. and Amy, G.L. (2007). Effects of natural organic matter (NOM) character and removal on efficiency of ozonation. *J. Water Supply Res. Technol. AQUA*, submitted for publication, April 2007.
- van der Helm, A.W.C., Rietveld, L.C., Baars, E.T. and van Dijk, J.C. (2007). Disinfection and by-product formation during ozonation in a pilot-scale plug flow reactor and CSTR. *J. Water Supply Res. Technol. AQUA*, submitted for publication, September 2007.

Conference proceedings

- Rietveld, L.C. and van der Helm, A.W.C. (2000). Modelling for control of drinking water production plants. *Proceedings of the IW(S)A workshop Modelling of conventional drinking water production processes*, Delft, the Netherlands, 2000.
- van der Helm, A.W.C. and Rietveld, L.C. (2000). Modelling of drinking water treatment processes within the Stimela environment. *Proceedings of the IWA conference Innovations in conventional and advanced water treatment processes*, Amsterdam, the Netherlands, 2000.
- van der Helm, A.W.C., Bosklopper, Th.G.J. and Rietveld, L.C. (2004). Ozone modelling for plant control. *Proceedings of the IOA-EA3G International Conference*, Barcelona, Spain, 2004.
- van der Helm, A.W.C., Smeets, P.W.M.H., Baars, E.T., Rietveld, L.C. and van Dijk, J.C. (2005). Dosing ratios for reduced bromate formation by dissolved ozone dosing. *Proceedings of the 3rd IWA Leading-Edge Conference and Exhibition on Water and Wastewater Treatment Technologies*, Sapporo, Japan, 2005.
- van der Helm, A.W.C., Smeets, P.W.M.H., Baars, E.T., Rietveld, L.C. and van Dijk, J.C. (2005). Modelling of ozonation for dissolved ozone dosing with reduced bromate formation. *Proceedings of the IOA-EA3G 17th world congress and exhibition*, Strasbourg, France, 2005.
- Barrios, R., Siebel, M.A., van der Helm, A.W.C., Bosklopper, Th.G.J. and Gijzen, H.J. (2005). Trends in impact reduction - The case of Amsterdam Water Supply. *Proceedings of the IWA Agua 2005 conference*, Cali, Colombia, 2005.
- Tapia, M., Siebel, M.A., van der Helm, A.W.C., Bosklopper, Th.G.J. and Gijzen, H.J. (2005). Environmental, financial and quality assessment of drinking water processes at Amsterdam Water Supply. *Proceedings of the IWA Agua 2005 conference*, Cali, Colombia, 2005.
- van der Helm, A.W.C. (2006). Integral modelling of drinking water treatment plant Weesperkarspel of Amsterdam Water Supply. *Proceedings of the Yearly Congress Water Research Centre Delft*, Delft, the Netherlands, 2006.
- van der Helm, A.W.C., Rietveld, L.C., Baars, E.T. and van Dijk, J.C. (2006). Modelling of ozonation: ozone decay, disinfection and formation of bromate and AOC, applied to a pilot scale continuous ozone plug flow reactor. *Proceedings of the Delft University of Technology Workshop Developments in Drinking Water Treatment Modelling*, Delft, the Netherlands, 2006.

- van der Helm, A.W.C., Grefte, A., Baars, E.T., Rietveld, L.C., van Dijk, J.C. and Amy, G.L. (2006). Effects of natural organic matter (NOM) character and removal on efficiency of ozonation. *Proceedings of the Delft University of Technology Workshop Developments in Drinking Water Treatment Modelling*, Delft, the Netherlands, 2006.
- Rietveld, L.C., van der Helm, A.W.C., van Schagen, K.M., van der Aa, L.T.J. and van Dijk, J.C. (2006). Integral deterministic modelling of drinking water treatment. *Proceedings of the Delft University of Technology Workshop Developments in Drinking Water Treatment Modelling*, Delft, the Netherlands, 2006.
- van der Helm, A.W.C., Rietveld, L.C., van der Aa, L.T.J. and van Dijk, J.C. (2006). Integral optimisation of drinking water treatment plants. *Proceedings of the AWWA Water Quality Technology Conference and Exposition*, Denver, USA, 2006.
- van der Helm, A.W.C. (2007). Integral modelling of drinking water treatment plant Weesperkarspel of Waternet. *Proceedings of the Yearly Congress Water Research Centre Delft*, Delft, the Netherlands, 2007.
- Ross, P.S., van der Helm, A.W.C., van den Broeke, J., van der Aa, L.T.J., Rietveld, L.C. and van Dijk, J.C. (2007). Characterization of NOM by UV-spectrography in drinking water treatment processes to assess biological stability. *Proceedings of the 4th IWA Leading-Edge Conference and Exhibition on Water and Wastewater Technologies*, Singapore, Republic of Singapore, 2007.
- Grefte, A., Dignum, M., van der Helm, A.W.C., Rietveld, L.C., Cornelissen, E.R., Amy, G.L. and van Dijk, J.C. (2007). Removal of NOM fractions by different anion exchange and sorbent resins. *Proceedings of the 4th IWA Leading-Edge Conference and Exhibition on Water and Wastewater Technologies*, Singapore, Republic of Singapore, 2007.
- van den Broeke, J., Ross, P.S., van der Helm, A.W.C., Baars, E.T. and Rietveld, L.C. (2007). Use of on-line UV/Vis-spectrometry in the measurement of dissolved ozone and AOC concentrations in drinking water treatment. *Proceedings of the IWA AutMoNet 2007 conference*, Gent, Belgium, 2007.
- van den Broeke, J., Ross, P.S., van der Helm, A.W.C., Baars, E.T. and Rietveld, L.C. (2007). On-line monitoring of drinking water treatment efficacy using UV/Vis-spectrometry. *Proceedings of the AWWA Water Quality Technology Conference and Exposition*, Charlotte, USA, 2007.

National publications

- van der Helm, A.W.C., Rietveld, L.C. and van Dijk, J.C. (1999). Is de praktijk gebaat bij modellen van intensieve gasuitwisselingssystemen? (Does practice benefit from models for gas exchange systems?). *H2O*, 32(11), 27-31.
- Riemersma, M., van der Helm, A.W.C. and Hendriks, A. (2001). Het gebruik van GIS bij leidingnetmodellering (The use of GIS for water distribution network modelling). *H2O*, 34(24), 24-25.
- van der Plas, A., Perfors, G., van der Helm, A.W.C. and Nijdam, P.C. (2002). Automatische distributieregeling voor PS Scheveningen (Automatic distribution control for drinking water production plant Scheveningen). *H2O*, 35(1), 23-25.
- van der Helm, A.W.C., Kramer, O., Bosklopper, Th.G.J. and Hofman, J.A.M.H. (2003). Hogere ambities vragen andere bedrijfsvoering (Higher ambitions demand a different control strategy). *H2O*, 36(18), 32-34.
- van der Helm, A.W.C. and Schilperoort, R. (2005). Van medicijnen wordt water niet beter (Water isn't getting well from medicines). *H2O*, 38(2), 4-6.
- van der Helm, A.W.C., Tuin, B., Hijnen, W.A.M. en Cornelissen, E.R. (2005). Nadruk op membraanonderzoek op derde LET-conferentie in Japan (Emphasis on membrane research at third LET-conference in Japan). *H2O*, 38(16), 26-27.
- van Leenen, M.T., van der Helm, A.W.C., Baars, E.T. and Rietveld, L.C. (2006). NOM-verwijdering met ionenwisseling kan leiden tot lagere kosten en betere waterkwaliteit (NOM removal with ion exchange can lead to lower costs and a better water quality). *H2O*, 39(6), 54-57.

National books

- van der Helm, A.W.C., Smeets, P.W.M.H. and Bosklopper, Th.G.J. (2005). Technologie kan ons helpen (Technology can help us). Chapter in *Door water verbonden (United by water)*, ISBN 90-407-2573-X.

Curriculum vitae

Alexander Wilhelmus Cornelis (Alex) van der Helm was born on February 23, 1972 in Nootdorp, the Netherlands. In 1990 he graduated from Gymnasium (College Preparatory High School) at Sint-Janslyceum in 's-Hertogenbosch. In 1991 he started his civil engineering studies at Delft University of Technology. Van der Helm finished his Master's thesis entitled "Modeling of gas transfer systems", a drinking water supply emphasis, in 1998. Supervised by dr. ir. L.C. Rietveld and Prof. J.C. van Dijk, van der Helm received the faculty award for best Master's thesis. Since 1998 he has worked at DHV B.V. (a consultancy and engineering company) as a water supply consultant. In 2003 he started his PhD research on integrated modeling of ozonation for optimization of drinking water treatment. The PhD research was carried out at Delft University of Technology. Currently, van der Helm also works part-time at the Delft University of Technology as a researcher.



In 2050, models will predict water quality and determine set points for the control of drinking water treatment plants. Models will be run continuously and will assist operators, whose daily duties will be automated. Off-line and on-line water quality data will be fed to models for continuous adjustment of treatment to ensure high quality drinking water.

This thesis identifies the objectives to be used for optimization of the operation of drinking water treatment and it describes integrated modeling of ozonation. Different control strategies for ozonation are assessed, a new design for ozone installations is developed, and the character and removal of natural organic matter (NOM) prior to ozonation is studied.

The results of this research contribute to the fulfillment of the vision for drinking water treatment in the year 2050.